High Throughput Discovery, Metabolism and Disposition of Chemopreventive Agents using Mass Spectrometry

BY

LIAN CHEN
B.S., Wuhan University, Wuhan, China, 2006

THESIS

Submitted in partial fulfillment of the requirements
for the degree of Doctor of Philosophy in Pharmacognosy
in the Graduate College of the
University of Illinois at Chicago, 2013

Chicago, Illinois

Defense Committee:
Richard B. van Breemen, Chair and Advisor
Joanna E. Burdette
Scott G. Franzblau
Brian T. Murphy
Hyun-Young Jeong, Biopharmaceutical Sciences

This dissertation is dedicated to my husband, Zhe Li, my parents, Shanyue Chen and

Cixiu Cao, and my daughter Jessica Yixuan Li

for their support, encouragement and love.

ACKNOWLEDGEMENTS

TABLE OF CONTENTS

LIST OF TABLES

LIST OF FIGURES

LIST OF ABBREVIATIONS

9cRA	9-*cis*-retinoic acid
ADH	Alcohol dehydrogenase
ADME	Absorption, distribution, metabolism and elimination
AKR	Aldo-keto reductase
ALDH	Aldehyde dehydrogenases
AP	Apical
BL	Basolateral
*B*max	Maximum binding capacities
CID	Collision - induced dissociation
CL_{int}	Hepatic intrinsic clearance
CYP450	Cytochromes P450
DMEM	Dulbecco's modified Eagle's medium
DMSO	Dimethylsulfoxide
ER	Estrogen receptors
FBS	Fetal bovine serum
FMO	Favin-containing monooxygenase
GSH	Glutathione
GST	Glutathione-S-transferase
HBSS	Hank's balanced salt solution
HLM	Human liver microsomes
IC_{50}	The concentration to inhibit 50% of enzyme activity
IR	Induction ratio
IT	Ion trap
K_D	Dissociation constant
LC-MS	Liquid chromatography - mass spectrometry
LC-MS/MS	Liquid chromatography - tandem mass spectrometry
LOQ	Limit of quantitation
LXR	Liver X receptors
m	Milli
M	Molar
m/z	Mass-to-charge ratio
MAO	Monoamine oxidases

MHz	Megahertz
min	Minute(s)
MNU	Methylnitrosourea
Moco	Molybdenum cofactor
MS^n	Mutiple-stage tandem mass spectrometry
n	Nano
NAT	*N*-acetyltransferase
$p21^{WAF1/CIP1}$	Cyclin-dependent kinase inhibitor
PAPA	*p*-aminobenzoic acid
PAPS	3'-phosphoadenosine-5'-phosphosulfate
PPAR	Peroxisome proliferator activated receptor
PPB	Plasma protein binding
PXR	Pregnane X receptor
QqTOF	Quadrupole time-of-flight
RAR	Retinoic acid receptors
RXR	Retinoid X receptors (RXR
RXRE	Retinoid X DNA Response Element
SAR	Structure-activity relationships
SF	Scaling factor
SIM	Selected ion monitoring
SMZ	Sulfamethazine
SRM	Selected reaction monitoring
SULT	Sulfotransferase
TEER	Transepithelial electrical resistance
Top 1	Topoisomerase I
TPA	12-*O*-tetradecanoylphorbol-13-acetate
u	Mass unit
UGT	UDP-glucuronosyltransferase
VDR	Vitamin D receptor
μ	Micro

SUMMARY

Cancer chemoprevention uses natural, synthetic, or biologic chemical agents to reverse, suppress or prevent the initial, promotion and/or progression of cancer. Most current chemoprevention agents like curcumin have low bioavailability or, like tamoxifen, have serious side effects. The successful development of new chemotherapeutic agents that target specific signal transduction pathways and achieve dramatic improvements in efficacy without significant cytotoxicity will be important for the future of cancer chemoprevention.

The control of gene expression offers a powerful strategy for the prevention and treatment of disease. Human gene expression is regulated by 48 nuclear receptors, approximately one-third of which require heterodimerization with one of the ligand-activated retinoid X receptors to bind to DNA and function efficiently. This situation has led to RXRs being dubbed the "master partner." As a nuclear receptor, the retinoid X receptor (RXR) is involved in the regulation of multiple anti-cancer pathways including several of those involved in cell proliferation, differentiation and apoptosis. Ligand-mediated activation of the RXR is a strategy for cancer chemoprevention and therapy. In an attempt to achieve the activation of multiple pathways, increase potency and reduce the toxicity of naturally occurring retinoids, various rexinoids have been developed and some have shown promising antitumor activity in preclinical and clinical studies.

Ultrafiltration mass spectrometry was invented and developed in the van Breemen laboratory for the screening of combinatorial library mixtures and natural

SUMMARY (continued)

product extracts in order to identify ligands to macromolecular targets, such as adenosine deaminase, dehydrofolate reductase, cycloxygenase-2, serum albumin, estrogen receptors (ER), and retinoid X receptor α. Following extensive screening for novel RXR ligands, we identified 3-amino-6-(3-aminopropyl)-5,6-dihydro-5,11-dioxo-11H-indeno[1,2-c]isoquinoline (AM6-36) as a ligand and agonist of RXR.

The indenoisoquinoline AM6-36 is an atypical rexinoid since it does not structurally resemble a retinoic acid. In order to validate the indenoisoquinolines as RXRα ligands and to understand the key features for RXR agonist activity, a SAR study was undertaken. New rexinoids, the indenoisoquinolines, have been identified and their potencies evaluated. The fact that indenoisoquinolines are structurally unique rexinoids offers the possibility of them having unique pharmacologic properties that could be clinically useful. Considering these factors as a whole, indenoisoquinoline rexinoids should be selected for further evaluation.

AM6-36 binds to RXRα and induces apoptosis in MCF-7 breast cancer cells. Because these data suggested that AM6-36 is a promising lead compound for the treatment or prevention of breast cancer, drug development studies were carried out in different *in vitro* and *in vivo* models combined with high performance liquid chromatography-mass spectrometry (LC-MS) and Liquid chromatography-tandem mass spectrometry (LC-MS/MS). AM6-36 formed seven Phase I and Phase II metabolites. Structures for all seven metabolites were proposed based on high resolution accurate mass tandem mass spectrometry, and six of these metabolites were

identified by comparison with synthetic standards. These preliminary metabolism studies suggest that AM6-36 will not form reactive, potentially toxic metabolites. AM6-36 showed moderate serum protein binding and moderate metabolic stability, and low first-pass liver metabolism is predicted. These properties are favorable for further investigation and development of AM6-36 as a potential chemoprevention and cancer therapeutic agent.

Topoisomerase I (Top1) is an essential enzyme that relaxes supercoiled DNA so that it may be replicated, transcribed and repaired. As Topl is overexpressed and DNA damage responses are defective in some human tumors, several Top1 inhibitors have been developed as chemotherapeutic agents. Two of these compounds, indimitecan (LMP776) and indotecan (LMP400) were promoted into Phase I clinical trials at the National Cancer Institute. These compounds appear to be stable and are powerful, cytotoxic Top1 poisons that induce long-lasting DNA breaks and overcome the drug resistance issues associated with the camptothecins.

The metabolism of LMP400 and LMP776 is currently under investigation, which has led to the synthesis of potential metabolites to be used as synthetic standards for metabolism studies. O-dealkylation and demethylenation are two major metabolic pathways of LMP400 and LMP776 observed to occur in human liver microsomes. As part of this study, the proposed metabolites are also being investigated for Top1 inhibitory activity. The discoveries of the very potent hydroxyindenoisoquinolines as metabolites of LMP400 and LMP77 have the potential

SUMMARY (continued)

to be as potent as the parent drug and to provide new starting points for the development of potent, cytotoxic Top 1 poisons.

In conclusion, high throughput screening, metabolism and disposition of pharmacologically active agents are critical in drug discovery and development. The combination of high-performance liquid chromatography and mass spectrometry (LC-MS) has become broadly used in all sectors in drug discovery and development. The analytical figures of high sensitivity, selectivity, reproducibility, and accessibility provide a powerful platform for analysis.

1. INTRODUCTION

1.1 <u>Cancer and chemoprevention</u>

Cancer is a leading cause of death worldwide and the total number of cases globally is increasing. Based on the GLOBOCAN 2008 estimates, about 12.7 million cancer cases and 7.6 million cancer deaths are estimated to have occurred in 2008. The World Health Organization estimates that 84 million people will die in the next 10 years if action is not taken. The most common new cancer diagnoses are lung, breast and colorectal cancer, while the most common causes of cancer death are lung, stomach and liver malignancies. More than 70% of all cancer deaths occur in low- and middle-income countries, where resources available for prevention, diagnosis and treatment of cancer are limited or nonexistent. The magnitude of the cancer problem, and the failure of advanced disease chemotherapy to effect major reductions in the mortality rates for the common types of malignancy, indicate that new approaches to the control of cancer are necessary.[1]

Cancer, a group of more than 200 different diseases, is an uncontrolled growth of cells that disrupts body tissues and organs. The multistage process of carcinogenesis is a gradual process with three phases: initiation, promotion and progression. The first phase involves genetic damage of a cell called initiation. The second phase is promotion, where carcinogens alter the cellular environment favoring the mutant cell. The final stage is progression, which involves further cell proliferation into clinically

detectable cancer.[2] The basic scientific knowledge of mechanisms of carcinogenesis can facilitate the design of rational new approaches for its prevention.
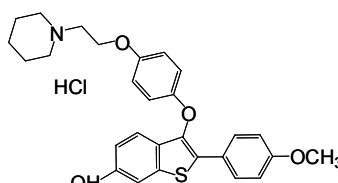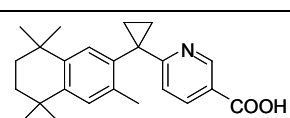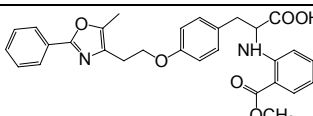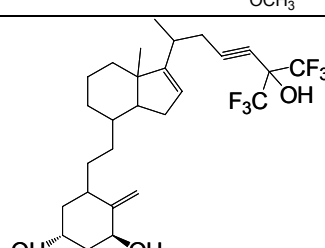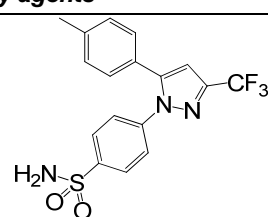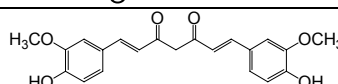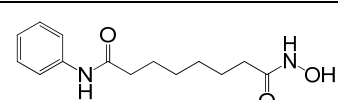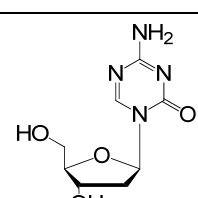
Cancer chemoprevention, as first defined by Sporn in 1976, uses natural, synthetic, or biologic chemical agents to reverse, suppress or prevent either the initial phase of carcinogenesis or the progression of neoplastic cells to cancer.[3] Today, cancer chemoprevention is considered possible at any stage, including the prevention of recurrence of clinically significant cancer in cancer survivors. During the last 30 years, the field of cancer chemoprevention has grown to the point where chemoprevention has been achieved in numerous animal experiments and validated in several major clinical trails. Although encouraging progress toward chemoprevention of human cancer has been made, this field is still in its earliest stages of development. The principal need in the chemoprevention of cancer remains the discovery of new agents that are safe, tolerable and clinically effective. [4, 5]

Nuclear receptors are one of the most abundant classes of transcriptional regulators and are important in eukaryotic development, differentiation, reproduction, and metabolic homeostasis. As nuclear receptors bind small molecules that can easily be modified by drug design, and control functions associated with major diseases, they are promising pharmacological targets. Nuclear receptors that are involved in carcinogenesis and have been targeted for chemoprevention include the estrogen receptors ERα and ERβ, the androgen receptor, the retinoic acid receptors (RARα, β and γ), the retinoid X receptors (RXRα, β and γ), the vitamin D receptor (VDR), and

the peroxisome proliferator activated receptor-γ (PPAR γ). Table I shows the structures of some chemopreventive agents with known molecular targets. For example, arzoxifene and tamoxifen are available as prescription drugs for the prevention of breast cancer, and celecoxib is approved for the prevention of familial polyposis. The ligands for the four nuclear receptors are all synthetic analogues of naturally occurring hormones or metabolites that bind to their cognate receptors.[6, 7, 8] The successful development of new chemotherapeutic agents that target specific signal transduction pathways and achieve dramatic improvements in efficacy without significant cytotoxicity will be important for the future of cancer chemoprevention.

TABLE I

CHEMOPREVENTIVE AGENTS WITH KNOWN MOLECULAR TARGETS.[7]

	Molecular target	Successful use of this class for prevention in animals	Clinical trials of this class of agent
Ligands for nuclear receptor			
Arzoxifene (SERM)	Oestrogen receptors	Breast cancer, prostate cancer	Successful (breast)
LG100268 (Rexinoid)	Retinoid X receptors	Breast cancer	Planned
GW7845 (SPARM)	Peroxisome proliferator-activated receptor-γ	Breast cancer	Planned
Ro24-5531 (Deltanoid)	Vitamin D receptor	Breast cancer, colon cancer prostate cancer	Planned
Anti-inflammatory agents			
Celecoxib	Cyclooxygenase-2	Colon cancer	Successful
Curcumin	Nuclear factor κB	Breast cancer, colon cancer	Planned
Chromatin modifiers			
SAHA	Histone deacetylase	Breast cancer	In progress
5-Aza-2'-deoxycytidine	DNA (demethylating agent)	Colon cancer, lung cancer	Drug too toxic at present

1.2 <u>Cancer chemoprevention by natural products</u>

Natural products have been used for the treatment of cancer throughout history. There are numerous reports of cancer chemopreventive activities of natural products. During the period from 1981 to 2002, it was reported that >60% of the approved drugs for cancer treatment are natural products or derived from natural products.[9] These compounds not only serve as drugs or templates for drugs directly, but in many instances lead to a better understanding of cellular pathways involved in the disease process.[10] For example, signal transduction pathways (cyclooxygenase-2, activator protein-1 and mitogen-activated protein kinases, are now recognized as potential molecular targets for chemoprevention by natural products.[11, 12]

Although natural products have great potential in cancer prevention, to move from a crude starting material such as a plant extract to a prescription drug which is effective as a cancer chemopreventive agent is a time-consuming and expensive process. In order for natural product drug discovery to continue to be successful, sensitive and robust approaches are required. In particular, developing high-throughput screening approaches for natural product chemoprevention drug discovery would help re-establish natural products as a major source for drug discovery.[13]

1.3 <u>Application of liquid chromatography-mass spectrometry to drug discovery and development</u>

Over the past decade, the combination of high-performance liquid chromatography and mass spectrometry (LC-MS) has become broadly used in all sectors in drug discovery and development. The analytical figures of high sensitivity, selectivity, reproducibility, and accessibility provide a powerful platform for analysis. Drug discovery and development consists of four distinct stages: (1) drug discovery; (2) preclinical development; (3) clinical development; and (4) manufacturing. Table II is a brief summary of these four stages of drug development. Significant events are highlighted with respect to their relationship to mass spectrometry.[14]

TABLE II

THE FOUR STAGES OF DRUG DEVELOPMENT, THEIR CORRESPONDING

MILESTONES AND ANALYSIS REQUIREMENTS.[14]

Development Stage	Milestone	Analysis emphasis	LC-MS analysis activities
Drug discovery	Lead candidate	Screening	Protein target identification; natural product identification; metabolic stability profiles; molecular weight determination for combinatorial/ medicinal chemistry support
Preclinical development	IND/CTA filing	Evaluation	Impurity, degradant, and metabolite identification
Clinical development	NDA/MAA filing	Registration	Quantitative bioanalysis; structure identification
Manufacturing	Sales	Compliance	Impurity and degradant identification

1.3.1 <u>LC-MS applications in drug discovery</u>

Since the early 1990s, drug discovery research focused on high-throughput screening and combinatorial chemistry has altered the traditional serial process of lead identification and accelerated the pace of drug discovery.[15, 16, 17] The determination of structure and purity of compounds used for high-throughput screening, whether discrete compounds or combinatorial library mixtures, is typically carried out using mass spectrometry. The molecular mass, fragmentation patterns and high-resolution mass spectra which are necessary for the determination of elemental compositions can be provided by high performance quadrupole time-of-flight (QqTOF) and ion trap-TOF (IT-TOF) tandem mass spectrometers.

Combinatorial chemistry has also created a need for rapid and predictive methods for screening thousands of compounds for receptor binding to identify lead compounds.[18, 19] To address this requirement, a number of mass spectrometry-based screening assays have been developed that are suitable for screening complex mixtures including natural product extracts. These methods, which include pulsed-ultrafiltration mass spectrometry, frontal affinity chromatography mass spectrometry, and size-exclusion chromatography mass spectrometry, may ultimately prove to be quite successful for both early discovery as well as lead development.[20] Ultrafiltration mass spectrometry was invented and developed in the van Breemen laboratory for the screening of combinatorial library mixtures and natural product extracts in order to identify ligands to macromolecular targets, such as adenosine

deaminase,[21, 22] dehydrofolate reductase,[23] cycloxygenase-2,[24] serum albumin,[25] estrogen receptors (ER),[26] and retinoid X receptor α.[27]

There is no doubt that ADME/Tox drug properties are crucial to the clinical success of a drug candidate. High-throughput assays to assess absorption, distribution, metabolism, elimination, and toxicity of lead compounds are being developed and implemented earlier than ever during the drug discovery process to provide an early perspective of clinical success.[28] Again, LC-MS has emerged as an advantageous technique for drug development.

Metabolic stability studies in the drug discovery process are often aimed at locating the metabolic soft spots in the structure that may increase the rate of intrinsic metabolic clearance resulting in low oral bioavailability. Preliminary metabolite characterization is usually performed when a compound is determined to be optimally stable in *in vitro* systems. It is important to characterize major metabolites and to establish whether there are significant metabolic differences between species and to identify potential pharmacologically active, reactive, or toxic metabolites.[29] The structures of these putative metabolites are then determined using product ion MS/MS and MS^n experiments.[30] Precursor ion scanning and constant neutral loss scanning are particularly useful for revealing structural features of unknown metabolites. Product ion scanning may then be used to obtain detailed structure information of drug metabolites. Modern LC-MS instruments, such as linear ion trap systems, offer very high scan speeds such that multiple MS/MS experiments may be carried out on the

TABLE III

COMMON DRUG METABOLISM BIOTRANSFORMATIONS AND THEIR

CORRESPONDING ELEMENTAL COMPOSITIONS AND MASS CHANGES. [32]

Metabolic reaction	Molecular formula change	*m/z* change
Debenzylation	$-C_7H_6$	-90.0468
Tert–butyl dealkylation	$-C_4H_8$	-56.0624
Decarboxylation	$-CO_2$	-43.9898
Isopropyl dealkylation	$-C_3H_6$	-42.0468
Hydroxymethylene loss	$-CH_2O$	-30.0106
Deethylation	$-C_2H_4$	-28.0312
Decarboxylation	$-CO$	-27.9949
Dehydration	$- H_2O$	-18.0105
Demethylation	$- CH_2$	-14.0157
Hydroxylation+dehydration	$-H_2$	-2.0157
Alcohols to aldehyde/ketone	$-H_2$	-2.0157
Desaturation	$-H_2$	-2.0157
Ketone to alcohol	$+H_2$	2.0157
N, O, S methylation	$+CH_2$	14.0157
Hydroxylation	$+O$	15.9949
Hydration, hydrolysis	$+H_2O$	18.0106
Hydroxylation and methylation	$+CH_2O$	30.0105
2×hydroxylation	$+O_2$	31.9898
Acetylation	$+C_2H_2O$	42.0106
3×hydroxylation	$+O_3$	47.9847
Glycine conjugation	$+C_2H_3NO$	57.0215
Sulfation	$+SO_3$	79.9568
Cysteine conjugation	$+C_3H_5NOS$	103.0092
Decarboxylation and glucuronidation	$+C_5H_8O_5$	148.0372
Glucuronic acid conjugation	$+C_6H_8O_6$	176.0321
GSH conjugation	$+C_{10}H_{17}N_3O_6S$	307.0839
2×glucuronic acid conjugation	$+C_{12}H_{16}O_{12}$	352.0642

parent drug, as well as putative metabolites, during a single analysis.[31] The development of high-resolution MS instrumentation such as QqTOF, IT-TOF and Orbitrap mass spectrometers and advances in data processing techniques have also enhanced the quality and productivity of drug metabolite identification. Common drug biotransformations and corresponding mass changes are listed in Table III[32]

1.3.2 LC-MS applications in preclinical drug development

Preclinical development activities are routinely initiated during the mid-to-late stages of drug development to provide more specific and detailed information regarding metabolism, bioavailability and pharmacokinetics of drug leads. LC-MS-based quantitative analysis of the drug and drug-related substances in support of pharmacokinetics is intensely used during pre-clinical and clinical stages of development due to its high sensitivity and selectivity. Quantitative LC-MS assays generally involve four steps: sample preparation, assay calibration, sample analysis, and data management. Triple quadrupole mass spectrometers used with selected reaction monitoring (SRM) provide a high degree of selectivity and better limits of quantitation (LOQ) than scan modes or selected ion monitoring (SIM) for the analysis of complex mixtures.[33]

As the drug candidate moves further into development, *in vivo* animal ADME studies are performed, and safety assessment is carried out in multiple species. The most widely used approach for metabolite profiling and identification in drug development involves administration of radiolabeled drug. The determination of

metabolite structures using LC-MS and LC-MS/MS is an ideal match of the high sensitivity and selectivity of mass spectrometry with the trace levels of drugs and drug metabolites in complex biological samples. With the continuing technological improvements, mass spectrometry has impacted not only the discovery phase, but also the development phase of new drugs by facilitating both qualitative and quantitative analysis of trace levels of drugs and their metabolites.

1.4 <u>Hepatic drug metabolism</u>

ADME/Tox drug properties (absorption, distribution, metabolism, elimination, and toxicity) are crucial to the clinical success of a drug candidate. Drug metabolism is the process by which drug molecules are chemically altered, usually to more polar metabolites that exhibit increased water solubility, to facilitate their excretion in urine and bile.[34] The major reason to evaluate the metabolism of a drug candidate is to understand how metabolic processes terminate or limit its desired pharmacological effects (efficacy) as well as how other processes may lead to unintended consequences (toxicity).

Many organs in the body are involved in drug metabolism including kidneys, skin, lungs, and intestine.[35] However, the liver is the most metabolically active tissue in which the majority of drug metabolism takes place. After oral absorption, drugs are transported via the portal vein to the liver. Along with drug-metabolizing enzymes and drug transporters, the liver provides an effective barrier that prevents xenobiotics from entering the systemic circulation.

Drug metabolism may be divided into two types of reactions, Phase I and Phase II. Phase I reactions include oxidation, reduction and hydrolysis, while Phase II conjugation reactions include glucuronidation, sulfation, acetylation, and methylation, amongst others. Some drugs just undergo one or the other but the majority will undergo both Phase I and then Phase II reactions sequentially.

1.4.1 <u>Drug-metabolizing enzymes</u>

Phase I drug-metabolizing enzymes typically convert hydrophobic endogenous and exogenous compounds into more hydrophilic metabolites by introducing polar functional groups (-OH, -SH, -NH$_2$, or –COOH). These enzymes primarily include cytochromes P450 (CYP450) and flavin-containing monooxygenase (FMO). Phase II reactions lead to the formation of a covalent linkage between a functional group either on the parent compound or on one introduced as a result of a Phase I metabolism. Phase II reactions involve conjugative enzyme families such as UDP-glucuronosyltransferases (UGTs), glutathione-*S*-transferases (GSTs), sulfotransferases (SULTs), *N*-acetyltransferases (NATs), and monoamine oxidases (MAOs).[36] Among the enzymes involved in the metabolism of drugs, the dominant players (~75%) are the P450 enzymes, followed by UGTs and esterases (shown in Figure 1). Together, these reactions account for ~95% of drug metabolism.[37, 38]
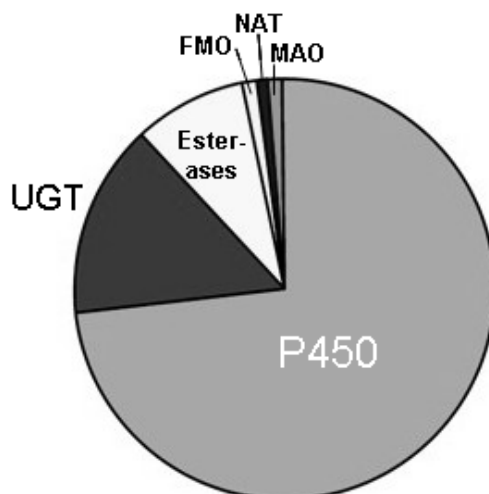
Figure 1 Fractions of drugs metabolized by various enzyme systems. [37]

1.4.1.1 **Phase I metabolic enzymes**

The P450 enzyme superfamily is a broad class of heme *b*-containing monooxygenase enzymes that dominate Phase I biotransformation in the liver. The vast majority of P450s catalyze reductive scission of molecular oxygen using electrons usually derived from coenzymes NADH and NADPH and delivered from redox partner proteins.[39] According to amino-acid-sequence homology, the P450 superfamily is classified into families, subfamilies and specific enzymes. Among the 57 functional CYP genes in humans, three families of CYPs (CYP1, CYP2 and CYP3) predominate in the oxidative metabolism of more than 90% of clinical drugs. Among various P450 isoforms, CYP3A4 is responsible for the majority of xenobiotic metabolism: almost 50% of known pharmaceuticals. CYP1A2 (4%), CYP2A6 (2%), CYP2C9 (10%), CYP2C19 (2%), CYP2E1 (2%), and CYP2D6 (30%) are the next most important P450 isoforms.[40, 41]

Genetic polymorphisms within P450s have a functional impact on the efficacy and adverse effects of drugs that are mainly eliminated by those particular enzymes. CYP2D6, CYP2C19 and CYP2C9 polymorphisms account for the most frequent variations in Phase I metabolism of drugs, since almost 42% of drugs in use today are metabolized by these enzymes. For example, CYP2D6 poor metabolizers are present in approximately 5-14% of Caucasians, 0-5% Africans, and 0-1% of Asians.[42] The genetic polymorphisms in the CYP family may have the most impact on variations of the fate of therapeutic drugs in individuals.

Like P450 reactions, FMO-catalyzed reactions are mixed-function oxidations and involve oxidation of heteroatoms, particularly nucleophilic atoms such as the nitrogen of amines.[43] FMOs have been implicated in the metabolism of a number of pharmaceuticals, pesticides and toxicants. Five mammalian forms of FMO are found in humans. FMO3 is the most abundant form in human liver. Polymorphism involves defects in FMO3 and results in deficient metabolism of trimethylamine and a resulting "fish-odor syndrome".[44]

Monoamine oxidases catalyze the oxidative deamination of monoamines. They are found in the outer mitochondrial membrane of liver and some neurogenic tissues. In humans, there are two types of MAO: MAO-A and MAO-B.[45,46]

Aldehyde oxidase and xanthine dehydrogenase are both molybdenum cofactor (Moco) containing enzymes. Xanthine is a substrate for xanthine dehydrogenase but not aldehyde oxidase; purines are substrates for both.[47] Alcohol dehydrogenases

(ADHs) are a group of dehydrogenase enzymes that occur in many organisms and facilitate the interconversion between alcohols and aldehydes or ketones. ADHs play the major role in the metabolism of ethanol in humans. Aldehyde dehydrogenases (ALDHs) are responsible for the oxidation of aldehydes to carboxylic acids. A number of polymorphisms have been identified that result in attenuation of catalytic activity.[48] Aldo-keto reductases (AKRs) constitute a large family of enzymes involved in reduction of various aldehydes and ketones. Epoxide hydrolase catalyzes the addition of H_2O to epoxides and functions in detoxication during drug metabolism.

1.4.1.2 Phase II metabolic enzymes

The UGTs are a superfamily of membrane-bound enzymes that catalyze the conjugation of glucuronic acid to a nucleophilic substrate.[49, 50, 51] Reactions can occur on phenols and aliphatic alcohols, carboxylic acids, primary, secondary, and tertiary amines, and even acidic carbon atoms.[50, 52] There are a large number of endogenous substrates for the UGTs. These include bilirubin, androgens, estrogens, progestogens, and glycolipids.[53] While the liver appears to be the major organ involved in glucuronidation, some UGT isoforms exist at high levels in the kidney and intestine, suggesting that extrahepatic glucuronidation can be significant.[51]

There are three subfamilies of UGTs in humans: UGT1A, 2B, and 2A. Like the P450 gene family, the UGTs can be altered by induction, inhibition and genetic variability.[50] This suggests that many drugs which are substrates for glucuronidation as part of their metabolism are significantly affected by inhibitors or inducers of their

specific UGT types. Genetic polymorphisms have been identified in all of the UGT enzymes that have been extensively evaluated. The most well-known polymorphism occurs in UGT1A1.[52]

The cytosolic sulfotransferase (SULTs) family catalyzes the transfer of a sulfonyl moiety from the cofactor 3'-phosphoadenosine-5'-phosphosulfate (PAPS) to hydroxyl, amino, sulfhydryl, and *N*-oxide groups of their substrates. The reaction is called sulfonation or sulfation.[54] Sulfonation results in inactivation of the majority of acceptors, including neurotransmitters, steroid hormones, and drugs, and is usually a detoxification pathway. The conjugated product has greater water solubility and is therefore excreted more readily from the body. In humans, 13 different SULT genes have been identified, and many SULTs have overlapping substrate specificity. Several chemicals are known to inhibit SULTs, and this leads to numerous drug–drug and food–drug interactions.[55, 56]

Glutathione-S-transferases (GSTs) activate the thiol of glutathione (GSH) into the more reactive thiolate anion within the active site, and thereby catalyze the reaction of glutathione with electrophiles to form glutathione conjugates. The major biological function of GSTs is believed to provide defense against electrophiles. Reactive metabolites of drugs formed by the cytochrome P450 system can be substrates for the GSTs, and this has been used in an analytical assay for identifying chemical species that have potential cytotoxicity and for detecting electrophilic metabolites.[57, 58]

One of the more common acetylation reactions is *N*-acetylation which is involved in the detoxification of a large number of arylamine and hydrazine drugs and chemical carcinogens. Arylamine *N*-acetyltransferases (NATs) are Phase II xenobiotic metabolizing enzymes, catalyzing acetyl-CoA-dependent acetylation reactions.[59] Human arylamine *N*-acetyltransferases are expressed as two polymorphic isoforms, NAT1 and NAT2, with sulfamethazine being selectively *N*-acetylated by NAT2 and with *p*-aminobenzoic acid being a specific substrate for NAT1. NAT1 is expressed in many other tissues, whereas NAT2 is expressed only in the liver and intestine.[60, 61] Individuals are classified as fast or slow acetylators depending on the variable rate of metabolism of certain drugs including isoniazid and hydralazine. The difference in acetylation rates in humans is one of the first genetic polymorphisms to be discovered.[62] Both NAT1 and NAT2 have been found to be polymorphic in human populations. Slow acetylator status has been associated with increased rates of adverse reactions to arylamine antibiotics, such as sulfamethoxazole.[63]

1.4.2 *In vitro* metabolic models

It has been estimated that nearly 50% of candidate drugs fail during development because of unacceptable efficacy, the major contributions being drug-drug interactions and metabolic stability.[64, 65] In order to speed up development and limit the number of late-stage failures of new chemical entities, reliable and relevant models with strong predictive power for human metabolism need to be established and implemented at an early stage.[66] *In vitro* drug metabolism studies

including the evaluation of metabolic stability, identification of metabolic pathways, identification of drug metabolizing enzymes, and evaluation of drug-drug interactions could make reliable predictions for clinical practice.

A number of different tissue matrices can be employed to study drug metabolism. These fall into four groups: organs, cells (primary cultures and cell lines), subcellular fractions (S9, cytosol and microsomes), and isolated enzymes (purified and recombinant systems).[67] The availability of materials, expense, ethical considerations, and *in vivo* relevance are factors that were used to determine the optimal model system for this dissertation.[68]

1.4.2.1 <u>Liver microsomes</u>

Human liver microsomes (HLM) are the most popular *in vitro* model currently in use due to their relevance, affordability and ease of use. Liver microsomes consist of vesicles of the hepatocyte endoplasmic reticulum, predominantly expressing Phase I enzymes, *e.g.*, CYPs, and some Phase II enzymes, *e.g.*, UGTs.[67] Therefore, by supplementing the microsomes with the appropriate cofactors, liver microsomes can be used to evaluate metabolic stability and *in vitro* intrinsic clearance, to identify reaction phenotyping, and to evaluate drug candidates as inhibitors of CYP and UGT enzymes. Liver microsomes from humans and toxicologically relevant species are also widely used for metabolic profiling.

However, there are several limitations regarding the use of liver microsomes as an *in vitro* model. First, the enriched CYPs and UGTs in the microsomal fraction can result in higher biotransformation rates than might be observed using intact cells or tissues. Secondly, because of the absence of other enzymes and cofactors, not all cellular metabolites might be formed using this *in vitro* model. These limitations make microsomes useful for qualitative but not quantitative prediction of *in vivo* human biotransformation.

1.4.2.2 Liver cytosol fractions

Liver cytosol is prepared from liver homogenate by differential centrifugation. The liver cytosolic fraction is comprised of the soluble Phase II enzymes including *N*-acetyl transferase, glutathione *S*-transferase and sulfotransferase. The primary use of this system is to determine what drug metabolites might be formed by the action of each of these soluble enzymes. Specific enzymes can be activated by adding specific exogenous cofactors, *e.g.*, acetyl coenzyme A for NAT; adenosine-3'-phosphate-5'-phosphosulfate (PAPS) for SULT; and glutathione for GST. Since there are only three major drug metabolizing enzyme types present in the liver cytosol, the contribution of soluble Phase II enzymes to drug metabolism can be studied separately or in combination depending on the cofactors added.

1.4.2.3 Liver S9 fractions

The liver S9 fraction is prepared by homogenizing the liver, disrupting the cells and then centrifuging at 9000g to obtain the supernatant. This fraction contains both cytosol and microsomes.[69] Compared with microsomes or cytosol, S9 fractions offer a more complete metabolic profile of drugs. Addition of exogenous cofactors to the respective incubation mixtures is necessary to ensure adequate reaction rates. Since the S9 fraction has lower enzyme activities than microsomes, it not used as often as microsomes for hepatic metabolism studies.

1.4.2.4 **Hepatocytes**

Hepatocytes are isolated from livers by a procedure called two-step collagenase digestion.[70] Compared with subcellular fractions, hepatocytes have an intact biological membrane and a complete set of all metabolic enzymes, receptors and cofactors needed for metabolic reactions at physiological concentrations. For long-term storage and convenient use of the isolated hepatocytes, cryopreservation procedures have been developed. Cryopreserved hepatocytes retain both Phase I and Phase II drug metabolizing enzyme activities and are stable for at least one year.[71, 72] Therefore, hepatocytes represent a physiologically relevant experimental model for the evaluation of liver-related human drug properties such as hepatotoxicity, metabolism and drug-drug interaction potential.[73] However, cryopreserved hepatocytes are comparatively expensive and require more complex incubation media than liver microsomes, S9 fraction or recombinant enzymes. Like human liver

microsomes, the problem of inter-individual variation can be overcome by using mixtures of hepatocytes from multiple donors.

1.4.2.5 <u>Liver slices</u>

The development of high-precision tissue slicers and dynamic organ culturing have made liver slices practical for *in vitro* biotransformation studies.[74, 75] One of the main advantages of liver slices is the maintenance of the intact tissue architecture of the liver so that they more closely mimic the *in vivo* enzyme environment than cell fractions or isolated enzymes. This makes it possible to probe the consequences of drug-drug interactions in the cellular environment of an intact isolated tissue. Also, subcellular fractions may be isolated from the same liver slices for direct comparative metabolic profiling.[76] Although liver slices are a relatively new addition to the in vitro assays of drug metabolism, their use has been limited due to inadequate penetration of the medium into the inner part of the slice, lack of optimal incubation methods and difficulties in storage and handling.

1.4.2.6 <u>Recombinant enzymes</u>

The availability of specifically expressed recombinant enzymes such as human CYPs, UGTs and NATs facilitates investigation of the contribution of individual metabolic enzymes to the overall biotransformation pathway. The advantages of using recombinant enzymes include the lack of interfering enzyme activities present in microsomes or other crude enzyme preparations and the flexibility to control and

optimize reaction components, especially for multi-enzyme systems. Easy to use and well characterized preparations of all major isoforms are now commercially available. The identification of the isozyme-specific drug biotransformation facilitate identification of metabolic structure-activity relationships (SAR) and predictions of drug-drug interactions.[77]

1.5 <u>Summary</u>

The specific aims of this dissertation are the discovery of new chemopreventive agents through high throughput screening and to initiate drug development studies of lead compounds including metabolism and disposition in different *in vitro* and *in vivo* models using LC-MS and LC-MS/MS. Ultrafiltration LC-MS will be used for screening and drug discovery because of its speed and selectivity, especially for the screening of natural product mixtures. Human liver microsomes, human hepatocytes and human liver cytosol will be used instead of S9 fraction, liver slices for initial studies of drug metabolism, because of their abilities to predict in *vivo* studies and their relevance, affordability and ease of use.

2. SCREENING FOR LIGANDS OF HUMAN RETINOID X RECEPTOR-α USING ULTRAFILTRATION MASS SPECTROMETRY

2.1 Introduction

2.1.1 Retinoid X receptor

Retinoid receptors are nuclear, ligand-regulated transcription factors of the steroid/thyroid hormone receptor superfamily.[78] There are two distinct classes of retinoid receptor, retinoic acid receptors (RAR) and retinoid X receptors (RXR), with three known subtypes within each class (α, β, γ).[79] RARs and RXRs are distinguished by their differential affinities for naturally occurring ligands. Although 9-*cis*-retinoic acid (9cRA) is a ligand for both groups, only RARs bind all *trans*-retinoic acid (see structures in Figure 2).[80]

Nuclear receptors are cellular proteins that control gene expression[81] and regulate cell functions such as growth, differentiation, apoptosis and metabolism.[82] There are 48 nuclear receptors,[83] all of which share a similar structural organization.[84, 85] The preferred binding partner for one-third of the nuclear receptors is retinoid X receptor. Because of this property, this protein has been called the "master partner."[86, 87] RXR forms three different types of dimmers: RXR homodimer, permissive heterodimers and nonpermissive heterodimers. RXR homodimers and RXR permissive heterodimers, including dimers with peroxisome proliferator-activated receptors, liver X receptors (LXRs), and pregnane X receptor (PXR), activate
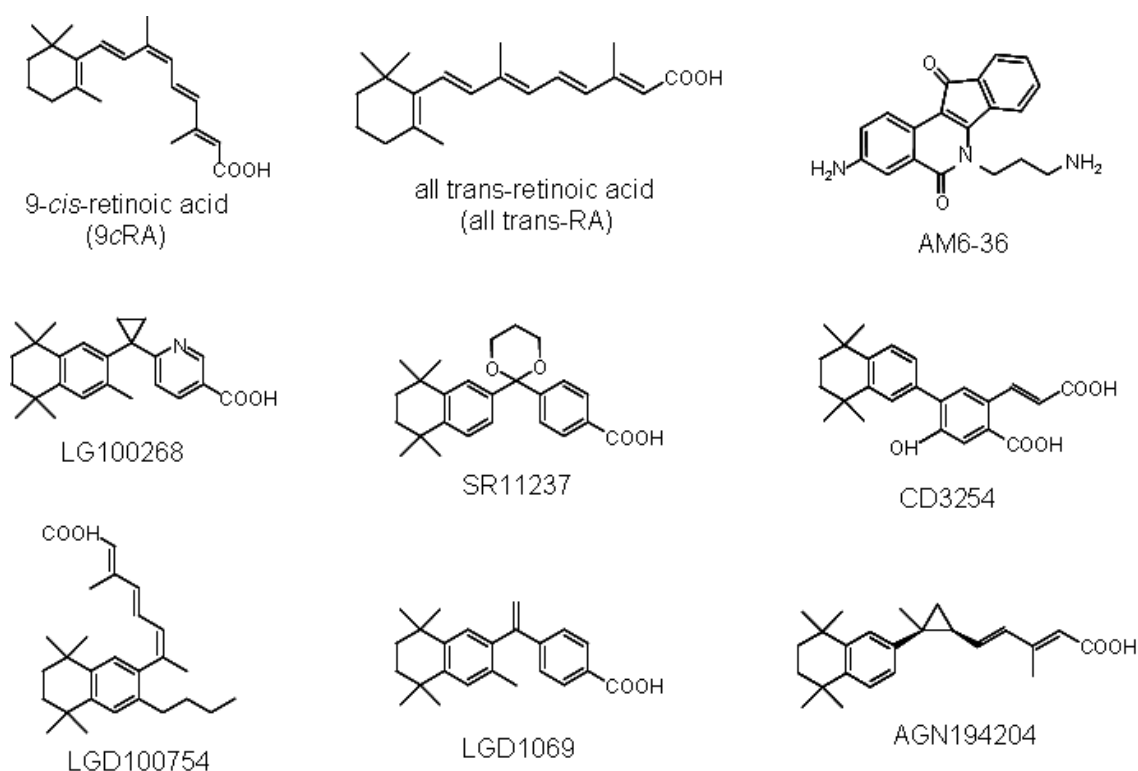
Figure 2 Structures of RXRα ligands and related test compounds used during this investigation.

transcription in response to RXR ligand binding because this class of dimer formation triggers a conformational change of the RXR that allows subsequent binding to the RXR. By contrast, nonpermissive heterodimers (*e.g.,* RAR, the vitamin D receptor and thyroid hormone receptors) can be activated only by the partner's ligand but not by an RXR ligand. In this situation, RXR serves as a silent binding partner because binding of nonpermissive heterodimers to the RXR does not permit ligand binding to the RXR.[78, 80, 88] Typical heterodimeric receptors such as RAR, or VDR can bind to their response elements as homodimers, but heterodimerization with RXR strongly increases the efficiency of DNA binding and transcriptional activity. Because RXRs

are obligate heterodimerization partners for a multitude of nuclear receptors, RXRs have the potential to regulate the activity of entire regulatory networks.

There are three isoforms of the RXR: α, which is mainly found in the kidney, liver and intestine, and is the major isotype found in the skin; β, which can be detected in nearly every tissue; and γ, which is found in the pituitary gland, brain and muscles.[89-93] Literature reports suggest that there is overlap between the functions of the three isoforms, but malfunction of RXRα has far worse consequences than those of the other two types. For example, knockout mouse studies showed that absence of the α isoform is fatal to fetal life, produces cardiac failure, and ocular malformations. Inactivation of the α type has an effect similar to the one observed in vitamin A-deficient fetuses, implying that this isoform is key for retinoid signaling.[78]

Similar to other nuclear receptors, RXRs require specific ligands to be functionally activated. The ligand-free RXR homodimers bind to DNA response elements (RXRE) and recruit corepressor protein complexes. Upon ligand binding, the RXRs undergo conformational changes that lead to dissociation of corepressor proteins and binding of coactivator proteins, triggering transcription. This up-regulates, for example, the production of cyclin-dependent kinase inhibitor (p21$^{\text{WAF1/CIP1}}$). Several reports have suggested that p21$^{\text{WAF1/CIP1}}$ upregulation causes apoptosis of cancer cells.[94] The RXR ligand mediated responses have also demonstrated the ability to influence metabolic processes, cellular differentiation and proliferation. Consequently, compounds that bind to an RXR and activate the RXRE

may function as chemopreventive agents. This effect is observed when an RXR is activated by one of its ligands, 9cRA. Various reports have documented the chemopreventive effects of 9cRA by itself or when combined with other substances.[95-98] However, therapies based on 9cRA or other retinoids are compromised by a variety of side effects caused by the requirement of large dosage, including headaches, alopecia, hypothyroidism, skin lesions, teratogenicity, and mucocutaneous toxicity.[99−105]

2.1.2 <u>Retinoid X receptor ligands and chemoprevention</u>

In an attempt to achieve the activation of multiple pathways, increase potency and reduce the toxicity of naturally occurring retinoids, RXR-selective ligands, known as rexinoids have been developed and have shown the potential to function as chemotherapeutic or chemopreventive agents[106-109] Although thousands of synthetic ligands are known for the retinoic acid receptors, a small number of synthetic ligands have been discovered for the RXRs, and these rexinoids include AGN194204, CD3254, LG100268, LGD1069, LGD100754 and SR11237 (Figure 2).[110] The chemopreventive efficacy of combinations of tamoxifen and a retinoid analog, 4HPR (fenretinide), have been shown in the prevention of contralateral disease in premenopausal women.[114] The combination of the rexinoid, LG100268 (Figure 2), and a selective estrogen receptor modulator, arzoxifene is synergistic in the prevention and treatment of mammary tumors.[115-117] The RXR selective retinoid, LGD1069 (bexarotene, Targretin), has been shown to prevent the development of

both estrogen receptor negative mammary tumors in transgenic mice without toxicity and estrogen receptor positive tumors in the methylnitrosourea (MNU)-induced rat mammary tumor model.[111-113] However, LGD1069 has been approved for drug use only for limited indications, namely topical and systemic treatment of cutaneous T cell lymphoma because of the significant adverse effects that may be due to the ability to activate the RARs.

2.1.3 Indenoisoquinolines

Topoisomerase I (Top1) is an essential enzyme that relaxes supercoiled DNA so that it may be replicated, transcribed and repaired.[118-121] As Top1 is overexpressed and DNA damage responses are defective in some human tumors, several Top1 inhibitors have been developed as chemotherapeutic agents.[121, 122] The alkaloid camptothecin[123] is not used clinically, but its derivatives topotecan and irinotecan are FDA-approved Top1 inhibitors.[118, 122, 124] Although potent, camptothecin derivatives suffer from many shortcomings, including poor solubility, dose-limiting toxicity, pharmacokinetic limitations resulting from the instability of the E-ring lactone under physiological pH, and binding of the lactone hydrolysis product to plasma proteins.[122, 125-127]

The indenoisoquinolines were therefore developed as therapeutic alternatives.[128, 129] Many optimization and SAR studies have produced indenoisoquinolines that are potent Top1 inhibitors with advantageous properties compared with camptothecins. AM6-36 is one of these synthetic indenoisoquinoline derivatives. Additional activities of indenoisoquinolines are also known, such as induction of cell-cycle arrest,

overcoming multidrug-resistance, and enhancement of the differentiation inducing activity of retinoids[130, 131] Therefore, some of the indenoisoquinolines were screened during this dissertation for binding of RXRα.

2.1.4 Ultrafiltration mass spectrometry

During ultrafiltration mass spectrometric screening, ligands in a mixture are allowed to bind to a receptor such as a protein therapeutic target, and then ultrafiltration is used to separate the receptor-ligand complexes from unbound low mass compounds.[21-27] The ligands are released by disrupting the ligand-receptor complexes using organic solvent, a pH change or other destabilizing conditions, and then analyzed using mass spectrometry or liquid chromatography-mass spectrometry. Control assays are carried out using inactive receptor or no receptor to test for non-specific binding to the macromolecule or the ultrafiltration membrane (Figure 3).
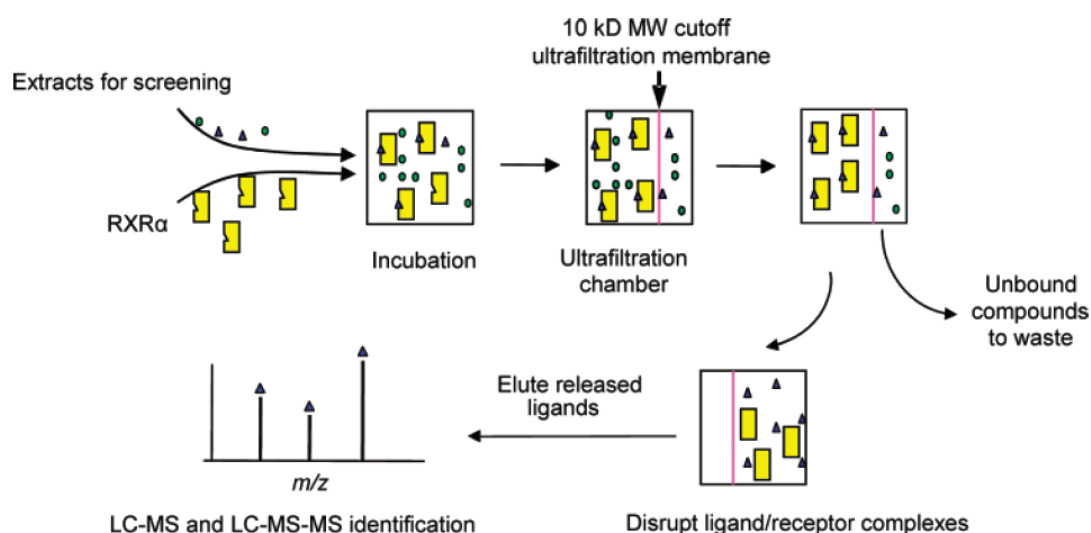
Figure 3 Experimental design of ultrafiltration LC-MS/MS screening of solutions for ligands to human RXRα.[27]

2.2 <u>Materials and methods</u>

2.2.1 <u>Materials</u>

Dulbecco's modified Eagle's medium (DMEM), fetal bovine serum (FBS), and antibiotics-antimycotics solution (100×) were purchased from Invitrogen (Carlsbad, CA). The translucent reporter vector carrying firefly luciferase under the control of RXRE (pRXRE) was purchased from Panomics (Fremont, CA). pBABE-puro vector encoding the cDNA for human RXRα (phRXRα) was purchased from Addgene Inc. (Cambridge, MA). *Renilla reniformis* luciferase vector (pRL) was purchased from Promega (Madison, WI).

The human RXRα ligand binding domain was expressed and purified by Prof. Michael Schimerlik at Oregon State University (Corvallis, OR). The RXRα was confirmed to be a homodimer by size-exclusion chromatography and mass spectrometry. Centrifugal ultrafiltration filters (Microcon YM-10) were purchased from Millipore (Bedford, MA). The RXR agonist LG100268 (Figure 2) was purchased from CVChem (Cary, NC). 9-*cis*-RA and all *trans*-RA were purchased from Sigma-Aldrich (St. Louis, MO). AM6-36 (Figure 2), its putative metabolites and other indenoisoquinolines were chemically synthesized in the laboratory of Dr. Mark Cushman of Purdue University (West Lafayette, IN). The purity of each synthetic indenoisoquinoline was determined to be >98% based on analysis using LC-MS. All organic solvents were HPLC grade or better and were purchased from Thermo Fisher (Hanover Park, IL). A Thermo Scientific (Rockford, IL) rapid equilibrium dialysis kit

was used according to the manufacturer's protocol to determine the dissociation constant for AM6-36 binding to RXRα.

2.2.2 <u>RXRE-luciferase reporter gene assay</u>

The RXRE-luciferase reporter gene assay was developed in the laboratory of our collaborator Dr. Pezzuto for the pre-screening of novel cancer chemopreventive and therapeutic agents capable of functioning as RXR agonists.[133] The ultrafiltration mass spectrometric assay serves as a secondary assay for the conformation of binding events. COS-1 African green monkey kidney fibroblast cells (1×10^4 cells/well) were plated in a 96-well culture plate and incubated in DMEM supplemented with 10% heat-inactivated FBS and antibiotics-antimycotics at 37°C in 5% CO_2 in a humidified incubator for 24 h. Then, 100 ng of pRXRE, 50 ng of phRXRα and 3 ng of pRL were transiently co-transfected into COS-1 cells in each well by using Lipofectamine 2000™ according to the manufacturer's protocol. After 24 h of transfection, cells were treated with compounds and further incubated for 24 h.   Cells were then lysed, and the RXRE transcriptional activities were determined by measuring the reporter luciferase activities using a dual-luciferase reporter assay system.

2.2.3 <u>Ultrafiltration mass spectrometric screening assay</u>

In preparation for ultrafiltration screening, 85 µL binding buffer consisting of 50 mM Tris-HCl (pH 7.5), 10% glycerol, 50 mM KCl, and 1 mM EDTA, 5 µL of a sample solution in DMSO, and 10 µL of RXRα (10 µM in binding buffer), were

mixed and incubated for 2 h at room temperature. The final concentration of the natural product extract in the incubation was 200 µg/mL and the final concentration of pure compounds in each incubation was 10 µM. LG100268 were used as a positive control in each batch of incubations.

Since the molecular mass of RXRα receptor is 27kD and the molecular mass of a homodimer is 54kD, 10,000 molecular mass cutoff filters were chosen for ultrafiltration analysis. After incubation, each mixture was filtered through a Microcon YM-10 centrifugal filter containing a regenerated cellulose ultrafiltration membrane with a 10,000 MW cutoff by centrifugation at 13,000 g for 10 min at 4 °C. The RXRα-ligand complexes were washed three times with 200 µL aliquots of 30 mM ammonium acetate (pH 7.5) followed by centrifugation again at 13,000g for 15 min at 4 °C to remove the unbound compounds. The washed RXRα-ligand solution (~10 µL) was transferred to a second filter where it was treated with 200 µL of 90% methanol in deionized water to disrupt the receptor-ligand complexes. The released ligands were then isolated from the denatured protein by centrifugation at 13,000g for 15 min. The solvent in the ultrafiltrate was evaporated under vacuum, and the ligands were reconstituted in 50 µL of methanol/water (80:20, v/v) containing 200 nM ketoconazole as an internal standard for analysis using LC-MS/MS as described below. For comparison, control analysis was carried out that was identical except for the use of denatured RXRα. All experiments were carried out under subdued light. Denatured RXRα was prepared by boiling the receptor at 90 ºC for 15 min.

2.2.4 Determination of equilibrium dissociation constant of AM6-36 from RXRα

Determination of the equilibrium dissociation constant of AM6-36 from RXRα was carried out using a rapid equilibrium dialysis kit. RXRα ligand binding domain (1 μM), spiked with different concentrations (0-100 μM) of AM6-36, was added to the sample chamber, and 350 mL of phosphate-buffered saline (containing 100 mM sodium phosphate and 150 mM sodium chloride, pH 7.4) was added to the buffer chamber. The plate was sealed and incubated at 37 °C on an orbital shaker at 100 rpm for 4 h. Note that 4 h incubation time was used since preliminary experiments indicated that AM6-36 binding to RXRα reached equilibrium by approximately 4 h. Aliquots (50 μL) were removed from the sample and buffer chambers and mixed with an equal volume of buffer or blank plasma, respectively. To each sample, 300 μL of ice-cold acetonitrile was added, and the matrix-matched samples were vortex mixed and incubated for 30 min on ice. After centrifugation at 13,000g for 15 min, the supernatants were removed, evaporated to dryness and then reconstituted in acetonitrile/water containing 0.1% formic acid (30:70, v/v) and 0.25 μM of ketoconazole (internal standard) prior to quantitative analysis using LC-MS/MS. The percentage of each compound bound to RXRα was calculated as follows:

% Free = (Concentration in buffer chamber/Concentration in RXRα chamber) × 100%

% Bound = 100% - % Free

The binding of AM6-36 (A) with RXRα (R) may be described by the equation,
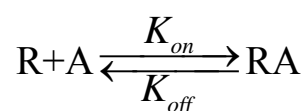
$$R+A \underset{K_{off}}{\overset{K_{on}}{\rightleftarrows}} RA$$

and the dissociation constant for this reaction is defined by the following equation:

$$K_\text{D} = \frac{K_{off}}{K_{on}} = \frac{[\text{R}][\text{A}]}{[\text{RA}]}$$

The binding coefficient is given by:

$$\text{Binding coefficient} = \frac{[Ligand]_{bound}}{[Protein]_{total}}$$

2.2.5 LC-MS/MS

Ultrafiltration screening of AM6-36 was analyzed using a Thermo Finnigan (San Jose, CA) TSQ Quantum triple quadrupole mass spectrometer equipped with a Waters 2695 HPLC. HPLC separations were carried out using a Waters (Milford, MA) Xterra 2.1×100 C_{18} column or a YMC (Wilmington, NC) C_{18} column (2.1×250 mm, 5 µm, 120 Å) with a mobile phase consisting of either a 12 min isocratic mobile phase of acetonitrile/aqueous 0.1% formic acid (40:60, v/v) or a 21 min linear gradient from 10-90 (v/v) aqueous methanol containing 0.01% formic acid at a flow rate of 200 µL/min. Positive ion electrospray ionization, collision-induced dissociation and selected reaction monitoring (SRM) were used to record the elution of each compound. The SRM transitions of *m/z* 364 to 254, *m/z* 320 to 303, *m/z* 301 to 159, and *m/z* 531 to 244 were monitored for LG100268, AM6-36, all *trans*-RA, and internal standard ketoconazole, respectively.

Quantitative analysis for dissociation constant determination was carried out on an Agilent (Santa Clara, CA) 6410 triple quadrupole mass spectrometer equipped with

an Agilent 1200 HPLC system. A Thermo Fisher (Bellefonte, PA) Hypersil GOLD 2.1×100 mm, 5 μm analytical column was used for chromatographic separations with a 6 min isocratic mobile phase consisting of acetonitrile/aqueous 0.1% formic acid (40:60, v/v) at a flow rate of 0.2 mL/min. Analytes were detected using positive ion electrospray, collision-induced dissociation and SRM at unit resolution. During SRM, the collision energy was 25 eV. The SRM transition of m/z 320 to m/z 303 and m/z 531 to m/z 489 was monitored for AM6-36 and the internal standard ketoconazole.

Ultrafiltration screening of indenoisoquinolines was carried out using UHPLC-MS-MS on a Shimadzu (Kyoto, Japan) Nexera UHPLC system interfaced with a Shimadzu LCMS-8040 triple quadrupole mass spectrometer. Analytes were separated on a Shimadzu Shim-pack XR-ODS III UHPLC column (2.0×50 mm, 1.6μm) using a 2.5 min linear gradient from 10-100% acetonitrile in 0.1% aqueous formic acid followed by re-equilibration at 10% methanol for 1.5 min. The flow rate was 0.5 mL/min. The mass spectrometer source parameters were as follows: DL temperature 300 °C, spray voltage 3500 V, nebulizing gas flow 3 L/min, and drying gas flow 20 L/min. LG100268 was detected using negative ion electrospray, collision-induced dissociation and SRM by recording the signal for the transition of the deprotonated molecule of m/z 362 to the most abundant fragment ion of m/z 318. Other analytes were detected using positive ion electrospray. The SRM transitions of m/z 531 to m/z 489, m/z 320 to m/z 303, m/z 319 to m/z 288, m/z 333 to m/z 288, m/z 348 to m/z 303, and m/z 420 to m/z 403 were monitored for ketoconazole, AM-6-36, MAR-VI-27, PVN-VI-36, PVN-VI-21, and PVN-VI-80, respectively.

2.3 Results

2.3.1 Ultrafiltration screening for RXRα ligands following RXRE-luciferase reporter gene assay pre-screening

Following screening of over 3,000 natural products and synthetic compounds using the RXRE-luciferase reporter gene assay, only one active lead was found, AM6-36 (see structure in Figure 2). As illustrated in Figure 4, AM6-36 greatly induced relative luciferase activities in a dose-dependent manner. Although the compound was less potent than 9-cis-RA, prominent induction was observed at higher concentrations (10 μmol/L, 4.1-fold; 15 μmol/L, 31.1-fold; and 20 μmol/L, 133.2-fold).[90]
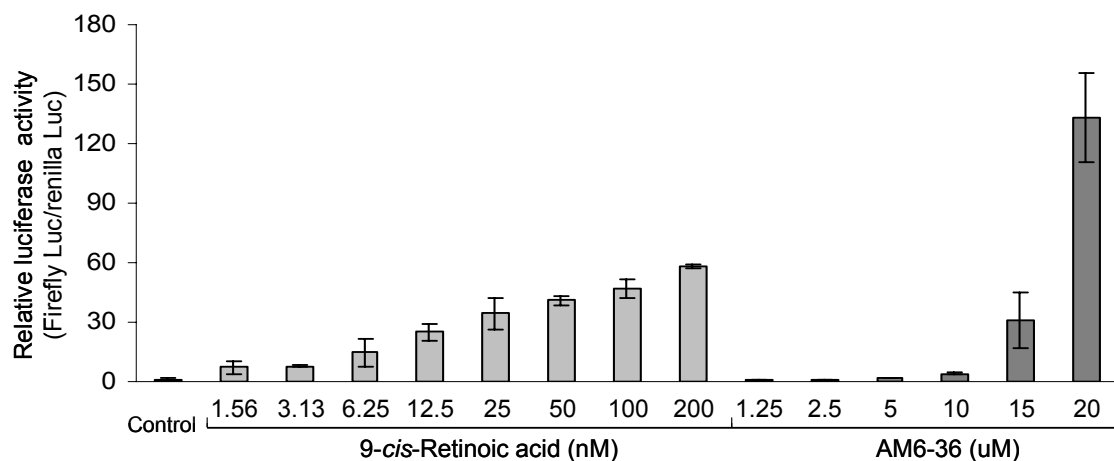
Figure 4 Effect of 9cRA and AM6-36 on RXR transcriptional activity.[90]

The active lead, AM6-36, was then investigated using ultrafiltration LC-MS. Figure 5 shows the LC-MS-MS analysis of an ultrafiltrate obtained following the incubation of LG100268, all trans-RA, and AM6-36 (10 μM) with 1 μM recombinant

human RXRα. The control incubations containing denatured RXRα were used to test for non-specific binding and adsorption of sample to the ultrafiltration apparatus. Enhancement of HPLC peak areas in the experimental incubations indicates specific binding of ligands to RXRα. As shown in Figure 5, LG100268, and AM6-36 showed enhanced peak areas relative to the control chromatograms.
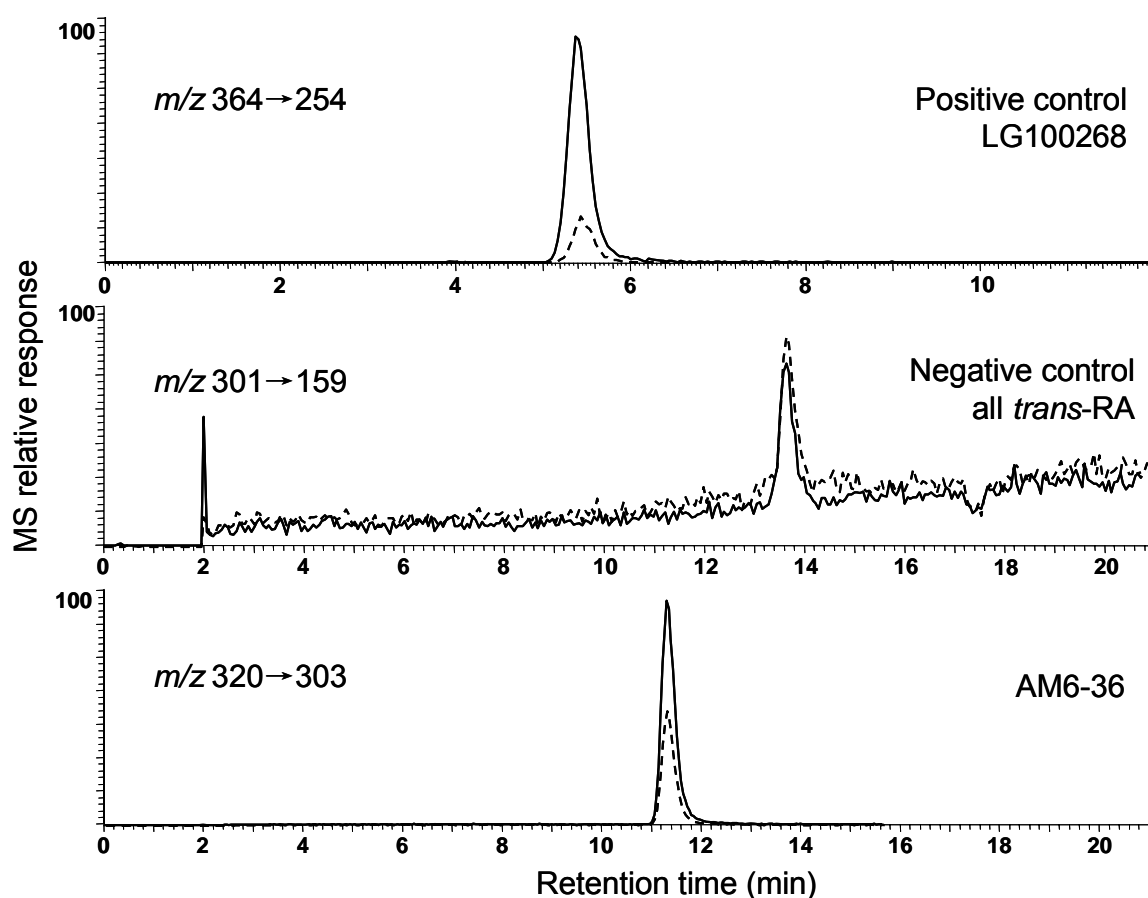
Figure 5 Ultrafiltration LC-MS testing of known ligand LG100268, negative control all trans-RA and AM6-36 for binding to RXRα. All compounds were tested at 10 μM. Binding of the test compound to RXRα produced peak enhancement (solid line) relative to the incubation using denatured RXRα (dashed lines).

2.3.2 Equilibrium dissociation constant of AM6-36 from RXRα

The maximum binding capacity (Bmax) and dissociation constant (K_D) for the binding between AM6-36 and RXRα were studied by equilibrium dialysis using the RXRα ligand binding domain. The binding constant was calculated by GraphPad Prism 6.0 (GraphPad Software, San Diego, CA) using a nonlinear regression model. Typical binding curves are shown in Figure 6. These experimental results indicate the existence of a single binding site. Since the saturation status cannot be reached within the range of tested concentration, the values for Bmax and K_D cannot be estimated.
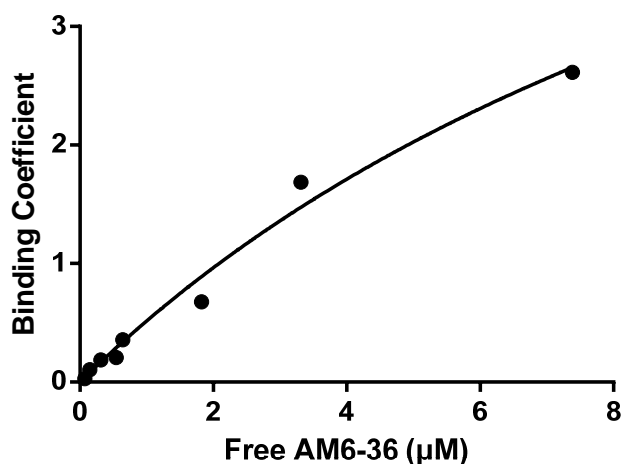
Figure 6 Saturation plot of equilibrium binding between AM6-36 and RXRα.

2.3.3 <u>Ultrafiltration screening of indenoisoquinolines for RXRα ligands following RXRE-luciferase reporter gene assay pre-screening</u>

On the basis of the unexpected yet unique ability of AM6-36 to serve as an RXR agonist, an SAR study was undertaken in order to validate the indenoisoquinolines as RXRα ligands and to understand their key structural features for RXR agonist activity. More than 100 indenoisoquinolines which had been synthesized in the laboratory of

Mark Cushman (Purdue University, West Lafayette, IN) were assayed using the RXRE-luciferase reporter gene assay, and 19 of these compounds were found to be active. The structures of these compounds and maximum induction ratios (IR) are shown in Table IV.

These 19 indenoisoquinolines were then screened for binding to RXRα using ultrafiltration LC-MS. The control incubations containing denatured RXRα were used to test for non-specific binding and adsorption of sample to the ultrafiltration apparatus. When specific binding to RXRα occurred, the peak area of the ligand was greater in the chromatogram corresponding to incubation with active RXRα than in the chromatogram of sample incubated with denatured RXRα. As shown in Figure 7, only 5 out of the 19 indenoisoquinolines that were active in the RXRE-luciferase assay showed binding to RXRα. These compounds, AM6-36, MAR-VI-27, PVN-VI-36, PVN-VI-21, and PVN-VI-80, showed enhanced peak areas relative to the control chromatograms. Examples of ultrafiltration LC-MS chromatograms of indenoisoquinolines that did not show binding to RXRα are shown in Figure 8. The specific binding (expressed as a binding ratio of the ligand peak area for the experiment to that of the control) may be used to rank ligands in order of their affinities for the receptor (Table IV). The maximum induction ratio is the highest point on the titration curve when compounds are tested at variable concentrations. The ranking obtained by the ultracentrifugation assay corresponds with the transcriptional activation results (Table IV).
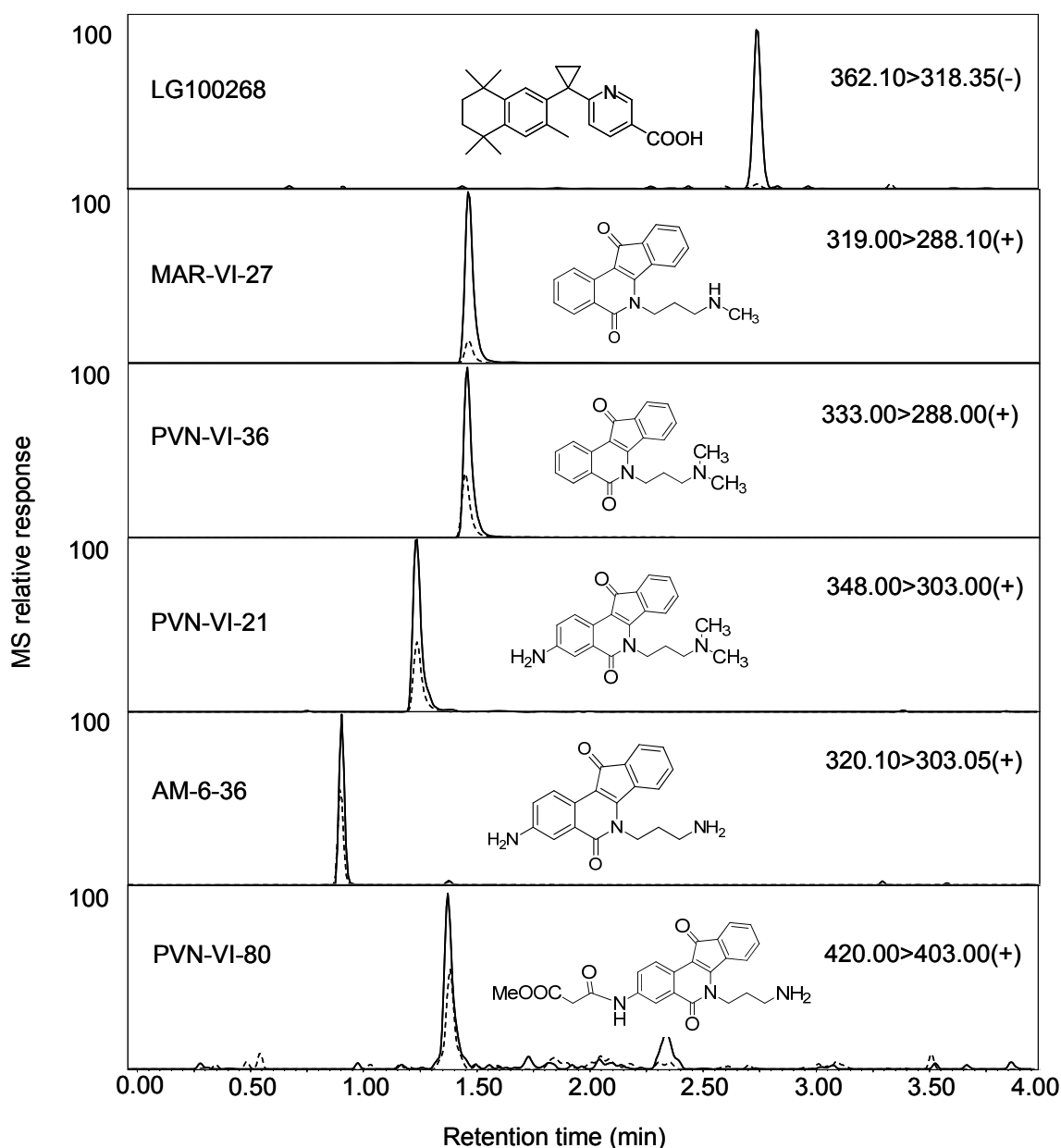
Figure 7 Ultrafiltration LC-MS testing of known ligand LG100268 and the indenoisoquinolines MAR-VI-27, PVN-VI-36, PVN-VI-21, AM-6-36, and PVN-VI-80 for binding to RXRα. Out of 19 indenoisoquinolines that were active in the RXRE-luciferase assay, only these 5 were confirmed to be ligands of RXRα using ultrafiltration LC-MS. Binding of the test compound to RXRα produced peak enhancement (solid line) relative to the incubation using denatured RXRα (dashed lines).
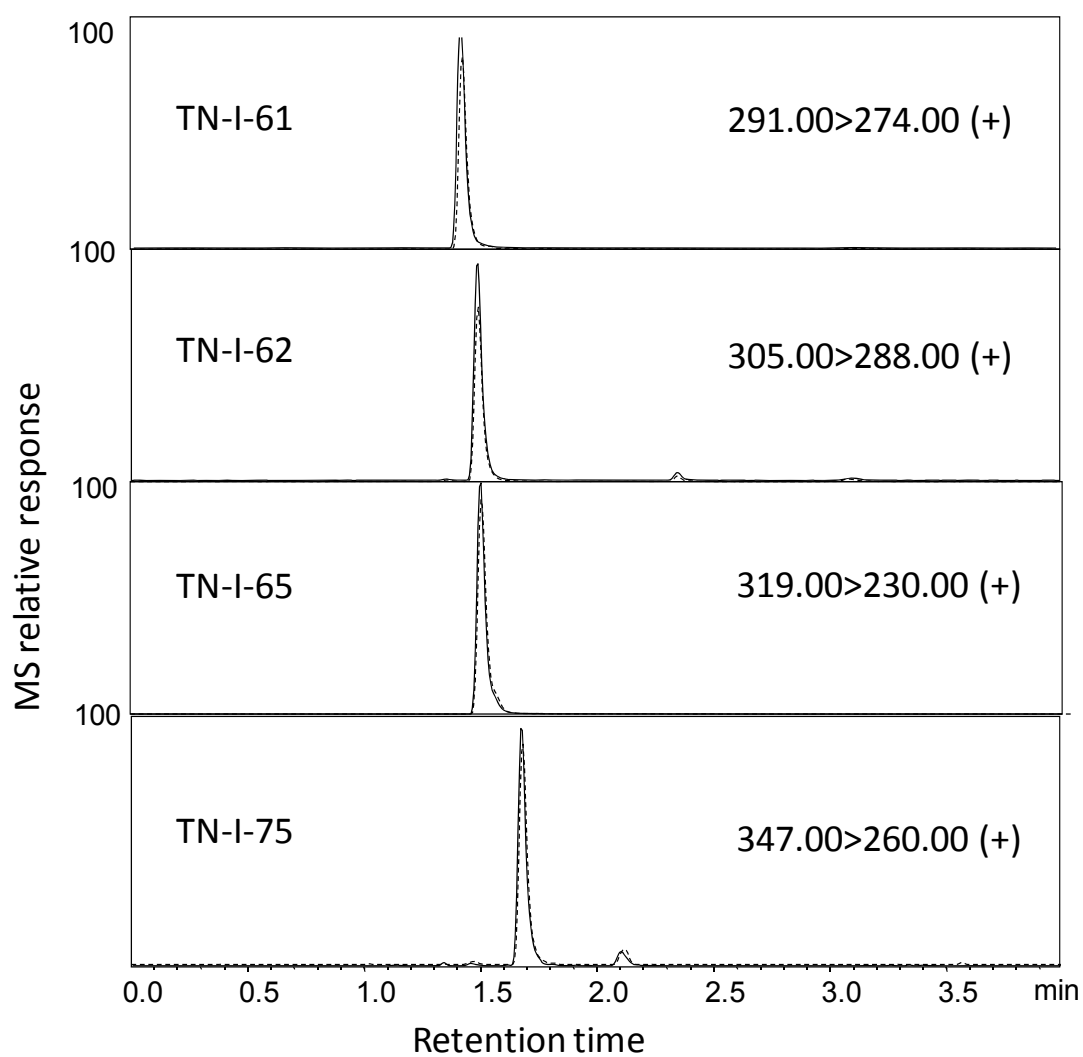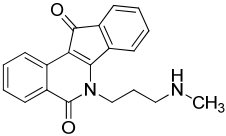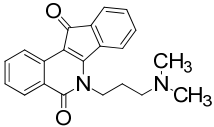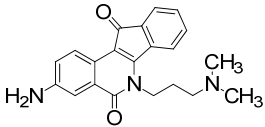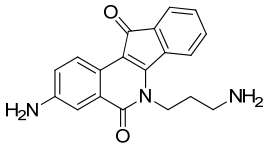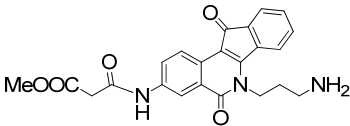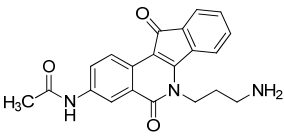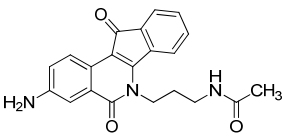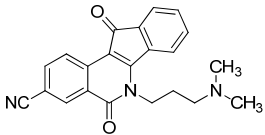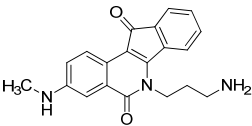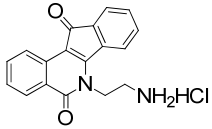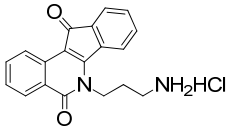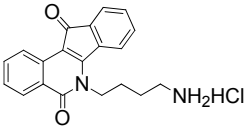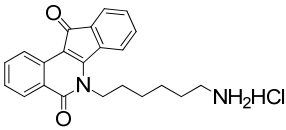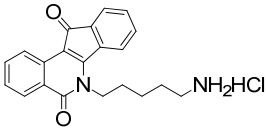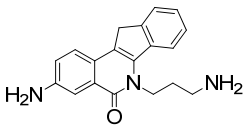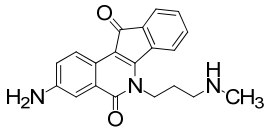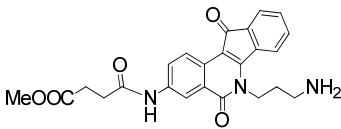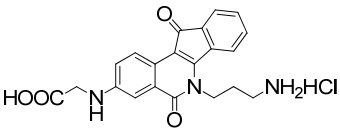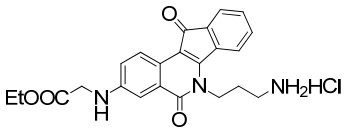
Figure 8 Examples of ultrafiltration LC-MS chromatograms of indenoisoquinolines that did not show binding to RXRα (see structures in Table IV). Binding of the test compound to RXRα produced peak enhancement (solid line) relative to the incubation using denatured RXRα (dashed lines).

TABLE IV

BINDING AFFINITY RANKING OF ACTIVE INDENOISOQUINOLINES

BASED ON ULTRAFILTRATION LC-MS AND LUCIFERASE ASSAY.

Compound	Structure	Max IR	Binding ratio	Binding affinity rank
MAR-VI-27		56.56	7.6	1
PVN-VI-36		31.13	2.6	2
PVN-VI-21		17.69	2.5	3
AM6-36		15.01	1.9	4
PVN-VI-80		4.34	1.7	5
MAR-V-80		18.75	-	-
MAR-VI-28		9.32	-	-
MAR-VI-73		7.14	-	-
MAR-VII-14		8.32	-	-

Compound	Structure	Max IR	Binding ratio	
TN-I-61		18.82	-	-
TN-I-62		35.31	-	-
TN-I-65		32.67	-	-
TN-I-75		37.44	-	-
TN-II-37		30.95	-	-
PVN-VI-15		20.87	-	-
PVN-VI-43		8.03	-	-
PVN-VI-48		10.87	-	-
PVN-VII-50		9.32	-	-
PVN-VII-51		10.00	-	-

1. Max IR: the maximum induction ratio observed when compounds are tested at variable concentrations.
2. Binding ratio: the ligand peak area for the experiment to that of the control.

2.4 <u>Discussion</u>

RXRs regulate the expression of genes that affect diverse physiological responses including proliferation, inflammation, differentiation, apoptosis, reproduction, bone development, hematopoesis, and embryonic development.[134] Receptor-selective rexinoids that have reduced toxicity are now being developed as potential chemopreventive agents. Unlike other nuclear receptors, RXRs are expressed in human carcinomas, and overexpression of RXR enhances the transcriptional response after binding of ligands.[135]

On the basis of these considerations, our chemoprevention discovery project utilized a RXR-specific response element (RXRE) reporter gene assay for the determination of RXR-mediated transcriptional responses in addition to demonstrating binding affinity towards RXR.[133] An RXR based ultrafiltration LC-MS assay served as a secondary assay for the confirmation of binding events.[27] During ultrafiltration mass spectrometric screening, the specific binding (expressed as a ratio of the ligand peak area for the experiment to that of the control) was used to rank ligands in order of their affinities for the receptor. The ranking obtained by the ultracentrifugation assay corresponded with the transcriptional activation results in this incvestigation. These results indicate that the ultrafiltration mass spectrometric screening assay functioned well for the screening for ligands of RXRα and facilitated the ranking of these ligands in order of affinity to RXRα.

RXR forms three different types of dimers; RXR homodimer, permissive heterodimers, and nonpermissive heterodimers. RXR, RAR and VDR roles in cancer regulation have many overlapping actions, such as the upregulation of the cyclin dependent kinase inhibitor p21.[92, 137] On the basis of DNA microarray analysis, AM6-36 upregulated the expression of CDKN1A, a target gene of RXR, by 35-fold. In accord with this response, the expression of the corresponding protein, p21[WAF1/CIP1], was increased in the presence of AM6-36.[133] Since both assays used for this discovery are expected to be due to the interaction of a test substance with RXR-RXR homodimers, further investigation was carried out to determine the potential of any lead, including AM6-36, to interact with other nuclear receptors.[136] Therefore, the ultrafiltration LC-MS testing of AM6-36 for binding to RAR and VDR were also investigated by Dr. Jerry White and Mr. Ke Huang to check for AM6-36 cross reactivity. RXR ligand AM6-36 was found to be a dual acting ligand binding to both RXR and VDR but not to RAR.[138]

Both RAR and VDR form nonpermissive heterodimers with RXR. In nonpermissive heterodimer complexes, the binding of the nonpermissive partner to the RXR receptor suppresses the RXR ligand-induced transcriptional activity of the RXR receptor; thus, RXR can be described as a "silent partner". However, if ligands for both receptors bind either to permissive or nonpermissive heterodimer complexes, these complexes are synergistically activated.[110] Therefore, AM6-36 was able to activate both partner receptors of RXR/VDR heterdimers synergistically as a dual acting ligand. In the case of RXR/RAR, because the RAR/RXR heterodimers bind to

the RARE with high affinity, the RAR/RXR heterodimer prevents RXR homodimer-mediated p21 promoter activation.[110] Binding of AM6-36 to RXR but not to RAR indicated that the upregulation of p21 by AM6-36 would not be prevented in the presence of RAR.

AM6-36 is one of a series of synthetic indenoisoquinoline derivatives initially synthesized as potential camptothecin-based topoisomerase I inhibitors. The indenoisoquinoline AM6-36 is an atypical rexinoid since it does not contain a carboxylic acid[104, 105, 139] and it does not structurally resemble a retinoic acid. In order to validate the indenoisoquinolines as RXRα ligands and to understand the key features for RXR agonist activity, an extensive SAR study was undertaken. Various novel precursors were functionalized and synthesized using different methodologies. New rexinoids, the indenoisoquinolines, have been identified and their potencies evaluated. These compounds present a novel scaffold, which can be functionalized to tune the properties of the new ligands. A novel motif, an aminopropyl side chain, has been identified as a key feature for RXR transcriptional activation. In comparison with known rexinoids, most of which contain carboxylic acids, the indenoisoquinoline rexinoids constitute a fundamentally different type of RXR ligand. The fact that indenoisoquinolines are structurally unique rexinoids offers the possibility of them having unique pharmacologic properties that could be clinically useful. Considering these factors as a whole, indenoisoquinoline rexinoids should be selected for further evaluation.

3. METABOLISM AND DISPOSITION OF AM6-36, A PROMISING LEAD FOR CANCER CHEMOPREVENTION

3.1 Introduction

The control of gene expression offers a powerful strategy for the prevention and treatment of disease. Human gene expression is regulated by 48 nuclear receptors, approximately one-third of which require heterodimerization with one of the ligand-activated retinoid X receptors to bind to DNA and function efficiently.[81] As a nuclear receptor, the retinoid X receptor (RXR) is involved in the regulation of multiple anti-cancer pathways including several of those involved in cell proliferation, differentiation and apoptosis. Ligand-mediated activation of the RXR is a strategy for cancer chemoprevention and therapy.

Following extensive screening for novel RXR ligands, we identified 3-amino-6-(3-aminopropyl)-5,6-dihydro-5,11-dioxo-11H-indeno[1,2-c]isoquinoline (AM6-36; Figure 2) as a ligand and agonist of RXR.[133] AM6-36 is an indenoisoquinoline, which is a class of compounds synthesized initially as potential topoisomerase I inhibitors.[140] We found that AM6-36 inhibited the proliferation of MCF7 breast cancer cells in a concentration-dependent manner accompanied by G2/M phase arrest at lower concentrations and enhanced S phase arrest at higher concentrations. A small collection of structural derivatives were also evaluated in the RXRE assay. AM6-36 mediated the strongest induction of RXRE transcriptional activity, as well as the strongest growth inhibitory effect with MCF7 cells. RXRα

transcriptional activity was upregulated with subsequent expression of RXR target gene *CDKN1A*. In accord with this response, the expression of the corresponding protein, p21$^{\text{WAF1/CIP1}}$, was increased in the presence of AM6-36. Strong indications of cancer chemopreventive potential were observed with HL-60 cells, 12-*O*-tetradecanoylphorbol-13-acetate (TPA)-treated JB6 Cl41 cells, and rats bearing mammary tumors. [133]

Because data suggest that AM6-36 is a promising lead compound for the treatment or prevention of breast cancer, drug development studies were carried out that included evaluation of intestinal permeability, metabolic stability, intestinal permeability, metabolic transformation by human liver microsomes and human hepatocytes, enzymes indentification, human plasma proteins binding, and preliminary disposition studies in rats.

The evaluation of the absorption, distribution, metabolism, excretion and toxicity (ADMEt) related properties of an investigational new drug are essential during preclinical drug development. Human liver microsomes are the most popular *in vitro* model currently in use for the investigation of xenobiotics metabolism due to their relevance, affordability and ease of use. But due to the absence of other enzymes and cofactors, not all cellular metabolites might be formed using this model. Human hepatocytes are another *in vitro* model developed. Since human hepatocytes contain both Phase I and Phase II enzymes as well as their co-factors such as NADPH and UDPGA, this model is more complete than human liver microsomes for the study of

hepatic drug-transformation reactions.[141] Metabolite structures were then predicted using high resolution LC-MS/MS and then identified by comparison with synthetic standards.

The liver cytosolic fraction is comprised of the soluble Phase II enzymes including *N*-acetyl transferase, glutathione *S*-transferase and sulfotransferase. The primary use of this system is to determine what drug metabolites might be formed by the action of each of these soluble enzymes. Human arylamine *N*-acetyl transferase (NAT) is encoded at two different loci. The enzyme encoded at one locus has a wide tissue distribution, is responsible for acetylation of *p*-aminobenzoic acid (PABA), and is termed NAT1. The second locus encodes an enzyme, which has a more restrictive tissue distribution with higher levels of expression in the liver and red blood cells, is responsible for the acetylation of sulfamethazine (SMZ), and is termed NAT2.[142] The NAT isoforms involvel in the generation of AM6-36 metabolite were identified using specific NAT inhibitors in a human liver cytosol model.

The degree of plasma protein binding (PPB) determines which fraction of the total plasma concentration of a compound is bound to plasma proteins, and therefore, not available for interaction with its biological target (receptors, enzymes, transporters, etc.). The effect of plasma protein binding on distribution volume and clearance highlights the importance of evaluation this property when investigating drug pharmacokinetics, efficacy and safety.

The metabolism studies of lead compounds such as indenoisoquinoline AM6-36 provide information regarding metabolic stability,[143, 144] the potential of forming potentially toxic metabolites,[145] and the possibility of metabolic transformation to more active (or inactive) products.[146] The results of these studies might be useful for the prediction of *in vivo* ADME in preparation for clinical trials.

3.2 Materials and methods

3.2.1 Materials

The Caco-2 cell line, Eagle's minimum essential medium, and fetal bovine serum were purchased from the American Type Culture Collection (Rockville, MD). Trypsin/EDTA, Hank's balanced salt solution (HBSS), HEPES buffer solution, PBS, penicillin, and streptomycin were purchased from Life Technology (Grand Island, NY). Transwell polycarbonate inserts (12 mm diameter, 1.1 cm^2 surface area, 0.4 μm pore size) were purchased from Corning Costar (Cambridge, MA). Transepithelial electrical resistance (TEER) was measured using a Millicell-ERS instrument from Millipore (Bedford, MA).

AM6-36 and putative metabolites of AM6-36 were synthesized as reported previously.[133, 147] and the purity was determined to be >98% based on analysis using liquid chromatograph-mass spectrometry (LC-MS). Pooled human liver microsomes and cryopreserved human hepatocytes were purchased from In Vitro Technologies

(Baltimore, MD) and were handled according to the supplier's instructions. Human liver cytosol was purchase from BD Biosciences (San Jose, CA).

Human plasma (K3EDTA) was purchased from Bioreclamation (Westbury, NY). Binding of AM6-36 to human plasma proteins was determined using a Thermo Scientific rapid equilibrium dialysis kit, which consists of a Teflon base plate which holds up to 48 disposable dialysis inserts. Each single-use, disposable insert is made of two side-by-side chambers separated by a vertical cylinder of dialysis membrane (in 8K MWCO).

All other chemicals were purchased from Sigma-Aldrich (St. Louis, MO). All organic solvents were HPLC grade or better and were purchased from Thermo Fisher (Hanover Park, IL).

Synthesis of 3-Amino-6-(3-aminopropyl)-11-hydroxy-6,11-dihydro-5H-indeno[1,2-c] isoquinolin-5-one (M1)

AM6-36 (107 mg, 0.30 mmol) was dissolved in methanol (15 mL), and the reaction mixture was cooled to 0 $^{\circ}$C. Sodium borohydride (1.03 g, 27.2 mmol) was added in portions, and the reaction mixture was stirred for 45 min, keeping the temperature constant. An aqueous solution of saturated ammonium chloride (50 mL) was added, and the solution extracted with dichloromethane (5 x 20 mL). The organic extracts were dried with sodium sulfate and the solvent removed. The obtained solid was washed with hexane-dichloromethane, 2:1. The desired compound

was obtained as a dark yellow solid (73 mg, 76%): mp 194 $^{\circ}$C (dec). IR (KBr) 3348, 3222, 3065, 2931, 2866, 1627, 1576, 1469, 1379, 1318, 1181, 1113, 833, 762 cm^{-1}; ^{1}H NMR (300 MHz, DMSO-d_6) δ 7.81-7.75 (m, 2 H) 7.57 (d, J = 6.9 Hz, 1 H), 7.39-7.27 (m, 3 H), 7.05 (dd, J = 6.5 Hz, J = 1.9 Hz, 1 H), 5.66-5.63 (m, 3 H), 5.43 (d, J = 8.8 Hz, 1 H), 4.49 (br t, J = 7.1 Hz, 2 H), 2.65 (br t, 2 H), 1.80 (br s, 2 H). (see structure in Figure 13).[147]

Synthesis of N-[6-(3-Aminopropyl)-5,11-dioxo-6,11-dihydro-5H-indeno[1,2-c] isoquinolin-3-yl]acetamide (M2)

To synthesize M2, 5 drops of acetic anhydride were added to a solution of AM6-36 (3 mg) in water (500 μL) at room temperature. Purification was carried out by semi-preparative HPLC equipped with a Shimadzu SPD-20A UV detector at 290 nm. Two acetylation products were separated using a YMC-Pack ODS 10×250 mm, 5μm column with a linear gradient from 20% to 60% methanol over 30 min. ^{1}H-NMR (δ, ppm, DMSO-d6, 400 MHz): 1.90 (t, 2H, J = 8.0 Hz, 2'-H), 2.10 (s, 3H, 12'-H), 2.75 (t, 2H, J = 8.0 Hz, 1'-H), 4.53 (t, 2H, J = 8.0 Hz, 3'-H), 7.46 (d, 1H, J = 4.0 Hz, 7-H), 7.54 (dd, 2H, J = 4.0 Hz J = 12.0 Hz, 5,6-H), 7.91 (d, 1H, J = 8.0 Hz, 9'-H), 7.95 (d, 1H, J = 8.0 Hz, 8'-H), 8.49 (d, 1H, J = 8.0 Hz, 4'-H), 8.56 (s, 1H, 10'-H), 10.32 (s, 1H, 11'-H) (see structure in Figure 19).

3.2.2 Cell culture

Caco-2 cells were cultured in Eagle's minimum essential medium with 10% fetal bovine serum, 100 units/mL penicillin and 100 μg/mL streptomycin in a humidified atmosphere of 5% CO_2 and 95% air at 37 °C. When the cells had reached approximately 70-80% confluence, thay were removed using 0.25% trypsin/EDTA, seeded onto polycarbonate membranes fitted into Transwell 6-well plates at a density of 2×10^5 cells/insert and cultured until late confluence. The cell culture medium was changed every other day after seeding. The integrity of each monolayer of differentiated cells was monitored by measuring the TEER. Only monolayers with TEER values >300 Ω/cm^2 were utilized.

3.2.3 Cellular transport experiments

Cellular transport experiments were carried out by Dr. Soyoun Ahn. In preparation for the Caco-2 cell monolayer assays, the cell culture medium was removed from both the apical (AP) and basolateral (BL) chambers. The cells were washed three-times and pre-incubated with HBSS containing 25 mM HEPES, pH 7.4, for 30 min at 37 °C on a shaker bath at 50 rpm. A 20 mM stock solution of AM6-36 in dimethylsulfoxide (DMSO) was diluted to different concentrations in HBSS/HEPES buffer (the final concentration of DMSO was less than 1%). These test solutions containing AM6-36 were added to either the apical chambers (for AP→BL measurement) or the basolateral chambers (for BL→AP assay), and blank HBSS/HEPES buffer was added to the other side. As a test of the integrity of the monolayer and as a marker of low permeability, sucrose (50 μM final concentration)

was added to the apical chambers. Propranolol (10 μM final concentration) was also added as a marker for compounds that are highly permeable. The total volumes of solution in the apical and basolateral chambers were 1.5 and 2.6 ml, respectively. The solutions in the recipient compartments were removed and replaced with fresh medium. The samples were stored at −20°C until analysis of AM6-36 by LC-MS-MS as described below for the analysis of extracts of serum and tissue. At the end of each experiment, basolateral samples were also analyzed by LC-MS for sucrose and propranolol. The apparent permeability coefficients (P_{app}, $\times 10^{-6}$ cm/sec ± S.D.) were then calculated. The P_{app} of sucrose from the apical to the basolateral side of each well was also measured and remained acceptably low at 0.16×10^{-6} cm/sec.[148]

Data were analyzed statistically using the Student's t-test, and linear regression analysis was carried out using GraphPad Prism. Difference between means of measurements of $p<0.05$ were considered significant.

3.2.4 Metabolic stability

To investigate metabolic stability, AM6-36 (1 μM) or propranolol (reference compound with medium metabolic stability[149]) was incubated with human liver microsomes (1 mg protein/mL) as described above except that the total incubation volume was 500 μL. Aliquots (50 μL each) were removed at 0, 5, 10, 20, 30, 40, 50, and 60 min, and mixed with 10 μL ice-cold acetonitrile/water/formic acid (90:10:4, v/v/v) containing ketoconazole (2.5 μM) as an internal standard. After centrifugation

to remove the precipitated protein, the concentration of AM6-36 or propranolol was determined in each supernatant using LC-MS/MS.

The hepatic intrinsic clearances of AM6-36 and propranolol were determined based on the rates of substrate disappearance during incubation with human liver microsomes. The slope of the linear regression curve ($-k_e$) from log percentage remaining of each compound versus incubation time was used to compute half-life using the following equation: $t_{1/2} = 0.693/ k_e$. Hepatic intrinsic clearance (CL_{int}, mL/min/kg) was calculated by using the following equation: [150]

$$CL_{int} = 0.693/ t_{1/2}\, SF$$

When liver microsomal preparation was used as the enzyme source,

$$SF = (G_{micrs}/W_{liver})(W_{liver}/W_{body})/C_{protein}, \quad \text{with}$$

SF, scaling factor (mL/ kg); G_{micrs}, the average quantity of microsomal protein in the liver (mg), W_{liver}, liver weight (g); W_{body}, body weight (kg); and $C_{protein}$, protein concentration in the reaction mixture (mg/mL). G_{micrs}/W_{liver} is usually considered to be approximately 50 mg/g, while W_{liver}/W_{body} is approximately 20 g/kg in humans[150]; thus,

$$CL_{int} = 1000 \times 0.693/ (t_{1/2}\, C_{protein}), \text{ in units of mL/min/kg.}$$

3.2.5 Testing for formation of electrophilic metabolites

AM6-36 (10 μM), human liver microsomes (1 mg protein/mL), glutathione (10 mM), and NADPH (1 mM) were incubated in 400 μL of 50 mM phosphate buffer (pH 7.4). A negative control was prepared containing no microsomes. The samples were incubated at 37 °C for 60 min and centrifuged. Aliquots of the supernatants were analyzed for glutathione conjugates using LC-MS/MS as described previously.[151]

3.2.6 <u>Incubation with human microsomes</u>

AM6-36 (1 μM) was incubated at 37 °C with pooled human liver microsomes (10 donors, mixed gender) containing 1 mg/mL of microsomal protein and 50 mM phosphate buffer at pH 7.4 in a total volume of 200 μL. After a 10 min preincubation, 1 mM NADPH was added to initiate reaction, and the mixture was incubated for an additional 60 min. The reaction was stopped by chilling the mixture on ice and by addition of 20 μL of ice-cold acetonitrile/water/formic acid (86:10:4, v/v/v) to precipitate proteins. Samples were centrifuged, supernatants were removed, evaporated to dryness under nitrogen, and the residues were dissolved in the mobile phase prior to analysis using LC-MS and LC-MS/MS. Control incubations were identical except for the elimination of microsomal protein or NADPH.

3.2.7 <u>Incubation with human hepatocytes</u>

Cryopreserved hepatocytes were thawed according to the supplier's instructions, and approximately 1×10^6 cells in a 1 mL suspension were incubated with 50 μM AM6-36 per well of a 6-well plate. Control experiments were identical except for the

use of heat-inactivated hepatocytes. The plate was incubated for 4 h at 37 °C with 5% CO_2 and 90% relative humidity. Incubations were terminated by the addition of 3 mL of ice-cold acetonitrile. The cell suspensions were centrifuged, and aliquots of the supernatants were analyzed using LC-MS and LC-MS/MS.

A 500 μL aliquot of the hepatocyte incubation was evaporated to dryness and reconstituted in 500μL sodium acetate buffer (100 mM, PH 5.0) containing β -glucuronidase (800 units). Enzymatic deconjugation was carried out at 37 °C for 6 h and terminated by the addition of ice-cold acetonitrile. After centrifugation, aliquots of the supernatants were analyzed using LC-MS/MS. Aliquots of samples not treated with β -glucuronidase were used as controls.

3.2.8 Biological evaluations of AM6-36 and its metabolites

RXRE-luciferase reporter gene assay and ultrafiltration mass spectrometric screening assay were carried out as described previously in section 2.2.2 and 2.2.3.

3.2.9 Identification of *N*-acetyltransferase isoforms responsible for AM6-36 metabolism

In preparation for inhibition and kinetics assays, the linearity of the formation of M2 was investigated by incubating AM6-36 (1 μM or 10 μM) with human liver cytosol up to 1 mg/ml. The reactions were stopped at various time points up to 60 min, and the major metabolites were measured using LC-MS as described below.

To identify specific arylamine *N*-acetyltransferase isoforms responsible for the formation of significant metabolites of AM6-36, incubations were carried out using chemical inhibitors of specific enzymes. Acetyl coenzyme A concentrations were fixed at 100 μM. Incubations contained 40 μL of human liver cytosol diluted to the appropriate concentration with 10 μL of acetyl coenzyme A (1 mM in water), and varying amounts of AM6-36, sulfamethazine, or para-aminobenzoic acid diluted in phosphate buffer consisting of 100 mM K_2HPO_4, 20 mM KH_2PO_4, 1 mM EDTA and 1 mM DTT, at pH 7.5 to start reactions. Reactions were terminated by addition of 300 μL of ice-cold acetonitrile containing ketoconazole as internal standard. After centrifugation, aliquots of the supernatants were analyzed using LC-MS/MS. Curve fitting of the kinetic data and the K_m and V_{max} were calculated using SigmaPlot 11.0 (Richmond, CA).

3.2.10 Equilibrium dialysis

Human plasma, spiked with 10 μM AM6-36, was added to the sample chamber of a rapid equilibrium dialysis kit, and 350 mL of phosphate-buffered saline (containing 100 mM sodium phosphate and 150 mM sodium chloride, pH 7.4) was added to the buffer chamber. The plate was sealed and incubated at 37 °C on an orbital shaker at 100 rpm for 5 h. Note that 5 h incubation time was used since preliminary experiments indicated that AM6-36 binding to human plasma proteins reached equilibrium by approximately 4.5 h. Aliquots (50 μL) were removed from the sample and buffer chambers and mixed with an equal volume of buffer or blank

plasma, respectively. To each sample, 300 μL of ice-cold acetonitrile was added, and the matrix-matched samples were vortex mixed and incubated for 30 min on ice. After centrifugation at $13,000 \times g$ for 15 min, the supernatants were removed, evaporated to dryness and then reconstituted in acetonitrile/water containing 0.1% formic acid (30:70, v/v) and 0.5 μM of caffeine (internal standard) prior to quantitative analysis using LC-MS/MS. The plasma protein binding of ketoconazole and atenolol, high and low plasma binding reference compounds, respectively, were also determined. The percentage of each compound bound to plasma protein was calculated as follows:

% Free = (Concentration in buffer chamber/Concentration in plasma chamber) ×100%

% Bound = 100% - % Free

3.2.11 <u>Animals</u>

Female Sprague-Dawley rats were obtained at 4-weeks-of-age from Sprague-Dawley (Indianapolis, IN) and placed on Takland diet. At 77 days-of-age, the rats were treated with AM6-36 by gavage (40 mg/kg; 0.5 ml; ethanol/polyethylene glycol 400; 10: 90, v/v), and the treatment was continued daily for three days. Sample collection and serum and tissue preprocessing were carried out by Dr. Clinton Grubbs of the University of Alabama at Birmingham (Birmingham, AL). Blood samples were collected (jugular vein) 3 h after the first treatment. Three hours after the final treatment, the animals were sacrificed, and blood, mammary tissue, liver, and perirenal fat were collected.

3.2.12 <u>Sample preparation</u>

After clotting, the blood samples were centrifuged at 100 ×g for 20 min. Serum and tissue samples were stored at -80°C until analysis. Rat liver was homogenized in 0.05 M phosphate buffer (pH 7.4), and mammary gland and perirenal fat tissues were homogenized in a mixture (50:50; v/v) of phosphate buffer and methanol to give homogenates containing 0.2 g tissue/mL. As an internal standard for quantitative analysis, UCN-01 (see structure in Figure 9) at 1 ng/mL was added to each homogenate and serum sample. Proteins in the homogenized tissue and serum samples were precipitated with four volumes of ice-cold acetonitrile. After centrifugation at 10,000 ×g for 5 min, each supernatant was removed, evaporated to dryness, and reconstituted in 100 μL of methanol/water (50:50; v/v) for analysis using LC-MS/MS.[152]

3.2.13 <u>LC-MS and LC-MS/MS</u>

Quantitative analysis of AM6-36 in the Caco-2 incubation buffer was carried out using an Agilent 1100 HPLC system interfaced with an Agilent MSD single quadrupole mass spectrometer. A Waters Xterra 2.1×50 mm, 3.5 μm analytical column was used for chromatographic separations with a isocratic mobile phase containing 0.1% formic acid in water and methanol (62:38 v/v) at a flow rate of 0.25 mL/min. AM6-36 were detected using positive ion electrospray and recorded using selected ion monitoring (SIM) at m/z 320.0 with the quadrupole mass spectrometer as follows: capillary voltage, 3800 V; nebulizer gas pressure, 35 psi; drying gas temperature. 315 °C; and drying gas flow rate, 10 L/min.

For quantitative analysis of AM6-36, internal standards and reference standards for metabolic stability studies, LC-MS/MS analyses were carried out on a Shimadzu Prominence HPLC system interfaced with an Applied Biosystems (Foster City, CA) API 4000 triple quadrupole mass spectrometer. A Thermo Fisher Hypersil GOLD 2.1×100 mm, 5 μm analytical column was used for chromatographic separations with a 10 min linear gradient from 10% to 90% acetonitrile in water containing 0.1% formic acid at a flow rate of 0.2 mL/min. Analytes were detected using positive ion electrospray, collision-induced dissociation and SRM at unit resolution. Nitrogen was used as the collision gas at 25 eV, and the dwell time was 1000 ms/ion. During SRM, AM6-36 was measured by recording the signal for the transition of the protonated molecule of m/z 320 to the most abundant fragment ion of m/z 303. The SRM transitions of m/z 531 to m/z 489 and m/z 260 to m/z 183 were monitored for ketoconazole and propranolol, respectively.
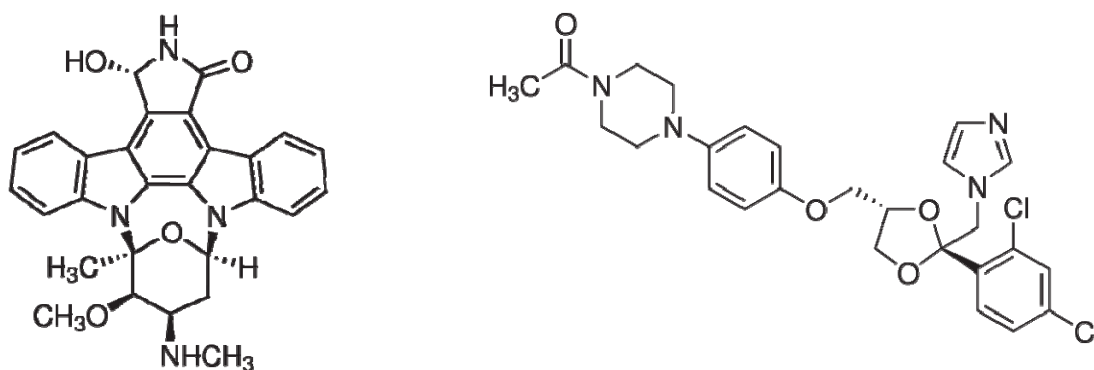
Figure 9 Structures of UCN-01 (Left) and ketoconazole (Right).

Analyses of AM6-36 and its metabolites were carried out using a Waters 2690 HPLC system equipped with a Waters Xterra 2.1×100 C_{18} column. The solvent system consisted of a linear gradient from 0.1% formic acid in water to methanol as

follows: 10% to 45% methanol over 35 min, 45% to 90% methanol over 10 min and isocratic 90% methanol for another 5 min. The column was equilibrated with 10% methanol for at least 10 min between analyses. The flow rate was 0.2 mL/min, and the column temperature was 33 °C. The HPLC was interfaced with a high resolution Waters Q-TOF Synapt hybrid quadrupole/time-of-flight mass spectrometer, and positive ion electrospray was used for sample ionization. For accurate mass measurements, leucine enkephalin ([M+H]$^+$ of m/z 556.2771) was introduced post-column as a lock mass. The mass accuracy obtained was < 5 ppm. Data were acquired from m/z 50-800. Tandem mass spectra were acquired at a collision energy of 25 eV using argon as the collision gas at a pressure of 2.0×10^{-5} mbar.

Ultrafiltration screening of AM6-36 metabolites was carried out using a Thermo Finnigan TSQ Quantum triple quadrupole mass spectrometer equipped with a Waters 2695 HPLC. HPLC separations were carried out using a Waters Xterra 2.1×100 C$_{18}$ column or a YMC (Wilmington, NC) C$_{18}$ column (2.1×250 mm, 5 μm, 120 Å) with a mobile phase consisting of either a 12 min isocratic mobile phase of acetonitrile/aqueous 0.1% formic acid (40:60, v/v) or a 21 min linear gradient from 10-90 (v/v) aqueous methanol containing 0.01% formic acid at a flow rate of 200 μL/min. Positive ion electrospray ionization, collision-induced dissociation and SRM were used to record the elution of each compound. The SRM transitions of m/z 364 to 254, m/z 320 to 303, m/z 322 to 305, m/z 362 to 345, m/z 321 to 303, m/z 323 to 305, m/z 364 to 347, m/z 363 to 345, m/z 301 to 159, and m/z 531 to 244 were monitored

for LG100268, AM6-36, M1, M2, M3, M4, M5, M6, all *trans*-RA, and internal standard, respectively.

Quantitative analysis for isoform identification studies were carried out using UHPLC-MS-MS on a Shimadzu Nexera UHPLC system interfaced with a Shimadzu LCMS-8040 triple quadrupole mass spectrometer. Analytes were separated on a Shimadzu Shim-pack XR-ODS III UHPLC column (2.0 x 50 mm, 1.6 μm) using a 2.5 min linear gradient from 10-100% acetonitrile in 0.1% aqueous formic acid with re-equilibration at 10% methanol for 1.5 min. The flow rate was 0.5 mL/min. Mass spectrometer ion source parameters were as follows: DL temperature 300 °C, spray voltage 3500 V, nebulizing gas flow 3 L/min, and drying gas flow 20 L/min. MAR-V-80 was detected using positive ion electrospray, collision-induced dissociation and SRM by recording the signal for the transition of the deprotonated molecule of *m/z* 362 to the most abundant fragment ion of *m/z* 345. The SRM transitions of *m/z* 531 to *m/z* 244 and *m/z* 320 to *m/z* 303, were monitored for ketoconazole and AM-6-36, respectively. Calibration curves were prepared using blank human liver cytosol that had been spiked with M2 ranging from 2 to 362 ng/mL. The calibration curves were obtained using linear regression analysis.

For quantitative analysis of AM6-36, internal standards and reference standards during plasma protein binding studies, LC-MS/MS analyses were carried out on a Shimadzu Prominence HPLC system interfaced with an Applied Biosystems API 4000 triple quadrupole mass spectrometer. A Thermo Hypersil GOLD 2.1×100

mm, 5 μm analytical column was used for chromatographic separations with a 10 min linear gradient from 10% to 90% acetonitrile in water containing 0.1% formic acid at a flow rate of 0.2 mL/min. Analytes were detected using positive ion electrospray, collision-induced dissociation and SRM at unit resolution. Nitrogen was used as the collision gas at 25 eV, and the dwell time was 1000 ms/ion. AM6-36 and ketoconazole were measured using SRM as described above. The SRM transitions of *m/z* 267 to *m/z* 145, and *m/z* 195 to *m/z* 138 were monitored for atenolol and caffeine, respectively.

LC-MS-MS quantitative analysis of AM6-36 in extracts of serum and tissues were carried out using a Shimadzu LC-20AD Prominence UFLC pump and SIL-20AC HT prominence autosampler interfaced to an Applied Biosystems API 4000 triple quadruple mass spectrometer. A Waters XTerra MS C_{18} column (2.1 mm × 100 mm, 3.5 μm) was used for HPLC separation with a 13-min linear gradient from 10-80% acetonitrile in 0.1% aqueous formic acid at a flow rate of 0.25 ml/min. Positive ion electrospray was used for ionization, and product ion mass spectra were recorded using collision-induced dissociation SRM as described above for AM6-36. For the internal standard (UCN-1), the SRM transition of m/z 483 to 130 was monitored with a dwell time of 300 ms. Calibration curves were prepared using blank serum or homogenized tissue from control animals that had been spiked with AM6-36 ranging from 0.5 to 500 ng/mL. The calibration curves were obtained using linear regression analysis.

3.3 <u>Results</u>

3.3.1 <u>Intestinal permeability</u>

Based on the Caco-2 cell permeability model, the apparent permeability coefficient for AM6-36 in the AP → BL direction was 2.75×10^{-6} cm/sec. This rate was 10-fold slower than that of the high permeability standard, propranolol, but was 17-fold faster than the low permeability standard, sucrose (Table V). The apparent permeability coefficient in the BL → AP direction was similar to that in the AP → BL direction (Table V). These measurements indicate that the intestinal absorption of AM6-36 should proceed at a moderate rate following oral administration. Since the apparent permeability coefficients in the AP → BL and in the BL → AP were not significantly different, AM6-36 does not appear to be a substrate for efflux proteins that might reduce its bioavailability.

TABLE V

APPARENT PERMEABILITY COEFFICIENTS OF AM6-36 THROUGH CACO-2 MONOLAYERS.[133]

		Papp ($\times 10^{-6}$ cm/sec ± S.D.)[1]	
		AP to BL[2]	**BL to AP[3]**
AM6-36[4]	5 μM	2.75 ± 0.78	3.95 ± 0.11
	10 μM	5.52 ± 0.2.9	3.25 ± 0.71
	25 μM	4.45 ± 0.71	8.26 ± 0.93
Standards	Propranolol 10 μM	27.6	
	Sucrose 50 μM	0.16	

1. Papp (apparent permeability coefficient) is expressed as cm/sec ($\times 10$-6).
2. AP to BL indicates apical to basolateral transport.
3. BL to AP indicates basolateral to apical transport.
4. Data are expressed as mean ± SD, n = 3

3.3.2 <u>Metabolic stability</u>

The concentration of AM6-36 decreased during incubation for 60 min with human liver microsomes (Figure 10). The elimination rate constant of AM6-36 was 0.0053, and the *in vitro* half-life was 130 min. Based on these data, the hepatic intrinsic clearance of AM6-36 was determined to be 5.33 mL/min/kg. Under identical conditions, the reference substrate propranolol, which has medium-low metabolic stability,[97] showed an elimination rate constant of 18.3 mL/min/kg and a half-life of 38 min.
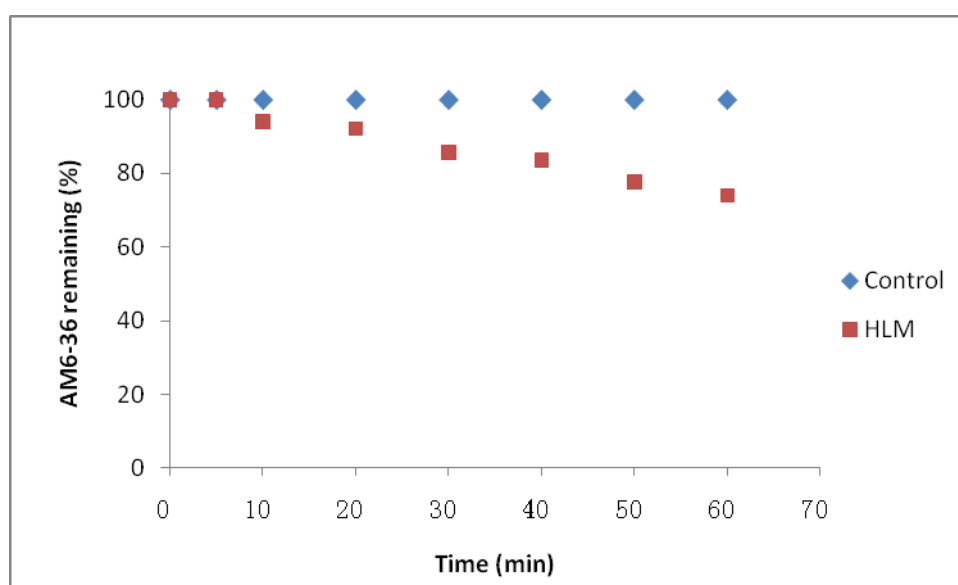
Figure 10 Disappearance of AM6-36 during incubation with pooled human liver microsomes.

3.3.3 <u>Test for electrophilic metabolites of AM6-36</u>

During the investigation of the metabolism of AM6-36 by human liver microsomes, a set of experiments was carried out containing the biological

nucleophile glutathione to trap any electrophilic metabolites that might form. Analysis of the metabolite mixture using LC-MS/MS showed no evidence of glutathione conjugates (data not shown). Therefore, human liver microsomal metabolism of AM6-36 does not appear to generate any electrophilic intermediates that can be trapped as glutathione conjugates.

3.3.4 Identification of AM6-36 metabolites during incubation with human liver microsomes
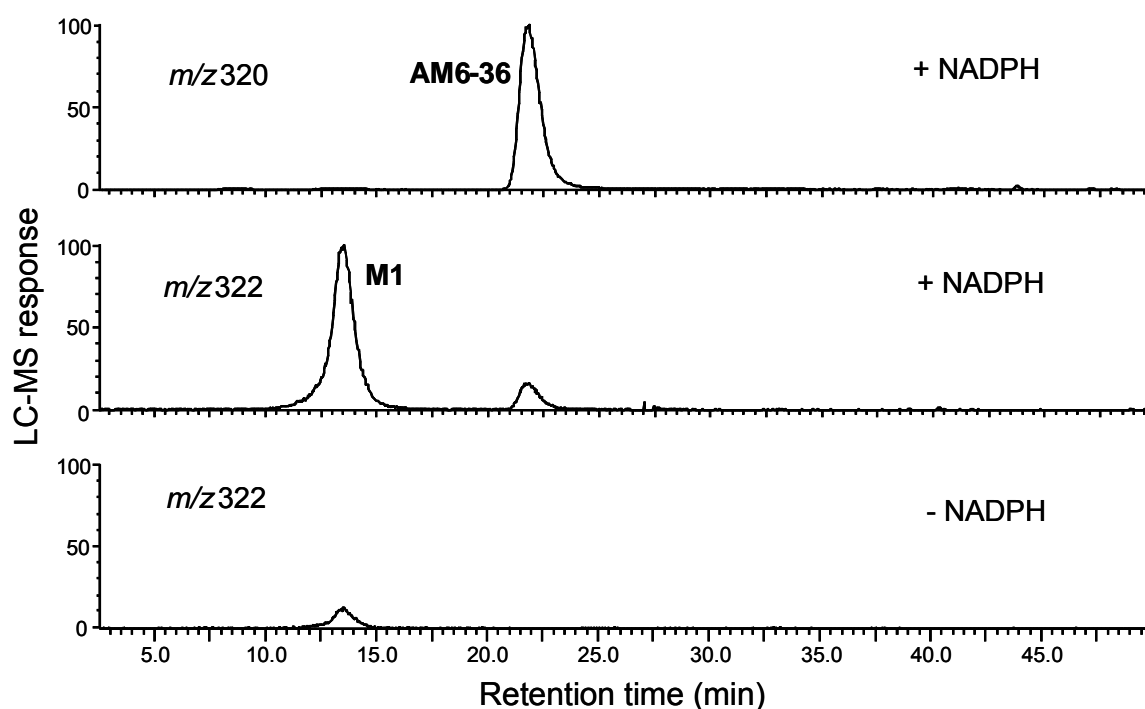
Figure 11 Computer-reconstructed mass chromatograms of m/z 320 and m/z 322 from the high resolution positive ion electrospray LC-MS analysis of an incubation of AM6-36 with pooled human liver microsomes. One Phase I metabolite, M1, was detected as a protonated molecule of m/z 322.1554 ($C_{19}H_{20}N_3O_2$, ΔM -0.2 ppm) at a retention time of 13.6 min.

The positive ion electrospray LC-MS analysis of the AM6-36 metabolite mixture after incubation with human liver microsomes is shown in Figure 11. One major metabolite M1 (retention time 13.6 min) was detected as a protonated molecule of *m/z* 322.1554 which is within -0.2 ppm of the elemental composition $C_{19}H_{20}N_3O_2$. This formula indicates that M1 is a reduction product of AM6-36 ($C_{19}H_{18}N_3O_2$) formed by the addition of two hydrogen atoms. The formation of M1 required both liver microsomes and NADPH because omission of either produced no detectable metabolites of AM6-36 (Figure 11). Possible chemical structures that are consistent with these data would include reduction of the ketone to an alcohol or reduction of a carbon-carbon double bond. The positive ion product ion tandem mass spectra of AM6-36 and M1 were obtained and are shown in Figure 12. The tandem mass spectrum of M1 (Figure 12) contained an abundant fragment ion of *m/z* 287.1107 ($C_{19}H_{15}NO$, -2.7 ppm), corresponding to the loss of ammonia and a molecule of water. Not observed in the tandem mass spectrum of AM6-36 (Figure 12), loss of water from M1 suggested that it was formed by reduction of the ketone group of AM6-36 to an alcohol. The corresponding alcohol was synthesized and found to coelute with M1 during LC-MS/MS and to produce an identical tandem mass spectrum. Therefore, M1 was identified as 3-amino-6-(3-aminopropyl)-11-hydroxy-6,11-dihydro-5*H*-indeno [1,2-*c*]isoquinolin-5-one (Figure 13).
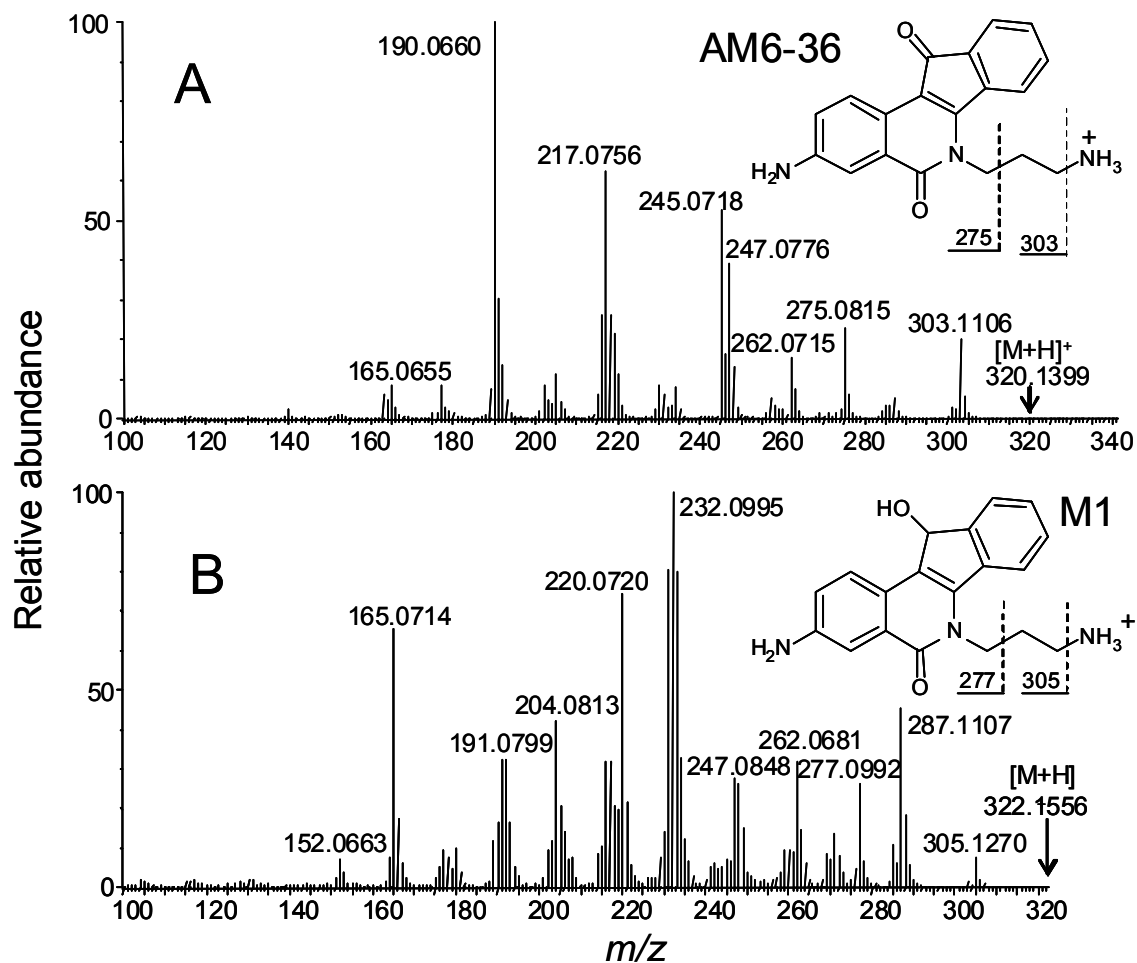
Figure 12 Positive ion electrospray product ion tandem mass spectra obtained using high resolution accurate mass measurement of A) AM6-36; and B) the abundant Phase I metabolite M1.The mass of the protonated molecule used as the precursor for product ion tandem mass spectrometry is indicated on each tandem mass spectrum.

Figure 13 Proposed metabolic pathway of human liver Phase I metabolites of AM6-36.

3.3.5 <u>Identification of AM6-36 metabolites during incubation with human</u>
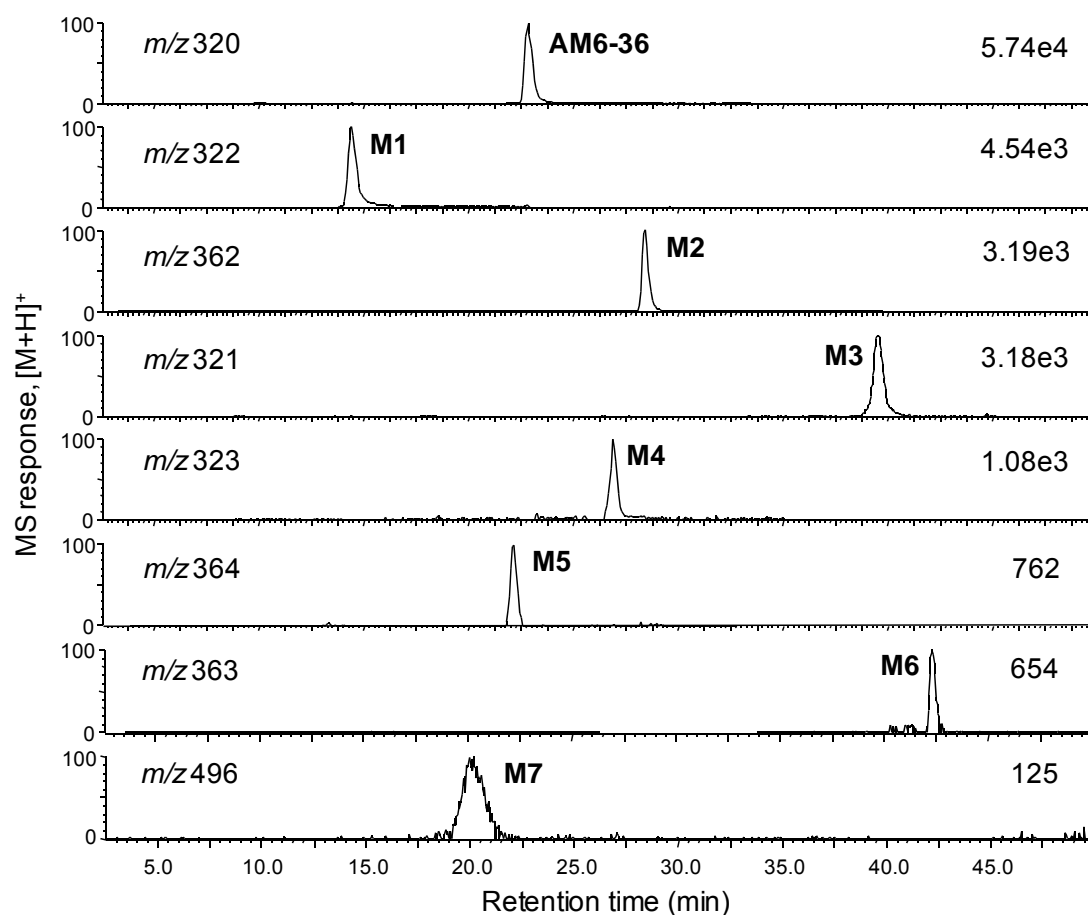
<u>hepatocytes</u>

Figure 14 Computer-reconstructed positive ion electrospray LC-MS chromatograms of AM6-36 and its seven Phase I and Phase II metabolites formed during incubation with human hepatocytes.

There were seven metabolites formed during incubation of AM6-36 with human hepatocytes (Figure 14), and one was identical to the liver microsomal metabolite M1. The most abundant of the new metabolites of AM6-36, M2, eluted at 27.8 min during LC-MS analysis (Figure 14) and formed a protonated molecule of m/z 362.1501. Accurate mass measurement of M2 indicated an elemental composition of $C_{21}H_{20}N_3O_3$ (ΔM -1.1 ppm) which corresponded to monoacetylation of AM3-36. The product tandem mass spectrum of protonated M2 is shown in Figure 15. The product ion of m/z 345.1220 in the positive ion tandem mass spectrum (Figure 15) was formed by a loss of ammonia, $[MH-NH_3]^+$ (ΔM -5.5 ppm). Loss of ammonia and the product ion of m/z 317 indicated that the acetyl group was not present on the aminopropyl side chain. Therefore, the acetyl group must be located on the aniline group (Figure 15). This proposed structure was then synthesized, and the M2 was identified as *N*-(6-(3-aminopropyl)-5,11-dioxo-6,11-dihydro-5*H*-indeno[1,2-c] isoquinolin-3-yl)acetamide by LC-MS/MS comparison with a synthetic standard (Figure 19).

Another abundant metabolite of AM6-36 formed by human liver microsomes, M3, was detected during LC-MS at a retention time of 39.6 min (Figure 14). The protonated molecule of M3 was measured as m/z 321.1247 which corresponded to an elemental composition of $C_{19}H_{17}N_2O_3$ (ΔM 2.5 ppm). Therefore, M3 was formed by the conversion of an amino group to an alcohol. Based on the observation of fragment ions of m/z 303 and m/z 275 in the product ion tandem mass spectrum which localized the alcohol to the propyl side chain (Figure 15), the putative metabolite was

synthesized for comparison using LC-MS/MS, and M3 was identified as 6-(3-hydroxypropyl)-3-amino-5*H*-indeno [1,2-*c*]isoquinoline-5,11(6*H*)-dione (Figure 19).

To determine if monoamine oxidases were responsible for the formation of M3, human liver microsomes were preincubated with the monoamine oxidase A inhibitor clorgiline or the monoamine oxidase B inhibitor pargyline (10 μM) immediately before incubation with AM6-36. Because these inhibitors did not alter the formation of M3 from AM6-36 (Figure 16), monoamine oxidases were not responsible for this metabolic transformation. These results indicate that AM6-36 will not interfere with monoamine oxidase metabolism.

Eluting at 26.9 min during LC-MS (Figure 14), the protonated molecule of M4 was detected at *m/z* 323.1383 and corresponded to a theoretical formula of $C_{19}H_{19}N_2O_3$ (ΔM -4.0 ppm). The fragment ions of *m/z* 305 ([MH-H$_2$O]$^+$), *m/z* 287 ([MH-2H$_2$O]$^+$), 277, and *m/z* 264 in the product ion tandem mass spectrum of M4 (Figure 17) indicated the presence of two alcohol groups with one located at the terminus of the propyl side chain. These data are consistent with reduction of the ketone to an alcohol and conversion of the amino propyl group to a propyl alcohol group. After synthesis of this proposed compound and comparison with the metabolite using LC-MS/MS, M4 was identified as 3-amino-11-hydroxy-6-(3-hydroxypropyl) -6,11-dihydro-5*H*-indeno[1,2-c]isoquinolin-5-one (Figure 19).

Metabolite M5 eluted at a retention time of 22.1 min during LC-MS (Figure 14) and was detected as a protonated molecule of *m/z* 364.1662. Accurate mass measurement indicated an elemental composition of $C_{21}H_{22}N_3O_3$ (ΔM 0.3 ppm) which likely corresponded to the addition of an acetyl group to M1. This putative structure is also consistent with several M5 fragment ions in the product ion tandem mass spectrum (Figure 17) that differed from M1 by 42 u (a ketene, C_2H_2O, which is a characteristic neutral loss of acetyl groups) including *m/z* 233, 275, 290, 319, 329, and 347. Since $[MH-NH_3]^+$ was observed as the base peak of *m/z* 347 (Figure 17), acetylation did not occur on the aminopropyl group. Therefore, a derivative of M1 was synthesized containing an acetyl group on the aniline group (Figure 17). Based on identical tandem mass spectra and co-elution during LC-MS/MS, M5 was identified as *N*-(6-(3-aminopropyl)-11-hydroxy-5-oxo-6,11-dihydro-5*H*-indeno[1,2-*c*] isoquinolin-3-yl)acetamide (Figure 19).

A minor metabolite of AM6-36, M6 eluted at a retention time of 42.3 min during LC-MS (Figure 14). Using positive ion electrospray with accurate mass measurement, protonated M6 was measured at *m/z* 363.1346 which was within 0.3 ppm of the elemental composition $C_{21}H_{19}N_2O_4$. This elemental composition suggested acetylation and conversion of an amino group to an alcohol. Since the tandem mass spectrum of M6 (Figure 18) was similar to that of M2 (Figure 15), M6 was likely to be acetylated like M6 but differ by conversion of the aminopropyl group to an alcohol. The predicted metabolite was synthesized and shown to co-elute with M6 during LC-MS/MS and to produce an identical tandem mass spectrum. Therefore, the

structure of M6 was determined to be *N*-[6-(3-hydroxypropyl)-5,11-dioxo-6,11-dihydro-5*H*-indeno[1,2-*c*] isoquinolin-3-yl] acetamide (Figure 19).

Metabolite M7 eluted at 20.2 min during LC-MS (Figure 14), and formed a protonated molecule of *m/z* 496.1734. Accurate mass measurement indicated an elemental composition of $C_{25}H_{26}N_3O_8$ (ΔM 2.8 ppm). Since the mass was 176 u higher than AM6-36, M7 was probably a monoglucuronide. After treatment with β-glucuronidase and reanalysis using LC-MS (data not shown), the peak of M7 disappeared and the peak corresponding to AM6-36 increased, which confirmed the identification of M7 as a glucuronide acid conjugate of AM3-36. The ion of *m/z* 479.1307 in the product ion mass spectrum of M7 (Figure 18) represented loss of an amino group from the protonated molecule, suggesting that the aminopropyl group was not conjugated with glucuronic acid. Although no authentic standard was synthesized for confirmation, M7 was probably an AM6-36 monoglucuronide conjugated on the nitrogen substituent of the A-ring (Figure 19).
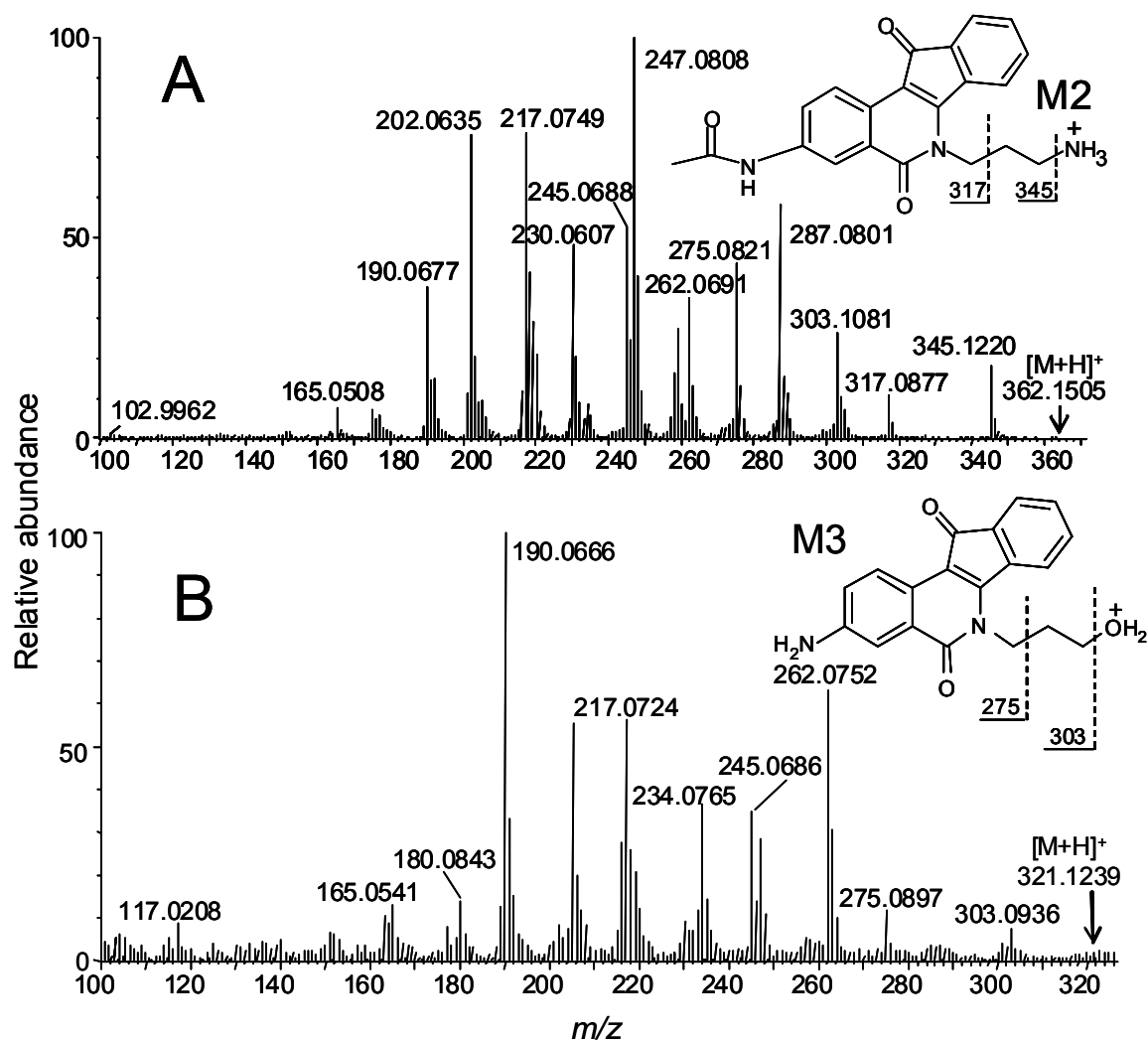
Figure 15 Positive ion electrospray product ion tandem mass spectra with high resolution accurate mass measurement of A) M2; and B) M3. The mass of the protonated molecule used as the precursor for product ion tandem mass spectrometry is indicated on each tandem mass spectrum.

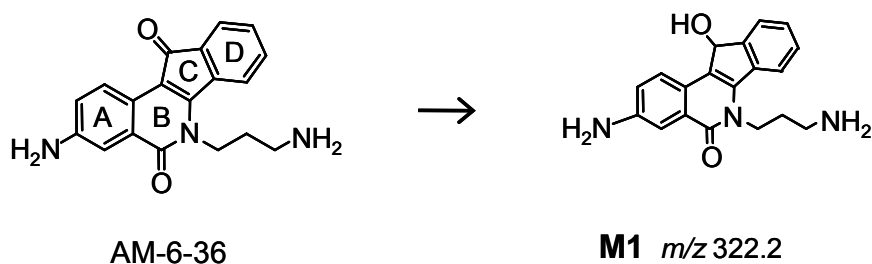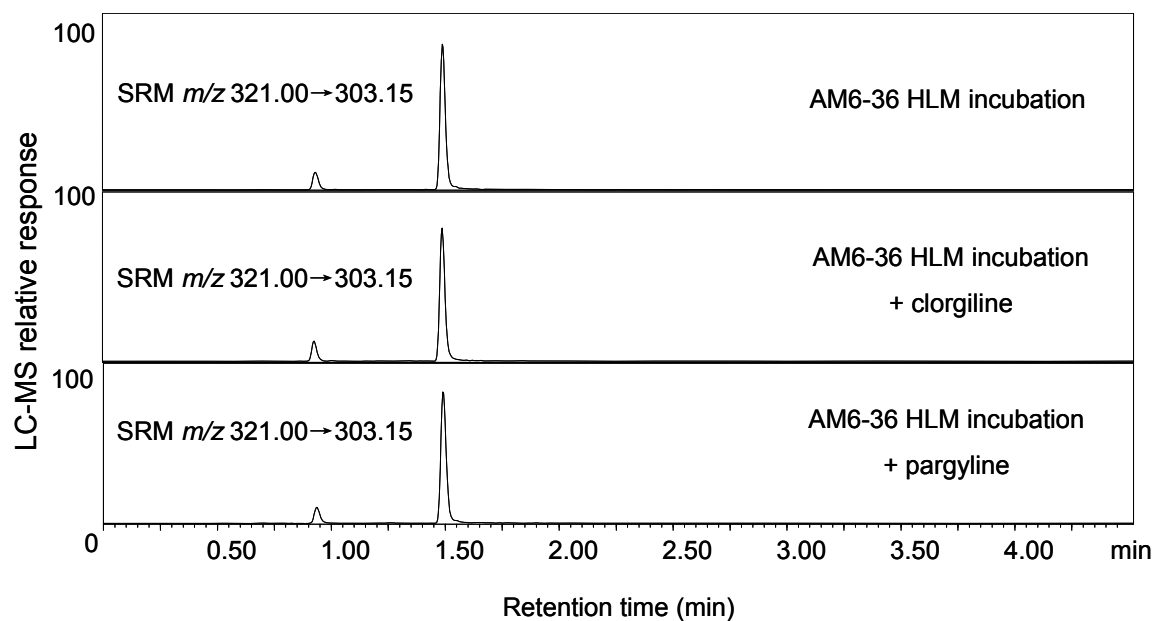**Figure 16** Positive ion electrospray LC-MS/MS with CID and SRM of the protonated

molecules of M3 formed during incubation of AM6-36 with pooled human liver

microsomes with or without monoamine oxidase A and B inhibitors clorgiline and

pargyline.
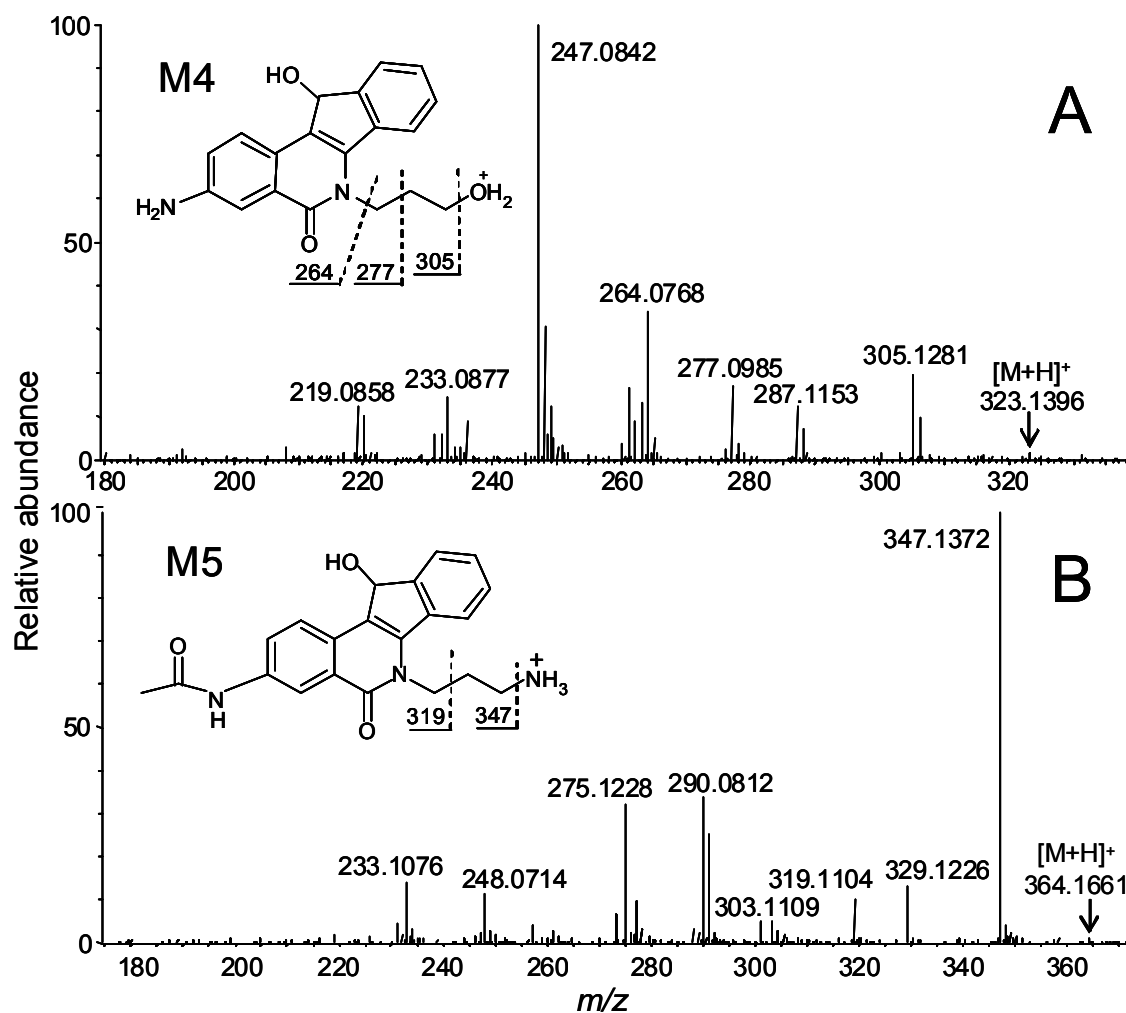
Figure 17 Positive ion electrospray product ion tandem mass spectra with high resolution accurate mass measurement of A) M4; and B) M5. The mass of the protonated molecule used as the precursor for product ion tandem mass spectrometry is indicated on each tandem mass spectrum.
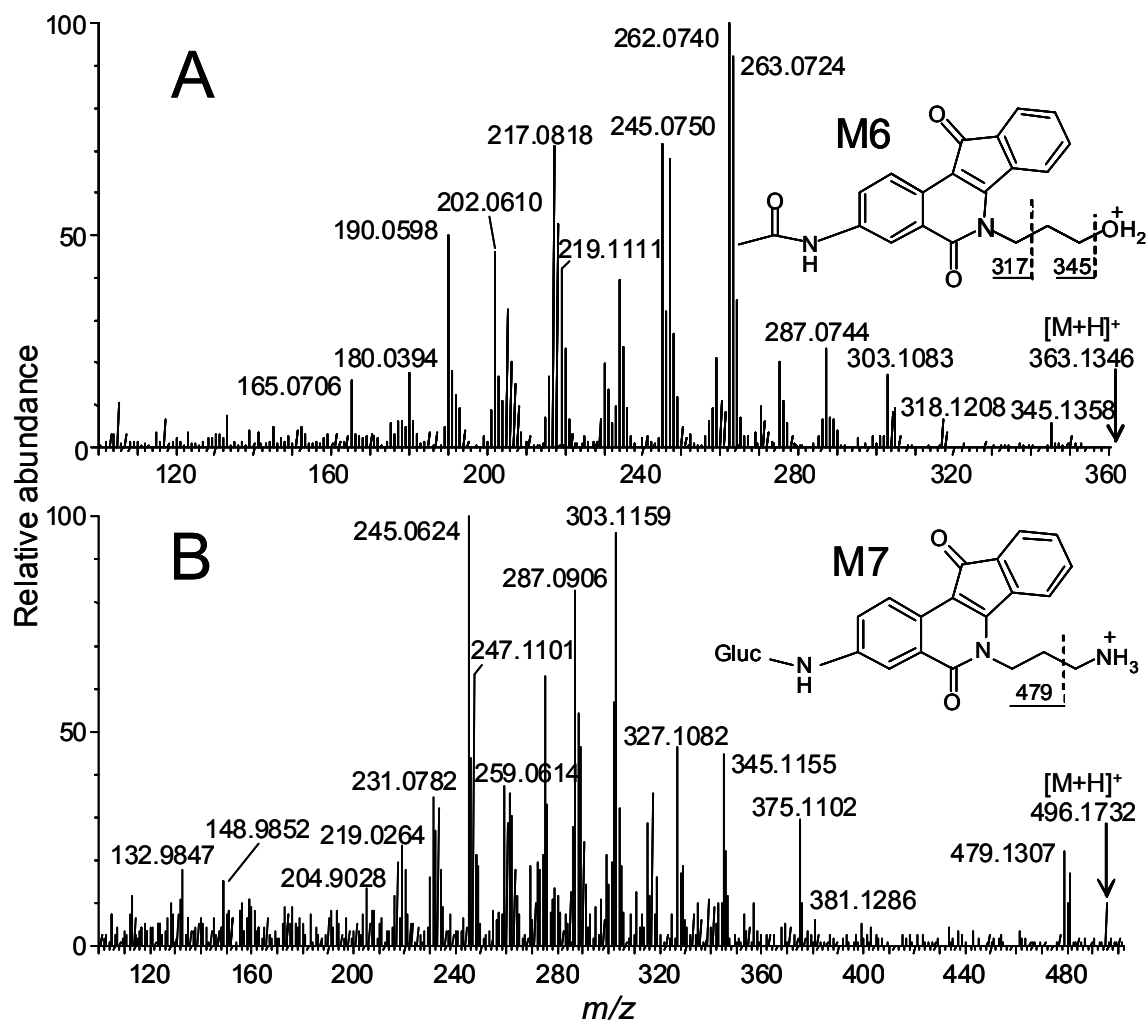
Figure 18 Positive ion electrospray product ion tandem mass spectra with high resolution accurate mass measurement of A) M6; and B) M7. The mass of the protonated molecule used as the precursor for product ion tandem mass spectrometry is indicated on each tandem mass spectrum.
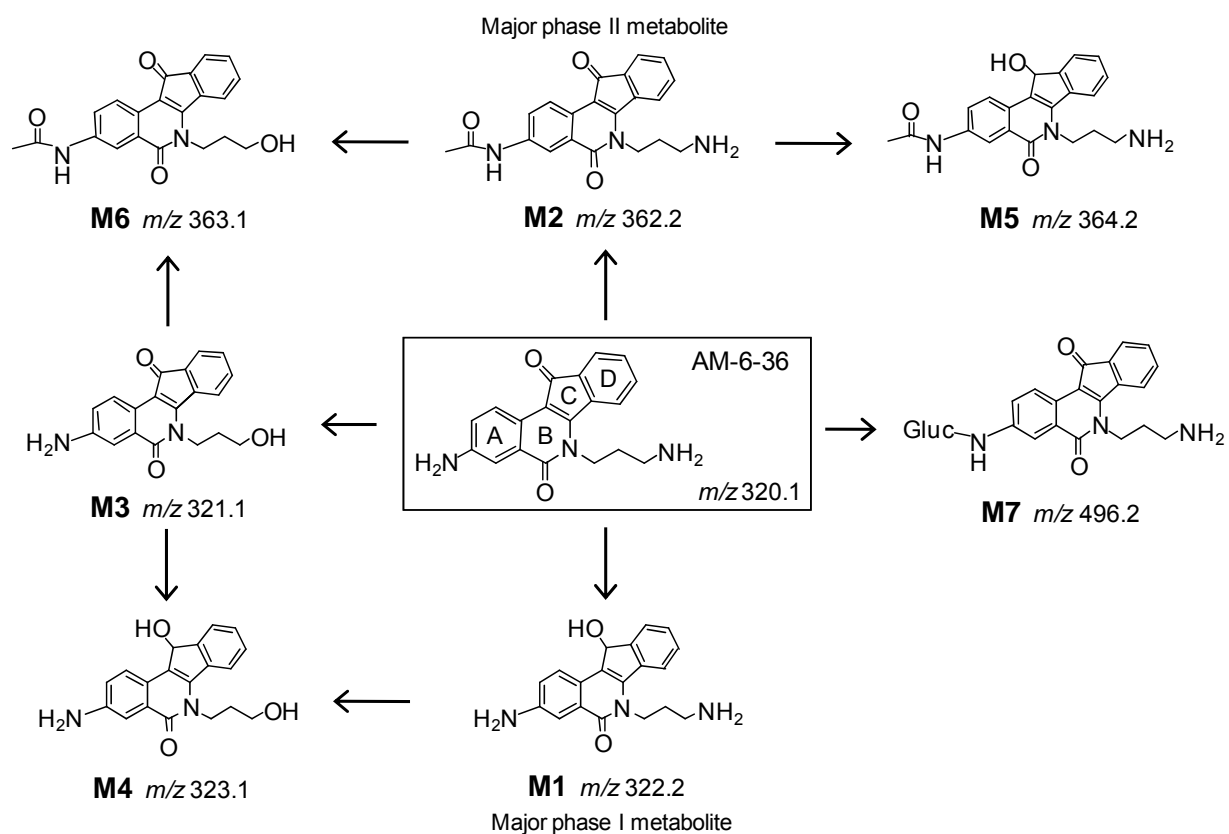
Figure 19 Structures and proposed metabolic pathways of all seven Phase I and II human hepatic metabolites of AM6-36.

3.3.6 <u>**Biological evaluation of AM6-36 and its metabolites**</u>

As described in Chapter 2, the induction of RXRE transcriptional activity is a valid chemopreventive strategy. Since AM6-36 is a rexinoid and agonist of RXRα, the metabolites of AM6-36 were tested against this target. Based on the affinity binding studies using ultrafiltation LC-MS, none of the metabolites of AM6-36 were found to be ligands of RXRα (Figure 20). The RXRE activity of each metabolite was tested in cell based bioassay, and the results are summarized in Table VI. One AM6-36 metabolite, M2, showed RXRE induction activity and showed a maximum induction ratio of 3.55 ± 0.53. This induction ratio was less than one-half that of AM6-36. All of the metabolites were less cytotoxic than AM6-36 (Table VI).
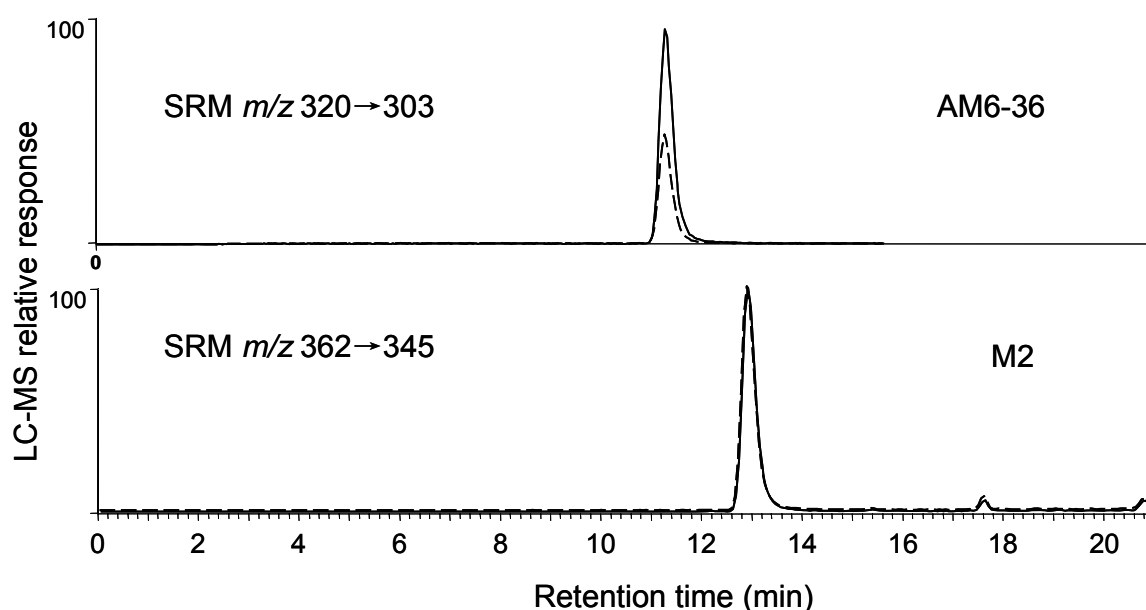
Figure 20 Ultrafiltration LC-MS/MS testing of AM6-36 and M2 for binding to RXRα. AM6-36 bound to RXRα. M1, M2, M3, M4, M5 and M6 also did not to RXRα (data not shown). Binding of the test compound to RXRα produced peak enhancement (solid line) relative to the incubation using denatured RXRα (dashed lines).

TABLE VI

BIOLOGICAL ACTIVITIES OF AM6-36 AND ITS METABOLITES.

Compound	% Cell survival[1]	Max IR[2]	Ultrafiltration binding
AM6-36	58.6 ± 0.3	7.67 ± 0.37	Binding
M1	87.5 ± 2.3	-	-
M2	74.5 ± 0.6	3.55 ± 0.53	-
M3	85.9 ± 6.3	-	-
M4	86.9 ± 2.9	-	-
M5	83.7 ± 1.3	-	-
M6	90.6 ± 0.7	-	-

1. Testing concentration: 50 μM.
2. Max IR: the maximum induction ratio observed when compounds are tested at variable concentrations.

3.3.7 <u>Determination of enzymes and factors involved in AM6-36 metabolism</u>

Determining Linear Conditions and Parameters for Michaelis-Menten Kinetics

The rates of formation of M2 from AM6-36 by human liver cytosol were investigated using LC-MS/MS. Retention times for AM6-36 and M2 were 0.9 and 1.1 min, respectively. Calibrations were linear and reproducible over the range of 2 to 362 ng/mL ($r^2 > 0.999$). Formation of M2 was linear up to 1 h with cytosolic protein concentrations up to 1 mg/ml (Figure 21 and Figure 22). Michaelis-Menten plot of M2 formation from AM6-36 by human liver cytosol was calculated by curve fitting using SigmaPlot 11.0 and the values for K_m and V_{max} were 15.4 μM and 885.0

pmol/min/mg, respectively, at an acetyl coenyzme A concentration of 100 μM (Figure 23).
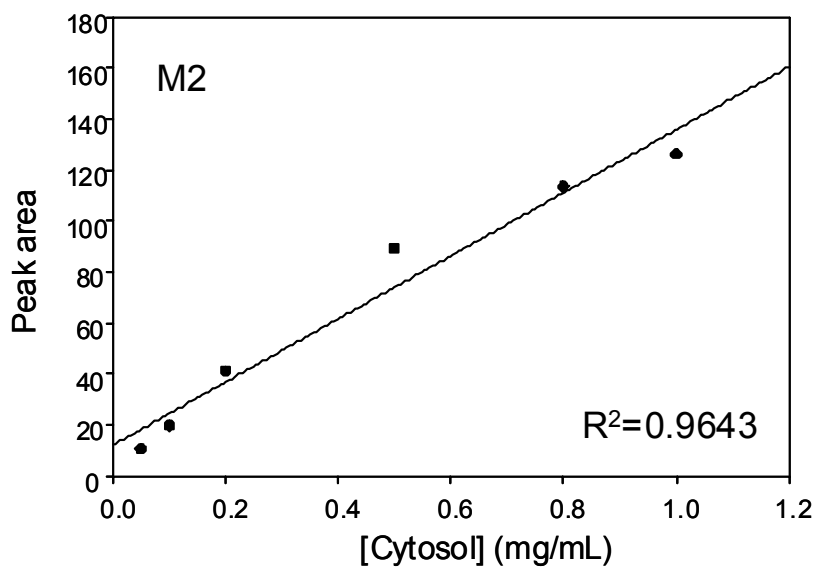
Figure 21 Formation of M2 from AM6-36 by human liver cytosol was linear with cytosol concentrations up to 1 mg/ml.
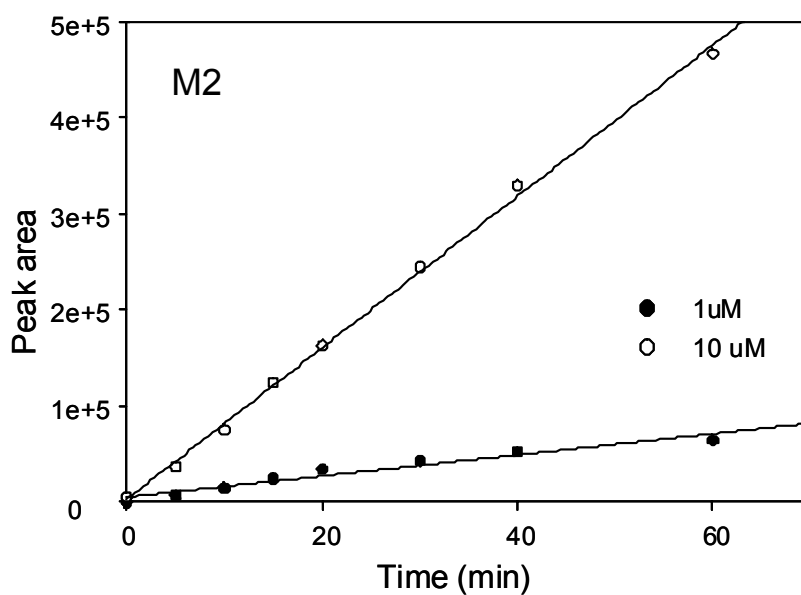
Figure 22 Formation of M2 from AM6-36 by human liver cytosol was linear up to 1 h.
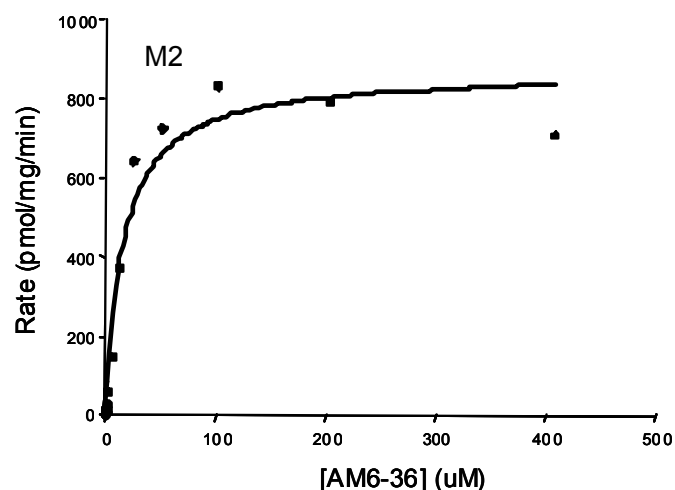
Figure 23 Michaelis-Menten plot of M2 formation from AM6-36 by human liver cytosol.

Isoform-Selective Inhibition Screening of N-Acetyl AM6-36 Formation

Selective inhibition screening in human liver cytosol using SMZ as the NAT2 probe and PABA as the NAT1 probe showed a dominant NAT2 component (Figure 24). Therefore, acetylation of AM6-36 to form M2 was catalyzed primarily by NAT2. The IC_{50} value was calculated to be 0.9 mM by curve fitting using Sigma Plot 11.0.
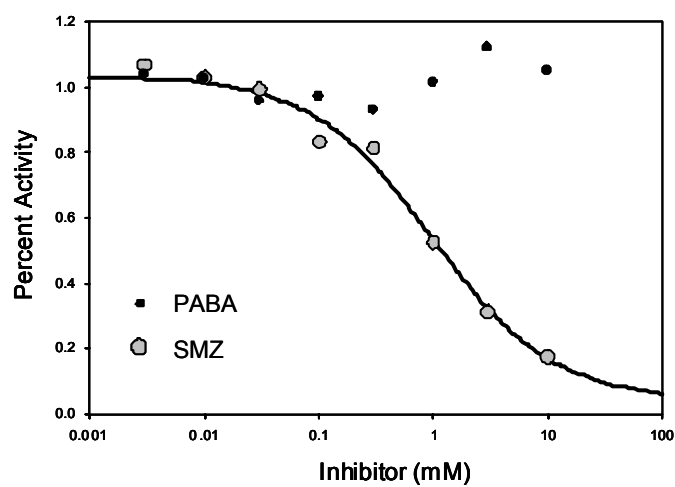
Figure 24 Inhibition of M2 formation from AM6-36 by sulfamethazine.

3.3.8 Human plasma protein binding of AM6-36

Equilibrium dialysis and LC-MS/MS were used to investigate the binding of AM6-36 to human plasma proteins. AM6-36 was found to be 75% bound to plasma proteins. For comparison, ketoconazole, which was used as a high protein binding control, was 95% bound to plasma proteins under identical conditions, and only 7% of the low protein binding control, atenolol, was found to be bound to plasma proteins.

3.3.9 Detection of AM6-36 and its metabolites *in vivo*

To assess absorption and metabolism, AM6-36 (40 mg/kg body weight) was administered to rats, by gavage, over a period of 3 days. Blood was collected on days 1 and 3, and tissues were collected at the end of the study. Quantitative analysis of AM6-36 was carried out with Dr. Jerry White. As summarized in Table VII, the concentration of AM6-36 in the rat serum was approximately 0.83 μg/mL. The concentration in liver (4.28 mg/g) was approximately 5 times higher. The amount of perirenal fat and mammary tissue obtained from each rat in this study was determined to be in insufficient amounts for quantitative analysis of the test compound. Therefore, perirenal fat from 3 rats was combined into a single sample for analysis, and mammary tissue from 3 rats was combined into a single sample. Appreciable quantities were found in the mammary gland (0.29 μg/g) and perirenal fat (0.28 μg/g). These data are consistent with moderate oral absorption and moderate metabolism/excretion.

TABLE VII

CONCENTRATION OF AM6-36 IN SERUM AND TISSUES FROM RATS.

Rat ID	Serum (μg/mL)		Liver (μg/g)	Mammary gland (μg/g)	Fat (μg/g)
	1-day	3-day	Pooled: *N*=3		
AM6-36 (40 mg/kg)[1]					
4	0.84 ± 0.008	0.82 ± 0.003	3.72 ± 0.07	-	-
5	0.84 ± 0.010	0.84 ± 0.007	5.03 ± 0.23	-	-
6	0.82 ± 0.004	0.82 ± 0.002	3.75 ± 0.13	-	-
Total	0.83 ± 0.010	0.83 ± 0.010	4.28 ± 0.65	0.29 ± 0.006	0.28 ± 0.001

1. Data are expressed as mean ± SD, n = 3

After administration of AM6-36 to rats by gavage, serum, liver and mammary tissues were obtained for analysis using high-resolution LC-MS and LC-MS/MS. The acetylated AM6-36 metabolite, M2, which was the most abundant Phase II metabolite *in vitro*, was also the most abundant metabolite observed *in vivo* (data not shown) and was detected in serum and rat liver but not in mammary tissue (Table VII). In addition to M2, metabolites M1, M3, M4, and M6 were detected in rat liver but not in serum or mammary tissue. The identities of these metabolites in rat serum and liver were confirmed by comparison of the tandem mass spectra and HPLC retention times of the metabolites with synthetic standards.

3.4 <u>Discussion</u>

One of the goals of cancer chemoprevention drug discovery is to identify drug candidates which possess appropriate ADME properties with low hepatic clearance and high oral bioavailability. Metabolic stability in the presence of liver microsomes is routinely obtained *in vitro* and used to eliminate compounds with undesirable ADME properties as early as possible in the drug discovery.[153] The substrate depletion method is often used to estimate the metabolic efficiency of compounds in liver.[150] The *in vitro* metabolic stability in human liver microsome should reasonably well predict *in vivo* clearance in human.

The metabolic half-life of AM6-36 (130 min) was longer than propranolol (38 min), and its hepatic intrinsic clearance was considerably smaller. Due to the instability of enzyme activity after 2h incubation, the exponential decay curve could not be obtained after 4 h or 6 h incubation. Although AM6-36 has a long half life, the metabolic stability study was carried out within 1 h according to the supplier's instructions. Note that the measured hepatic intrinsic clearance of propranolol, 18.3 mL/min/kg, was similar to the literature value of 13.0 mL/min/kg.[154] Therefore, AM6-36 is predicted to have low first-pass hepatic metabolism. During incubation with human liver microsomes and NADPH, one metabolite was observed, M1, which was formed by reduction of the ketone group on the C-ring to an alcohol (Figure 13). Since M1 was not observed in control incubations in which AM6-36 was incubated without human liver microsomes or NADPH, the formation of M1 requires enzymatic

catalysis. Finally, the metabolic activation experiments using glutathione as a trapping agent showed no evidence of the formation of electrophilic metabolites, which might be a source of toxicity.[151]

The large availability and simplicity in use make human liver microsomes the most popular *in vitro* model. However, because of the absence of other enzymes (e.g., NAT) and cytosolic cofactors, not all cellular metabolites might be formed using this model. In contrast, cryopreserved hepatocytes have been shown to retain both Phase I and Phase II drug metabolizing enzyme activities. Cryopreserved human hepatocytes, being closer to the in vivo liver system, have been widely utilized as the most versatile in vitro system which maintains both metabolizing and transporting activities.

In order to obtain more comprehensive information of metabolic transformation and to detect potentially toxic AM6-36 metabolites, metabolism studies were then carried out using human hepatocytes. Incubation with human hepatocytes produced seven metabolites; four of these were formed in approximately equal abundance (M1-M4) and three were minor metabolites (M5-M7) (Figure 19). Three of these hepatocyte metabolites, M1, M4 and M5, contained an alcohol on the C-ring due to reduction of the ketone. The abundant metabolite M2 was formed by acetylation of the amino group on the aromatic A-ring (Figure 19) instead of the amino group on the propyl side chain, probably due to pKa differences, which would cause the aliphatic amine to be protonated at physiological pH and therefore be less susceptible to

acetylation. M5 and M6, which were observed in low abundance, were probably formed from M2 by reduction of the ketone or conversion of the aliphatic amine to an alcohol, respectively. Alternatively, M6 could have been formed by acetylation of M3, which was generated from AM6-36 by conversion of the aliphatic amine to an alcohol. M4 was the only diol metabolite which might have been formed by reduction of the ketone of M3 or oxidation of the aliphatic amine of M1 followed by reduction of the intermediate aldehyde. Observed only as a minor metabolite, M7 was the only glucuronide formed from AM6-36 by human hepatocytes.

With the exception of the glucuronide, all of the AM6-36 metabolites were synthesized in order to obtain authentic reference standards that could be used to confirm the identities of the actual metabolites. The syntheses of the metabolites also provided enough material for investigation of their biological activities. Hepatic Phase I and Phase II enzymes might convert xenobiotics to inactive, active or even toxic metabolites. The biological evaluation indicated that none of the metabolites of AM6-36 were found to be ligands of RXRα based on ultrafiltration assay. One metabolite, M2 showed RXRE induction activity that was less than half that of AM6-36, and this weak activity might be the result of week binding to RXRα that was below the limit of detection of the ultrafiltration LC-MS assay. These data indicate that metabolic processes terminate or limit the desired chemoprevention activity and chemotherapeutic cytotoxicity of AM6-36. As a potential chemoprevention agent, these data indicate that AM6-36 is worthy of additional investigation.

NAT acetylation of AM6-36 in human liver cytosol is mediated by NAT2, as shown by the NAT2-specific sulfamethazine inhibition. NAT2 is expressed predominantly in the liver and gut, whereas NAT1 is expressed ubiquitously. NAT2 is a highly polymorphic enzyme that plays a key role in the detoxication and/or metabolic activation of certain therapeutic drugs, occupational chemicals and carcinogens. The enzyme produced by NAT2 acts on 1% of drugs in current clinical use including isoniazid and numerous chemicals. The enzyme activity is expressed at highly variable levels. Three phenotypes are identified: rapid acetylators, intermediate acetylators, or slow acetylators. Approximately 50% of people in the United States are slow acetylators and 40% intermediate acetylators. Like the identification of CYP isoform(s) involved in the metabolism of the drug candidate, the identification of specific NAT(s) are very useful for the evaluation of the effects of potential drug-drug interaction/genetic polymorphism for liver-targeted candidates. Slow acetylators exhibit different pharmacokinetics from normal individuals and are at increased risk of drug-induced side effects due to diminished drug elimination.

Equilibrium dialysis is one of the most frequently used approaches to determine the nonbound drug fraction in plasma, where the major drawbacks are the time to reach equilibrium (varying between 6 and 24 h) and a long assay preparation time. A rapid equilibrium dialysis (RED) device has recently become commercially available offering the potential for reduced preparation and equilibration times. The high surface-to-volume ratio of the membrane compartment allows rapid dialysis, where equilibrium can be reached in 4 hours with high levels of reproducibility and accuracy.

AM6-36 binding to human plasma proteins reached equilibrium by approximately 4.5 h. The data suggested that AM6-36 showed only moderate binding to serum proteins (75%) and should not produce drug-drug interactions due to displacement of highly bound drugs from serum proteins.

After administration of AM6-36 to rats by gavage, AM6-36 was detected in serum, liver and mammary tissues. Among the seven metabolites of AM6-36 observed in vitro, all except M5 and M7 were observed *in vivo* using rats. Among the AM6-36 metabolites detected *in vivo*, M2 was the most abundant (data not shown). These findings are consistent with the *in vitro* studies for the following three reasons: 1) M2 was a major metabolite of AM6-36 during incubations with human hepatocytes; and 2) M5 and M7 were only minor metabolites formed by human hepatocytes. Low levels of AM6-36 were found in mammary gland and fat tissues. Together with high abundance of M2 of AM6-36 found in rat liver and plasma, we conclude that extensive Phase II metabolism of AM6-36 is one of the main reasons leading to only moderate oral bioavailability in rats.

In conclusion, the metabolism of the indenoisoquinoline AM6-36, which is an agonist of RXR under investigation as a potential chemotherapeutic and chemoprevention agent, was investigated using human hepatocytes, human liver microsomes and rats. AM6-36 formed seven Phase I and Phase II metabolites. Structures for all seven metabolites were proposed based on high resolution accurate mass tandem mass spectrometry, and six of these metabolites were identified by

comparison with synthetic standards. These preliminary metabolism studies suggest that AM6-36 will not form reactive, potentially toxic metabolites. AM6-36 showed moderate serum protein binding, moderate metabolic stability, and low first-pass liver metabolism is predicted. These properties are favorable for further investigation and development of AM6-36 as a potential chemoprevention and cancer therapeutic agent.

4. *IN VITRO* HEPATIC METABOLISM STUDIES OF THE EXPERIMENTAL

CANCER TREATMENT DRUGS INDOTECAN AND INDIMITECAN

4.1 <u>Introduction</u>

Topoisomerases are nature's ubiquitous solution for managing the topology and torsional states of DNA. Topoisomerase I (Top1) is an essential enzyme that relaxes supercoiled DNA so that it may be replicated, transcribed and repaired.[118-121] The enzyme acts through a nucleophilic tyrosine residue (Tyr723), which nicks the phosphodiester backbone of double-stranded, supercoiled DNA and forms a transient "cleavage complex" in which the 3' end of the broken DNA strand is covalently linked to the enzyme. Within this "cleavage complex", the scissile (broken) strand undergoes "controlled rotation" around the unbroken strand, a process that relaxes the DNA. The catalytic cycle ends when the 5′ end of the scissile strand re-ligates the DNA and the enzyme is released. If this cycle is inhibited, DNA damage ensues, which in turn activates DNA damage responses, leading to cell cycle arrest or the eventual triggering of pro-apoptotic cascades.[155-159]

As Topl is overexpressed and DNA damage responses are defective in some human tumors, several Top1 inhibitors have been developed as chemotherapeutic agents.[121, 122] Representative examples are shown in Figure 25. The alkaloid camptothecin[123] is not used clinically, but its semisynthetic derivatives topotecan and irinotecan are FDA-approved.[118, 122, 124] Although potent, camptothecin derivatives suffer from many shortcomings, including poor solubility, dose-limiting toxicity,

pharmacokinetic limitations resulting from the instability of the E-ring lactone under physiological pH, and binding of the lactone hydrolysis product to plasma proteins.[122, 125-127]
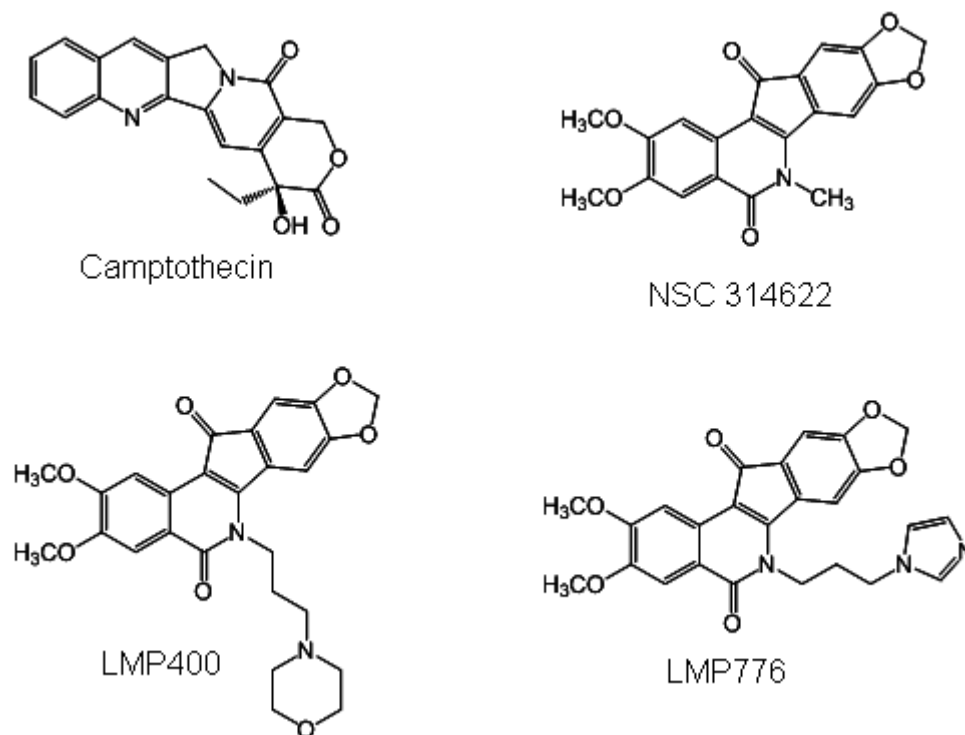
Figure 25 Representative Top1 Inhibitors.

To circumvent these limitations, the indenoisoquinolines were developed as therapeutic alternatives. In 1998, a COMPARE analysis[128, 129] was performed on NSC 314622 (Figure 25), which indicated that it may act in a manner similar to camptothecin and derivatives. Indeed, this compound was found to be a Top1 inhibitor.[160] Since then, many optimization and SAR studies have produced potent indenoisoquinolines. Two of these compounds, indimitecan (LMP776) and indotecan (LMP400) were promoted into Phase I clinical trials at the National Cancer Institute. These compounds appear to be stable and are powerful, cytotoxic Top1 poisons that

induce long-lasting DNA breaks and overcome the drug resistance issues associated with the camptothecins.[130, 161, 162]

4.2 Materials and methods

4.2.1 Materials

Indotecan (LMP400), indimitecan (LMP776), and putative metabolites of LMP400 and LMP776 were chemically synthesized in the laboratory of Dr. Mark Cushman of the Department of Medicinal Chemistry and Molecular Pharmacology at Purdue University (West Lafayette, IN). The purities were determined to be >98% based on analysis using LC-MS. Human liver microsomes were purchased from In Vitro Technologies (Baltimore, MD). All other chemicals were purchased from Sigma-Aldrich (St. Louis, MO). All organic solvents were HPLC grade or better and were purchased from Thermo Fisher (Hanover Park, IL).

4.2.2 Metabolic stability

Compounds (1 μM) were incubated separately with pooled human liver microsomes (1 mg protein/mL) as described previously in section III, 3.3.1.2. All experiments were carried out in duplicate.

The metabolic stability of propranolol, which has medium-low metabolic stability,[97] was used for reference in each set of experiments. The estimation of half-life was based on the rates of substrate disappearance during the 60 min

incubation with human liver microsomes. The results were converted to the percentage of substrate remaining, using t = 0 as 100%. The slope of the linear regression curve ($-k_e$) from log percentage remaining of each compound versus incubation time relationship was used in the conversion to *in vitro* value from the following equation: $t_{1/2} = 0.693/ k_e$.

4.2.3 <u>Incubation with human liver microsomes</u>

Compound LMP440 or LMP776 (10 μM) was incubated at 37 °C with pooled human liver microsomes (15 donors, mixed gender) containing 1 mg/mL of microsomal protein and 50 mM phosphate buffer at pH 7.4 in a total volume of 200 μL. After a 5 min preincubation, 1 mM NADPH was added to initiate reaction, and the mixture was incubated for an additional 60 min. The reaction was stopped by chilling the mixture on ice and by addition of 20 μL of ice-cold acetonitrile/water/formic acid (86:10:4, v/v/v) to precipitate proteins. Samples were centrifuged, supernatants were removed, evaporated to dryness under nitrogen, and the residues were dissolved in the mobile phase prior to analysis using LC-MS and LC-MS/MS. Control incubations were identical except for the elimination of microsomal protein or NADPH.

4.2.4 <u>LC-MS and LC-MS/MS</u>

Quantitative analyses of LMP400 and LMP776 were carried out using UHPLC-MS-MS on a Shimadzu Nexera UHPLC system interfaced with a Shimadzu

LCMS-8040 triple quadrupole mass spectrometer. Analytes were separated on a Shimadzu Shim-pack XR-ODS III UHPLC column (2.0 x 50 mm, 1.6µm) using a 2.5 min linear gradient from 10-90% acetonitrile in 0.1% aqueous formic acid with equilibration at 10% methanol for 1 min. The flow rate was 0.5 mL/min. Mass spectrometer source parameters were as follows: DL temperature 300 °C, spray voltage 3500 V, nebulizing gas flow 3 L/min, and drying gas flow 20 L/min. Analytes was detected using positive ion electrospray, collision-induced dissociation and SRM by recording the signal for the transition of the protonated molecule to the most abundant fragment ion. The SRM transitions of m/z 479 to m/z 392, m/z 460 to m/z 392, m/z 260 to m/z 183, and m/z 531 to m/z 244 were monitored for LMP400, LMP776, propranolol, and internal standard, respectively.

Analyses of LMP440, LMP776 and their metabolites were carried out using a Waters 2690 HPLC system equipped with a Waters Xterra 2.1×100 C_{18} column. The solvent system consisted of a linear gradient from 0.1% formic acid in water to methanol as follows: 20% to 45% methanol over 10 min, 45% to 90% methanol over 1 min and isocratic 90% methanol for another 2 min. The column was equilibrated with 20% methanol for at least 10 min between analyses. The flow rate was 0.2 mL/min, and the column temperature was 33 °C. The HPLC was interfaced with a high resolution Waters Q-TOF Synapt hybrid quadrupole/time-of-flight mass spectrometer, and positive ion electrospray was used for sample ionization. For accurate mass measurements, leucine enkephalin ([M+H]$^+$ of m/z 556.2771) was introduced post-column as a lock mass. The mass accuracy obtained was < 5 ppm.

Data were acquired from *m/z* 100-700. Tandem mass spectra were acquired at a collision energy of 20 eV using argon as the collision gas at a pressure of 2.0×10^{-5} mbar.

4.3 <u>Results</u>

4.3.1 <u>Metabolic Stability</u>

The metabolic stability values defined as the half-life during incubation with human liver microsomes and NADPH relative to propranolol (38 min) are summarized in Table VIII. Compared with the reference substrate propranolol, which is regarded as a drug with medium-low metabolic stability, metabolic stability studies indicated that LMP400 and LMP776 possess high degrees of metabolic stability during incubation with human liver microsomes.

TABLE VIII

THE METABOLIC STABILITY VALUES DEFINED AS THE HALF-LIFE

DURING INCUBATION WITH HUMAN LIVER MICROSOMES AND NADPH.

	$t_{1/2}$ (min)[1]	SRM transition (m/z)
LMP400	52.9	479 to 392
LMP776	42.9	460 to 392

4.3.2 Identification of LMP400 metabolites during incubation with human liver microsomes

Figure 26 Computer-reconstructed positive ion electrospray LC-MS chromatograms of LMP400 and its metabolites formed during incubation with human liver microsomes.

The positive ion electrospray LC-MS analysis of the LMP400 metabolite mixture after incubation with human liver microsomes is shown in Figure 26. Two major metabolites (M1 and M2) were detected as their protonated molecules. The formation of M1 and M2 required both liver microsomes and NADPH, since omission of either produced no detectable metabolites (data not shown).

The most abundant LMP400 metabolite M1 eluted at 12.3 min during LC-MS (Figure 26) and formed a protonated molecule of m/z 467.1823. Accurate mass measurement indicated an elemental composition of $C_{25}H_{27}N_2O_7$ (1.1 ppm) corresponding to the loss of one carbon atom. It is possible that the loss of carbon took place on the dimethoxy group or dioxolane group baesd on this information. The structure of M1 was then confirmed as 8,9-dihydroxy-2,3-dimethoxy-6-(3-morpholinopropyl)-5*H*-indeno[1,2-c]isoquinolin-5,11(6*H*)-dione by LC-MS/MS comparison with a synthetic standard PVN-9-12 (Figure 27).

Eluting at a retention time of 12.6 min (Figure 26), metabolite M2 produced a protonated molecule at *m/z* 465.1654 during positive ion electrospray, which was within -1.7 ppm of the elemental composition $C_{25}H_{25}N_2O_7$. This formula indicated that M2 was a demethylation product of LMP400. The putative metabolite was synthesized for comparison using LC-MS/MS (Figure 27), and M2 was identified as 3-hydroxy-2-methoxy-6-(3-morpholinopropyl)-5*H*-[1,3]dioxolo[4',5':5,6]indeno[1,2-c]isoquinoline-5,12(6*H*)-dione (PCL-3-65). The metabolism of LMP400 is summarized in Figure 28.

Figure 27 Positive ion electrospray product ion tandem mass spectra obtained using high resolution accurate mass measurement of LMP400, M1 and M2. The mass of the protonated molecule used as the precursor for product ion tandem mass spectrometry is indicated on each tandem mass spectrum.
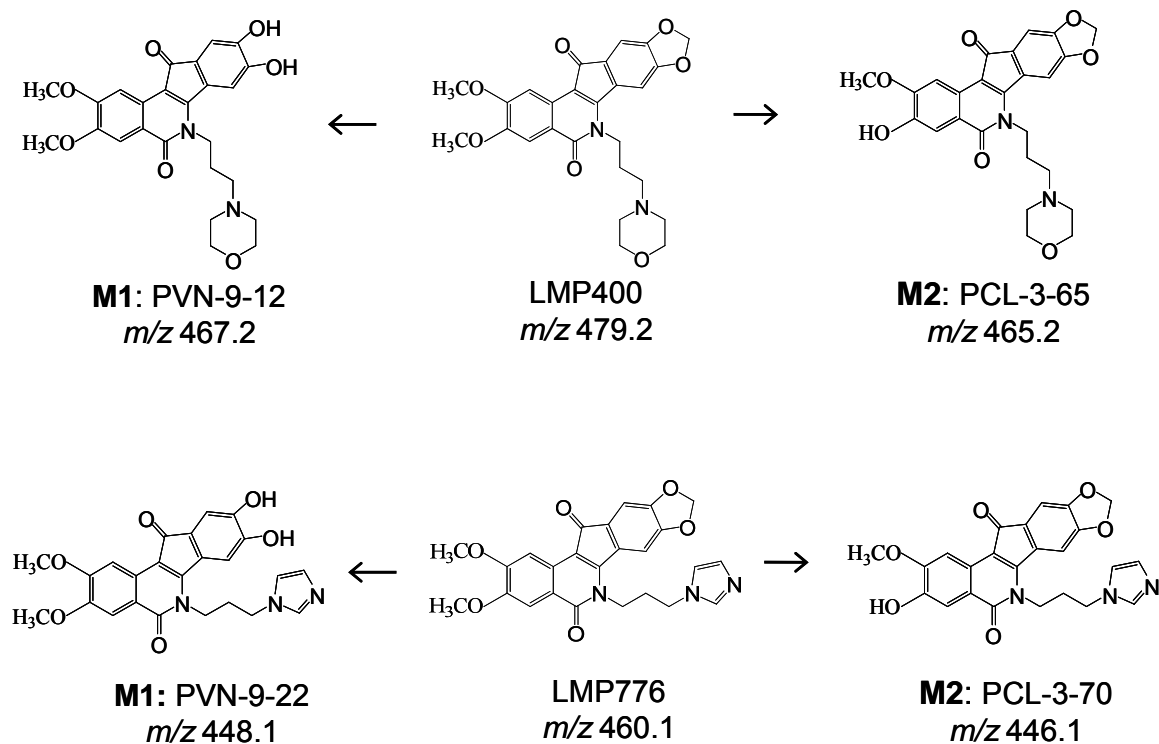
Figure 28 Structures and proposed metabolic pathways of human liver Phase I metabolites of LMP400 and LMP776.

4.3.3 Identification of LMP776 metabolites during incubation with human liver microsomes

The investigational Top1 inhibitor LMP776 was incubated with human liver microsomes, and the Phase I metabolites were characterized using LC-MS. The computer-reconstructed selected ion chromatograms for the positive ion electrospray LC-MS analysis of an incubation of LMP776 with pooled human liver microsomes are shown in Figure 29. Two major (M1 and M2) metabolites (based on abundances during LC-MS) were detected as their protonated molecules.

During LC-MS, the most abundant metabolite M1 was detected at the retention time of 12.8 min (Figure 29). Accurate mass measurement provided a value of *m/z* 448.1508, which was within -0.2 ppm of the theoretical formula of $C_{24}H_{22}N_3O_6$. This formula was consistent with the loss of a methylene group, and LC-MS/MS comparison with the synthetic standards (Figure 30) confirmed this metabolite as 6-(3-(1*H*-imidazol-1-yl)propyl)-8,9-bis(benzyloxy)-2,3-dimethoxy-5*H*-indeno[1,2-c]isoquinolin-5,11(6*H*)-dione.

A second abundant metabolite of LMP776, M2 eluted at a retention time of 13.2 min (Figure 29). Metabolite M2 produced a protonated molecule of *m/z* 446.1361, which corresponded to a loss of a methyl group with an elemental composition of $C_{24}H_{20}N_3O_6$ (2.0 ppm). After synthesis of one of the possible *O*-demethylated derivatives of LMP776 and comparison with the metabolite using LC-MS/MS (Figure 30), M2 was identified as 6-(3-(1*H*-imidazol-1-yl)-3-hydroxy-2-methoxy-5*H*-[1,3]dioxolo[4',5':5,6]indeno[1,2-*c*]isoquinoline-5,12(6*H*)-dione (PCL-3-70). Figure 28 summarizes the metabolism of both LMP400 and LMP776.
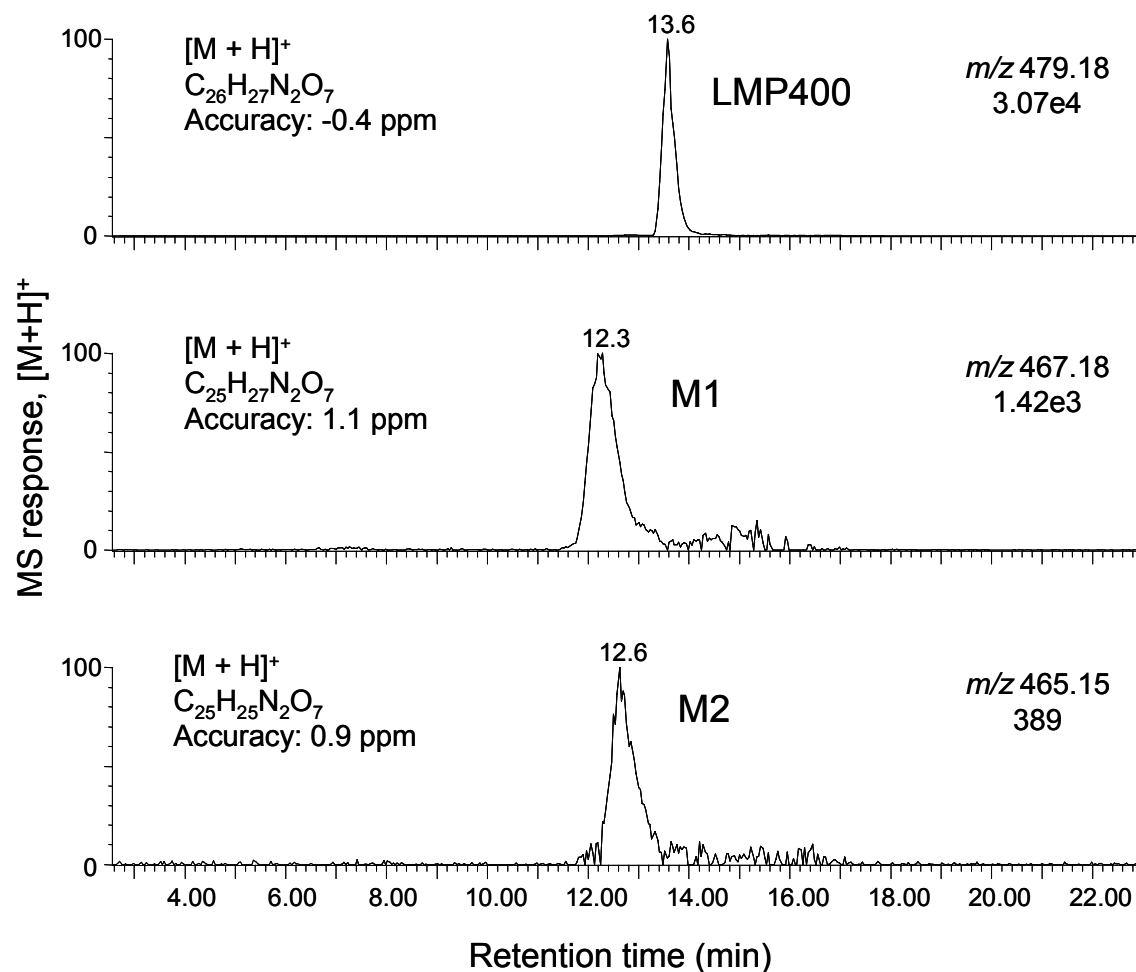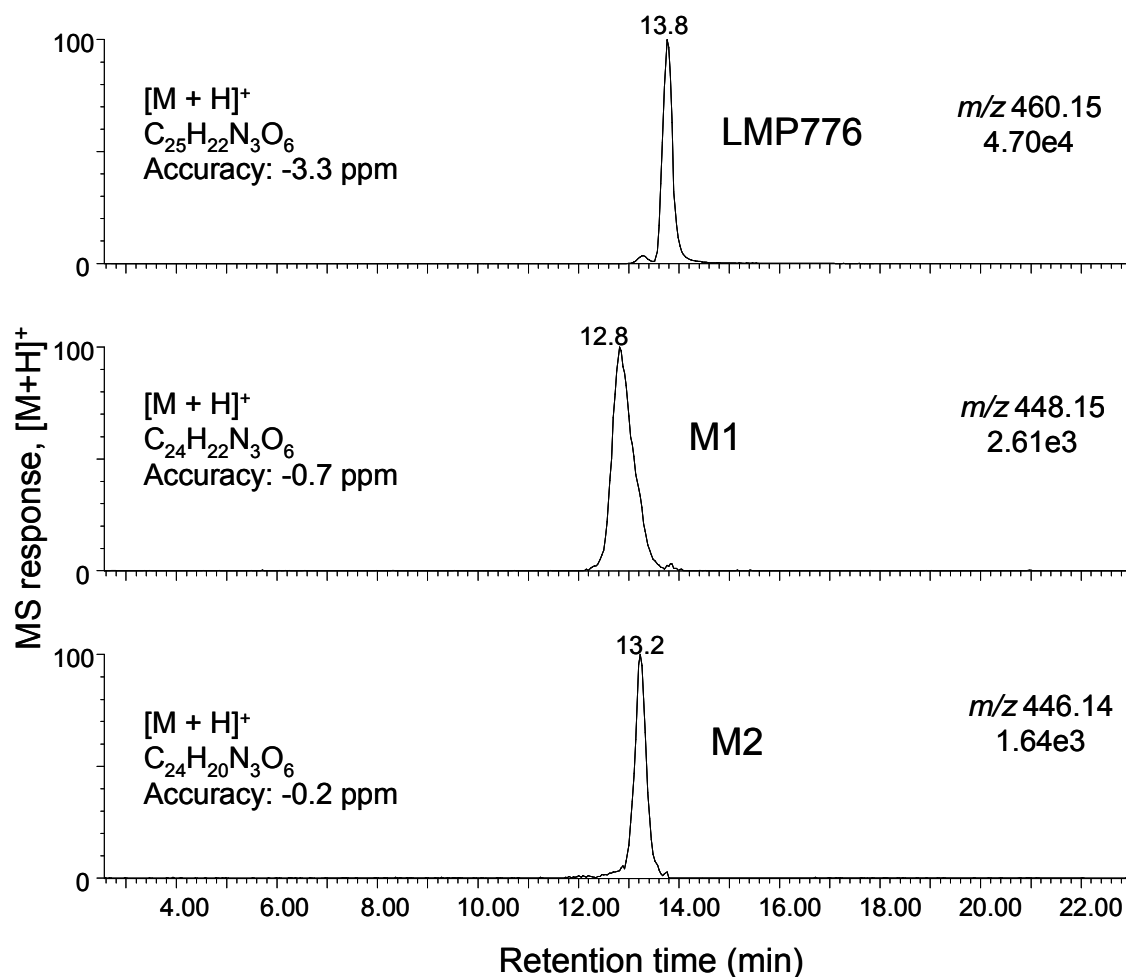
Figure 29 Computer-reconstructed positive ion electrospray LC-MS chromatograms of LMP776 and its metabolites formed during incubation with human liver microsomes.
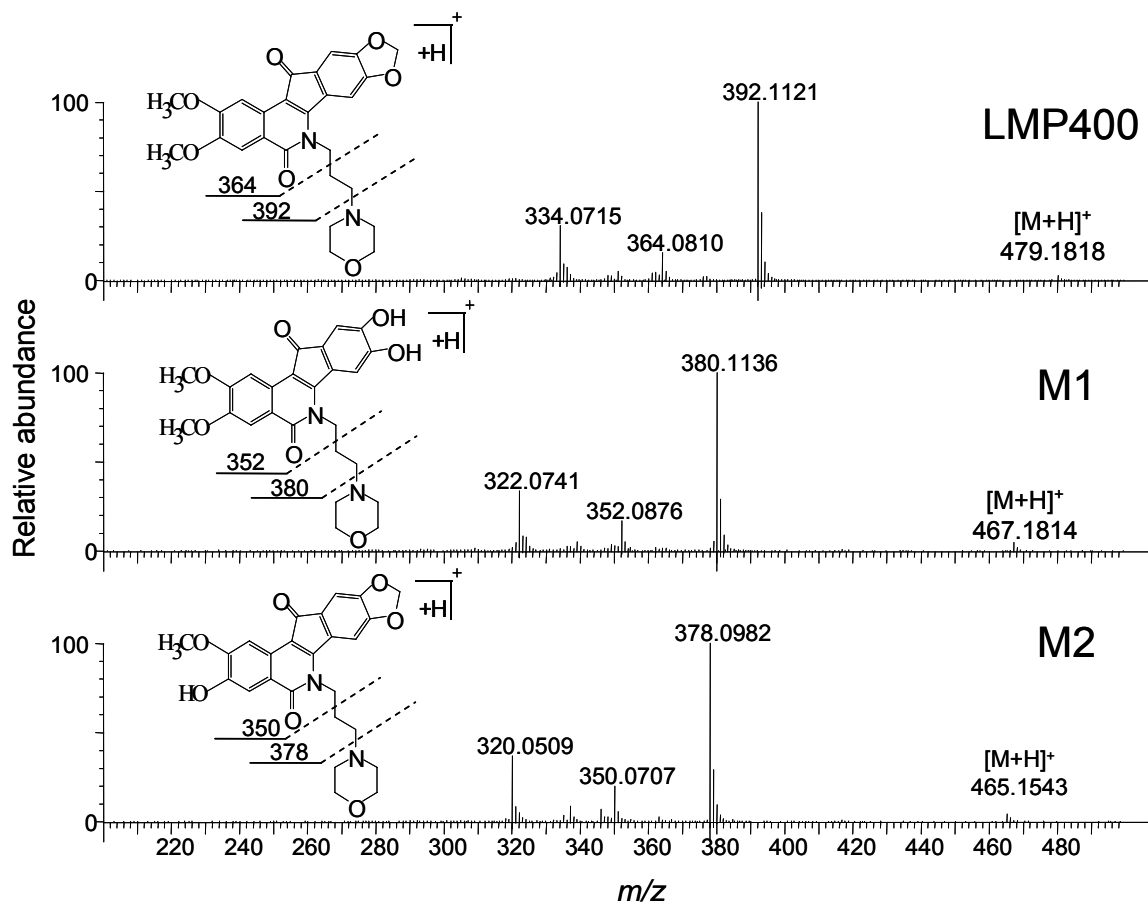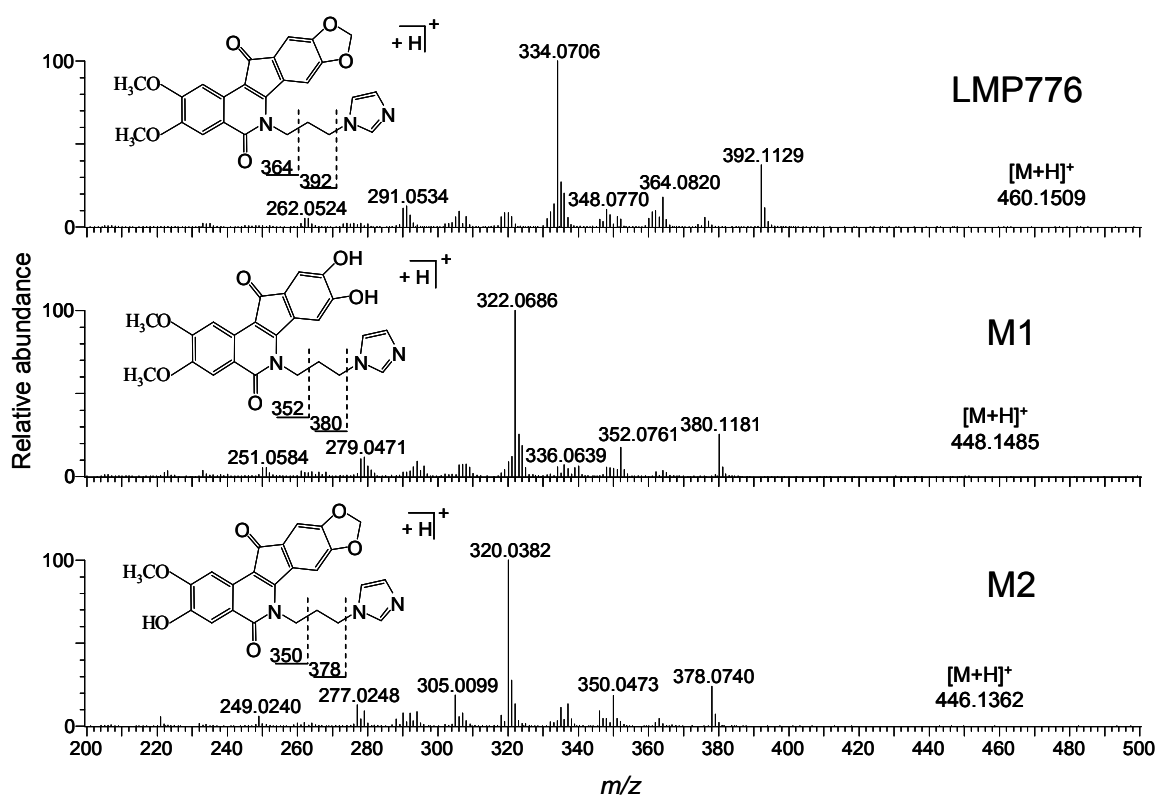
Figure 30 Positive ion electrospray product ion tandem mass spectra obtained using high resolution accurate mass measurement of LMP776, M1 and M2. The mass of the protonated molecule used as the precursor for product ion tandem mass spectrometry is indicated on each tandem mass spectrum.

4.4 <u>Discussion</u>

During incubation with human liver microsomes and NADPH, two similar Phase I metabolites were formed from each of LMP400 and LMP776 (Figure 28). Since M1 and M2 were not observed in control incubations without human liver microsomes or NADPH, their formation depended upon enzymatic catalysis. M1 was formed by loss of carbon from the dioxolane group, and M2 was an *O*-demethylation product. The structures were identified by comparison with synthetic standards.

O-dealkylation, catalyzed chiefly by hepatic cytochrome P450 enzymes, is a common and well-precedented metabolic process, and plays significant roles in human metabolism of the chemotherapeutic agents etoposide and teniposide,[163] opiates and opiate antagonists,[164, 165] and the topoisomerase inhibitors berberine and Genz-64482.[166, 167] Methylenedioxy rings are also sites of metabolic interference (likely via oxidation). Both demethylenation (to yield catechols) and demethylenation/alkylation processes (to yield *o*-methoxyphenols) are also observed in rodent and human metabolism of berberine,[166] safrole and piperonal derivatives,[168, 169] MDMA ("ecstasy"),[170] and the designer drug MDPPA.[171]

As part of this study, the metabolites of LMP400 and LMP776 are also being investigated for Top1 inhibitory and antiproliferative activity in the National Cancer Institute's Developmental Therapeutics Assay (the "NCI-60") against cell lines derived from a variety of human tumors (approximately 60 lines are being used).[172, 173] All of the metabolites possess significant anti-Top1 activity (shown in Appendix).

Although they were weaker Top1 poisons than LMP400 and LMP776, these metabolites might serve to prolong the antitumor effects of the parent drugs in vivo. As there are many examples of potent hydroxylated/phenolic Top1 poisons in the literature, the the hydroxyindenoisoquinolines metabolites are also new leads for the development of potent, cytotoxic Top1 poisons.

5. CONCLUSIONS AND FUTURE DIRECTIONS

Retinoid X receptor is a combinatorial partner for one-third of the 48 human nuclear receptor superfamily members and acts as a master coordinator of nuclear receptor signaling pathways involved in the control of cell growth and differentiation.

Although many derivatives and analogs of retinoids have been synthesized extensively investigated, therapies based on retinoids are compromised by a variety of side effects and reduced RAR expression in various cancer types. RXR ligands have shown promising chemopreventive and chemotherapeutic activities with mild toxicity in several cancer types tested, and RXR expression is rarely lost in human tumors. Ultrafiltration mass spectrometric screening greatly facilitated the screening for ligands of RXRα. AM6-36 was identified as structurally unique rexinoid and a leading chemopreventive agent based in high throughput screening.

LC-MS has provided superior sensitivity and selectivity needed for analytical challenges, making it well suited for drug metabolism as well as other ADME related evaluation of lead compounds from screening. The preliminary metabolism studies of AM6-36 suggest that AM6-36 will not form reactive, potentially toxic metabolites. AM6-36 showed moderate serum protein binding, moderate metabolic stability, and low first-pass liver metabolism is predicted. These properties are favorable for further investigation and development of AM6-36 as a potential chemoprevention and cancer therapeutic agent.

Despite many clinical trials, only two RXR agonists, LGD1069 and 9cRA have been approved for drug use and then only for limited indications. Both drugs have significant adverse effects that may be due to their abilities to activate the RARs. The effects of AM6-36 on other nuclear receptors such as PPARs and LXRs should also be examined in the future.

Continual screening of RXR ligands would be another direction of future work. A major limitation for the RXR ultracentrifugation screening was that the receptor must be purchased. Therefore, an in-house expression and purification of RXR should be accomplished in order to better facilitate the high throughput screening approach.

Since a recent report has indicated that RXR agonists may be of therapeutic utility in the treatment of Alzheimer's disease and its antecedent phases,[174] rexinoids for the treatment/prevention of Alzheimer's disease will also be an interesting direction for future investigation.

CITED LITERATURE

1.   Parkin DM, Bray F, Ferlay J and Pisani P: Global cancer statistics, 2002. CA Cancer J Clin. 2005, 55: 74-108.

2.   Joseph T. DiPiro, Robert L. Talbert, Gary C. Yee, Gary R. Matzke, Barbara G. Wells, L. Michael Posey. Pharmacotherapy: A Pathophysiologic Approach, 8th Edition

3.   Sporn MB. Approaches to prevention of epithelial cancer during the preneoplastic period. Cancer Res. 1976, 36: 2699–2702.

4.   Sporn MB, Liby KT. Cancer chemoprevention: scientific promise, clinical uncertainty. Nat Clin Pract Oncol. 2005, 2: 518-25.

5.   Prevention of cancer in the next millennium: Report of the Chemoprevention Working Group to the American Association for Cancer Research. Cancer Res. 1999, 59: 4743-58.

6.   Laudet V and Gronemeyer H 2002. The Nuclear Receptor Facts Book. San Diego: Academic Press.

7.   Sporn MB, Suh N. Chemoprevention: an essential approach to controlling cancer. Nat Rev Cancer. 2002, 2: 537-43.

8.   Robinson-Rechavi M, Escriva Garcia H, Laudet V. The nuclear receptor superfamily. J Cell Sci. 2003, 116: 585-6.

9.   Newman DJ, Cragg GM, Snader KM. Natural products as sources of new drugs over the period 1981-2002. J Nat Prod. 2003, 66: 1022-37.

10.   Gullo VP, McAlpine J, Lam KS, Baker D, Petersen F. Drug discovery from natural products. J Ind Microbiol Biotechnol. 2006, 33: 523-31.

11.   Surh YJ. Cancer chemoprevention with dietary phytochemicals. Nat Rev Cancer. 2003, 3: 768-80.

12.   Kwon KH, Barve A, Yu S, Huang MT, Kong AN. Cancer chemoprevention by phytochemicals: potential molecular targets, biomarkers and animal models. Acta Pharmacol Sin. 2007, 28: 1409-21.

13.   Lam KS. New aspects of natural products in drug discovery. Trends Microbiol. 2007, 15: 279-89.

14. Lee MS, Kerns EH. LC/MS applications in drug development. Mass Spectrom Rev. 1999, 18: 187-279.

15. Gordon EM, Gallop MA, Patel DV. Strategy and Tactics in Combinatorial Organic Synthesis. Applications to Drug Discovery. Acc Chem Res 1996, 29: 144–154.

16. Thompson LA, Ellman JA. Synthesis and Applications of Small Molecule Libraries. Chem Rev. 1996, 96: 555-600.

17. Loo JA. Mass spectrometry in the combinatorial chemistry revolution. Eur Mass Spectrom 1997, 3: 93–104.

18. Bevan P, Ryder H, Shaw I. Identifying small-molecule lead compounds: the screening approach to drug discovery. Trends Biotechnol. 1995, 13: 115-21.

19. Papac DI, Shahrokh Z. Mass spectrometry innovations in drug discovery and development. Pharm Res. 2001, 18: 131-45.

20. Geoghegan KF, Kelly MA. Biochemical applications of mass spectrometry in pharmaceutical drug discovery. Mass Spectrom Rev. 2005, 24: 347-66.

21. van Breemen RB, Huang CR, Nikolic D, Woodbury CP, Zhao YZ, Venton DL. Pulsed ultrafiltration mass spectrometry: a new method for screening combinatorial libraries. Anal Chem. 1997, 69: 2159-2164.

22. Zhao YZ, van Breemen RB, Nikolic D, Huang CR, Woodbury CP, Schilling A, Venton DL. Screening solution-phase combinatorial libraries using pulsed ultrafiltration. J Med Chem. 1997, 40:4006-4012.

23. Nikolic D, van Breemen RB. Screening for inhibitors of dihydrofolate reductase using pulsed ultrafiltration mass spectrometry. Comb Chem High Throughput Screen. 1998, 1: 47-55.

24. Nikolic D, Habibi-Goudarzi S, Corley DG, Gafner S, Pezzuto JM, van Breemen RB. Evaluation of cyclooxygenase-2 inhibitors using pulsed ultrafiltration mass spectrometry. Anal Chem. 2000, 72:3853-3859.

25. Gu C, Nikolic D, Lai J, Xu X, van Breemen RB. Assays of ligand-human serum albumin binding using pulsed ultrafiltration and liquid chromatography-mass spectrometry. Comb Chem High Throughput Screen. 1999, 2:353-359.

26. Sun Y, Gu C, Liu X, Liang W, Yao P, Bolton JL, van Breemen RB.

Ultrafiltration tandem mass spectrometry of estrogens for characterization of structure and affinity for human estrogen receptors. J Am Soc Mass Spectrom. 2005, 16:271-279.

27. Liu D, Guo J, Luo Y, Broderick DJ, Schimerlik MI, Pezzuto JM, van Breemen RB. Screening for ligands of human retinoid X receptor-alpha using ultrafiltration mass spectrometry. Anal Chem. 2007, 79: 9398-402.

28. van Breemen RB, Newsome AG and Dahl JH. Mass Spectrometry and Drug Discovery. In: Burger's Medicinal Chemistry, Drug Discovery and Development. pp. 97–125. 2010

29. Tozuka Z, Kaneko H, Shiraga T, Beppu M, Niwa T, Kawamura A, Kagayama A. New SRM data dependent exclusion (MS)n measurement for structural determination of drug metabolites using LC/ESI/Ion trap MS. Drug Metab Pharmacokinet. 2003, 18: 390-403.

30. Nassar AE, Talaat RE. Strategies for dealing with metabolite elucidation in drug discovery and development. Drug Discov Today. 2004, 9: 317-27.

31. Hopfgartner G, Varesio E, Tschäppät V, Grivet C, Bourgogne E, Leuthold LA. Triple quadrupole linear ion trap mass spectrometer for the analysis of small molecules and macromolecules. J Mass Spectrom. 2004, 39: 845-55.

32. Ma S, Chowdhury SK. Application of liquid chromatography/mass spectrometry for metabolite identification. In: Drug Metabolism in Drug Design and Development: Basic Concepts and Practice, eds. Zhang D, Zhu M and Humphreys WG, pp. 331-335. John Wiley & Sons, Inc., Hoboken, NJ, USA, 2007

33. Johnson J, Yost R. Tandem mass spectrometry for trace analysis. Anal Chem. 1985, 57: 758-768

34. Liddle C and Stedman C. Hepatic metabolism of drugs. In: Textbook of Hepatology: From Basic Science to Clinical Practice, eds. Rodes J, Benhamou JP, Blei AT, Reichen J and Rizzetto M, Blackwell Publishing Ltd, Oxford, UK, 2008

35. Lu FC. Biotransformation of toxicants. In: Basic Toxicology: Fundamentals, Target Organs and Risk Assessment, eds. Lu FC and Kacew S. pp. 27-39. Taylor and Francis, Washington, DC, 1996

36. Iyanagi T. Molecular mechanism of phase I and phase II drug-metabolizing enzymes: implications for detoxification. Int Rev Cytol. 2007, 260: 35-112.

37. Williams JA, Hyland R, Jones BC, Smith DA, Hurst S, Goosen TC, Peterkin V, Koup JR, Ball SE. Drug-drug interactions for UDP-glucuronosyltransferase substrates: a pharmacokinetic explanation for typically observed low exposure (AUCi/AUC) ratios. Drug Metab Dispos. 2004, 32: 1201-8.

38. Guengerich FP. Oxidative, reductive, and Hydrolytic metabolism of drugs. In: Drug Metabolism in Drug Design and Development: Basic Concepts and Practice, eds. Zhang D, Zhu M and Humphreys WG, pp. 15-31. John Wiley & Sons, Inc., Hoboken, NJ, USA, 2007

39. Munro AW, Girvan HM, McLean KJ. Cytochrome P450--redox partner fusion enzymes. Biochim Biophys Acta. 2007, 1770: 345-59.

40. Wilkinson GR. Drug metabolism and variability among patients in drug response. N Engl J Med. 2005, 352: 2211-21.

41. Rendic S, Di Carlo FJ. Human cytochrome P450 enzymes: a status report summarizing their reactions, substrates, inducers, and inhibitors. Drug Metab Rev. 1997, 29: 413-580.

42. Zhou SF, Liu JP, Chowbay B. Polymorphism of human cytochrome P450 enzymes and its clinical impact. Drug Metab Rev. 2009, 41: 89-295.

43. Cashman JR. Structural and catalytic properties of the mammalian flavin-containing monooxygenase. Chem Res Toxicol. 1995, 8: 166-81.

44. Al-Waiz M, Ayesh R, Mitchell SC, Idle JR, Smith RL. A genetic polymorphism of the N-oxidation of trimethylamine in humans. Clin Pharmacol Ther. 1987, 42: 588-94.

45. Tipton KF, Boyce S, O'Sullivan J, Davey GP, Healy J. Monoamine oxidases: certainties and uncertainties. Curr Med Chem. 2004, 11: 1965-82.

46. Shih JC, Chen K. Regulation of MAO-A and MAO-B gene expression. Curr Med Chem. 2004, 11: 1995-2005.

47. Panoutsopoulos GI, Kouretas D, Beedham C. Contribution of aldehyde oxidase, xanthine oxidase, and aldehyde dehydrogenase on the oxidation of aromatic aldehydes. Chem Res Toxicol. 2004, 17: 1368-76.

48. Crabb DW, Matsumoto M, Chang D, You M. Overview of the role of alcohol dehydrogenase and aldehyde dehydrogenase and their variants in the genesis of alcohol-related pathology. Proc Nutr Soc. 2004, 63: 49-63.

49. Meech R, Mackenzie PI. Structure and function of uridine diphosphate glucuronosyltransferases. Clin Exp Pharmacol Physiol. 1997, 24: 907-15.

50. Miners JO, Mackenzie PI. Drug glucuronidation in humans. Pharmacol Ther. 1991, 51: 347-69.

51. Radominska-Pandya A, Czernik PJ, Little JM, Battaglia E, Mackenzie PI. Structural and functional studies of UDP-glucuronosyltransferases. Drug Metab Rev. 1999, 31: 817-99.

52. Tukey RH, Strassburg CP. Human UDP-glucuronosyltransferases: metabolism, expression, and disease. Annu Rev Pharmacol Toxicol. 2000, 40: 581-616.

53. Remmel R, Nagar S, Argikar U. Conjugative Metabolism of Drugs. In: Drug Metabolism in Drug Design and Development: Basic Concepts and Practice, eds. Zhang D, Zhu M and Humphreys WG, pp. 37-84. John Wiley & Sons, Inc., Hoboken, NJ, USA, 2007

54. Glatt H, Engelke CE, Pabel U, Teubner W, Jones AL, Coughtrie MW, Andrae U, Falany CN, Meinl W. Sulfotransferases: genetics and role in toxicology. Toxicol Lett. 2000, 112-113: 341-8.

55. Chapman E, Best MD, Hanson SR, Wong CH. Sulfotransferases: structure, mechanism, biological activity, inhibition, and synthetic utility. Angew Chem Int Ed Engl. 2004, 43: 3526-48.

56. Vietri M, Vaglini F, Pietrabissa A, Spisni R, Mosca F, Pacifici GM. Sulfation of R(-)-apomorphine in the human liver and duodenum, and its inhibition by mefenamic acid, salicylic acid and quercetin. Xenobiotica. 2002, 32: 587-94.

57. Harder A, Escher BI, Landini P, Tobler NB, Schwarzenbach RP. Evaluation of bioanalytical assays for toxicity assessment and mode of toxic action classification of reactive chemicals. Environ Sci Technol. 2003, 37: 4962-70.

58. Johnson BM, Qiu SX, Zhang S, Zhang F, Burdette JE, Yu L, Bolton JL, van Breemen RB. Identification of novel electrophilic metabolites of piper methysticum Forst (Kava). Chem Res Toxicol. 2003, 16: 733-40.

59. Evans DA. N-acetyltransferase. Pharmacol Ther. 1989, 42: 157-234.

60. Vatsis KP, Weber WW, Bell DA, Dupret JM, Evans DA, Grant DM, Hein DW, Lin HJ, Meyer UA, Relling MV, et al. Nomenclature for *N*-acetyltransferases. Pharmacogenetics. 1995, 5: 1-17.

61. Grant DM, Blum M, Beer M, Meyer UA. Monomorphic and polymorphic human arylamine *N*-acetyltransferases: a comparison of liver isozymes and expressed products of two cloned genes. Mol Pharmacol. 1991, 39: 184-91.

62. Hughes HB, Biehl JP, Jones AP, Schmidt LH. Metabolism of isoniazid in man as related to the occurrence of peripheral neuritis. Am Rev Tuberc. 1954, 70: 266-73.

63. Wolkenstein P, Carriere V, Charue D, Bastuji-Garin S, Revuz J, Roujeau JC, Beaune P, Bagot M. A slow acetylator genotype is a risk factor for sulphonamide-induced toxic epidermal necrolysis and Stevens-Johnson syndrome. Pharmacogenetics. 1995, 5: 255-8.

64. Hodgson J. ADMET-turning chemicals into drugs. Nat Biotechnol. 2001, 19: 722-6.

65. Grime K, Riley RJ. The impact of in vitro binding on in vitro-in vivo extrapolations, projections of metabolic clearance and clinical drug-drug interactions. Curr Drug Metab. 2006, 7: 251-64.

66. Gomez-Lechon MJ, Donato T, Ponsoda X, Castell JV. Human hepatic cell cultures: in vitro and in vivo drug metabolism. Altern Lab Anim. 2003, 31: 257-65.

67. Jones BC, Middleton DS, Youdim K. Cytochrome P450 metabolism and inhibition: analysis for drug discovery. Prog Med Chem. 2009, 47: 239-63.

68. Brandon EF, Raap CD, Meijerman I, Beijnen JH, Schellens JH. An update on in vitro test methods in human hepatic drug biotransformation research: pros and cons. Toxicol Appl Pharmacol. 2003, 189: 233-46.

69. Peters FT, Meyer MR. In vitro approaches to studying the metabolism of new psychoactive compounds. Drug Test Anal. 2011, 3: 483-95.

70. Berry MN, Friend DS. High-yield preparation of isolated rat liver parenchymal cells: a biochemical and fine structural study. J Cell Biol. 1969, 43: 506-20.

71. Loretz LJ, Li AP, Flye MW, Wilson AG. Optimization of cryopreservation procedures for rat and human hepatocytes. Xenobiotica. 1989, 19: 489-98.

72. Li AP, Lu C, Brent JA, Pham C, Fackett A, Ruegg CE, Silber PM. Cryopreserved human hepatocytes: characterization of drug-metabolizing enzyme activities and applications in higher throughput screening assays for hepatotoxicity, metabolic stability, and drug-drug interaction potential. Chem

Biol Interact. 1999, 121: 17-35.

73. Li AP. Human hepatocytes: isolation, cryopreservation and applications in drug development. Chem Biol Interact. 2007, 168: 16-29.

74. Krumdieck CL, dos Santos JE, Ho KJ. A new instrument for the rapid preparation of tissue slices. Anal Biochem. 1980, 104: 118-23.

75. Smith PF, Gandolfi AJ, Krumdieck CL, Putnam CW, Zukoski CF 3rd, Davis WM, Brendel K. Dynamic organ culture of precision liver slices for in vitro toxicology. Life Sci. 1985, 36: 1367-75.

76. Thohan S, Rosen GM. Liver slice technology as an in vitro model for metabolic and toxicity studies. Methods Mol Biol. 2002, 196: 291-303.

77. McGinnity DF, Riley RJ. Predicting drug pharmacokinetics in humans from in vitro metabolism studies. Biochem Soc Trans. 2001, 29: 135-9.

78. Germain P, Chambon P, Eichele G, Evans RM, Lazar MA, Leid M, De Lera AR, Lotan R, Mangelsdorf DJ, Gronemeyer H. International Union of Pharmacology. LXIII. Retinoid X receptors. Pharmacol Rev. 2006, 58: 760-72.

79. Yu VC, Delsert C, Andersen B, Holloway JM, Devary OV, Näär AM, Kim SY, Boutin JM, Glass CK, Rosenfeld MG. RXRβ: a coregulator that enhances binding of retinoic acid, thyroid hormone, and vitamin D receptors to their cognate response elements. Cell 1991, 67: 1251-1266.

80. Leid M, Kastner P, Lyons R, Nakshatri H, Saunders M, Zacharewski T, Chen JY, Staub A, Garnier JM, Mader S, et al. Purification, cloning, and RXR identity of the HeLa cell factor with which RAR or TR heterodimerizes to bind target sequences efficiently. Cell. 1992, 68: 377-95.

81. Mangelsdorf DJ, Thummel C, Beato M, Herrlich P, Schutz G, Umesono K, Blumberg B, Kastner P, Mark M, Chambon P, Evans RM. The nuclear receptor superfamily: the second decade. Cell. 1995, 83: 835-9.

82. Evans RM. The steroid and thyroid hormone receptor superfamily. Science. 1988. 240: 889–895.

83. Robinson-Rechavi M, Carpentier AS, Duffraisse M, Laudet V. How many nuclear hormone receptors are there in the human genome? Trends Genet. 2001, 17: 554–556.

84. Bertrand S, Brunet FG, Escriva H, Parmentier G, Laudet V, Robinson-Rechavi

M. Evolutionary genomics of nuclear receptors: from twenty-five ancestral genes to derived endocrine systems. Mol Biol Evol. 2004, 21: 1923–37.

85.   Olefsky JM. Nuclear receptor minireview series. J Biol Chem. 2001, 276: 36863-4.

86.   Wagner CE, Jurutka PW, Marshall PA, Groy TL, van der Vaart A, Ziller JW, Furmick JK, Graeber ME, Matro E, Miguel BV, Tran IT, Kwon J, Tedeschi JN, Moosavi S, Danishyar A, Philp JS, Khamees RO, Jackson JN, Grupe DK, Badshah SL, Hart JW. Modeling, synthesis and biological evaluation of potential retinoid X receptor (RXR) selective agonists: novel analogues of 4-[1-(3,5,5,8,8-pentamethyl-5,6,7,8-tetrahydro-2-naphthyl)ethynyl]benzoic acid (bexarotene). J Med Chem. 2009, 52: 5950–66.

87.   Chen ZP, Iyer J, Bourguet W, Held P, Mioskowski C, Lebeau L, Noy N, Chambon P, Gronemeyer H. Ligand- and DNA-induced dissociation of RXR tetramers. J Mol Biol. 1998, 275: 55–65.

88.   Zhang XK, Hoffmann B, Tran PB, Graupner G, Pfahl M. Retinoid X receptor is an auxiliary protein for thyroid hormone and retinoic acid receptors. Nature. 1992, 355: 441-6.

89.   Hamada K, Gleason SL, Levi BZ, Hirschfeld S, Appella E, Ozato K. H-2RIIBP, a member of the nuclear hormone receptor superfamily that binds to both the regulatory element of major histocompatibility class I genes and the estrogen response element. Proc. Natl Acad Sci USA. 1989, 86: 8289–8293.

90.   Dolle P, Fraulob V, Kastner P, Chambon P. Developmental expression of murine retinoid X receptor (RXR) genes. Mech Dev. 1994, 45: 91–104.

91.   Mangelsdorf DJ, Borgmeyer U, Heyman RA, Zhou JY, Ong ES, Oro AE, Kakizuka A, Evans RM. Characterization of three RXR genes that mediate the action of 9-cis retinoic acid. Gene Dev. 1992, 6: 329–344.

92.   Mangelsdorf DJ, Ong ES, Dyck JA, Evans RM. Nuclear receptor that identifies a novel retinoic acid response pathway. Nature. 1990, 345: 224–229.

93.   Nagpal S, Chandraratna RA Retinoids as anti-cancer agents. Curr Pharm.1996, 2: 295-316.

94.   Tanaka T, Suh KS, Lo AM, De Luca LM. P21(WAF1/CIP1) is a common transcriptional target of retinoid receptors. J Biol Chem. 2007, 282, 29987-29997.

95. Teplitzky SR, Kiefer TL, Cheng Q, Dwivedi PD, Moroz K, Myers L, Anderson MB, Collins A, Dai J, Yuan L, Spriggs LL, Blask DE, Hill SM. Chemoprevention of NMU-induced rat mammary carcinoma with the combination of melatonin and 9-cis-retinoic acid. Cancer Lett. 2001, 168: 155−163.

96. Teplitzky SR, Blask DE, Cheng Q, Myers L, Hill SM. Melatonin and 9-cis-retinoic acid in the chemoprevention of NMU-induced rat mammary carcinoma. Adv Exp Med Biol. 1999, 460: 363-7.

97. Zanardi S, Serrano D, Argusti A, Barile M, Puntoni M, Decensi A. Clinical trials with retinoids for breast cancer chemoprevention. Endocr Relat Cancer. 2006, 13: 51-68.

98. Lee HY, Chang YS, Han JY, Liu DD, Lee JJ, Lotan R, Spitz MR, Hong WK. Effects of 9-cis-retinoic acid on the insulin-like growth factor axis in former smokers. J Clin Oncol. 2005, 23: 4439−4449.

99. Zusi FC, Lorenzi MV, Vivat-Hannah V. Selective retinoids and rexinoids in cancer therapy and chemoprevention. Drug Discovery Today. 2002, 7, 1165-1174.

100. Alvarez RD, Conner MG, Weiss H, Klug PM, Niwas S, Manne U, Bacus J, Kagan V, Sexton KC, Grubbs CJ, Eltoum IE, Grizzle WE. The efficacy of 9-cis-retinoic acid (aliretinoin) as a chemopreventive agent for cervical dysplasia: results of a randomized double-blind clinical trial. Cancer Epidemiol Biomarkers Prev. 2003, 12: 114-9.

101. Ruzicka T, Lynde CW, Jemec GB, Diepgen T, Berth-Jones J, Coenraads PJ, Kaszuba A, Bissonnette R, Varjonen E, Holló P, Cambazard F, Lahfa M, Elsner P, Nyberg F, Svensson A, Brown TC, Harsch M, Maares J. Efficacy and safety of oral alitretinoin (9-cis retinoic acid) in patients with severe chronic hand eczema refractory to topical corticosteroids: results of a randomized, double-blind, placebo-controlled, multicentre trial. Br J Dermatol. 2008,158: 808-17.

102. Ponthan F, Kogner P, Bjellerup P, Klevenvall L, Hassan M. Bioavailability and dose-dependent anti-tumour effects of 9-cis retinoic acid on human neuroblastoma xenografts in rat. Br J Cancer. 2001, 85: 2004-9.

103. Miller WH Jr, Jakubowski A, Tong WP, Miller VA, Rigas JR, Benedetti F, Gill GM, Truglia JA, Ulm E, Shirley M, et al. 9-cis retinoic acid induces complete remission but does not reverse clinically acquired retinoid resistance in acute promyelocytic leukemia. Blood. 1995, 85: 3021-7.

104. de Lera AR, Bourguet W, Altucci L, Gronemeyer H. Design of selective nuclear receptor modulators: RAR and RXR as a case study. Nature Rev. Drug Discovery 2007, 6, 811-820.

105. Altucci L, Leibowitz MD, Ogilvie KM, de Lera AR, Gronemeyer H. RAR and RXR modulation in cancer and metabolic disease. Nature Rev Drug Discovery. 2007, 6: 793−810.

106. Furmick JK, Kaneko I, Walsh AN, Yang J, Bhogal JS, Gray GM, Baso JC, Browder DO, Prentice JL, Montano LA, Huynh CC, Marcus LM, Tsosie DG, Kwon JS, Quezada A, Reyes NM, Lemming B, Saini P, van der Vaart A, Groy TL, Marshall PA, Jurutka PW, Wagner CE. Modeling, synthesis and biological evaluation of potential retinoid X receptor-selective agonists: novel halogenated analogues of 4-[1-(3,5,5,8,8-pentamethyl-5,6,7,8-tetrahydro -2-naphthyl)ethynyl]benzoic acid (bexarotene). ChemMedChem. 2012, 7: 1551-66.

107. Esteva FJ, Glaspy J, Baidas S, Laufman L, Hutchins L, Dickler M, Tripathy D, Cohen R, DeMichele A, Yocum RC, Osborne CK, Hayes DF, Hortobagyi GN, Winer E, Demetri GD. Multicenter phase II study of oral bexarotene for patients with metastatic breast cancer. J Clin Oncol. 2003, 21: 999-1006.

108. Sherman SI, Gopal J, Haugen BR, Chiu AC, Whaley K, Nowlakha P, Duvic M. Central hypothyroidism associated with retinoid X receptor-selective ligands. N Engl J Med. 1999, 340: 1075-9.

109. Gniadecki R, Assaf C, Bagot M, Dummer R, Duvic M, Knobler R, Ranki A, Schwandt P, Whittaker S. The optimal use of bexarotene in cutaneous T-cell lymphoma. Br J Dermatol. 2007, 157: 433-40.

110. Tanaka T, De Luca LM. Therapeutic potential of "rexinoids" in cancer prevention and treatment. Cancer Res. 2009, 69: 4945-7.

111. Wu K, Zhang Y, Xu XC, Hill J, Celestino J, Kim HT, Mohsin SK, Hilsenbeck SG, Lamph WW, Bissonette R, Brown PH. The retinoid X receptor-selective retinoid, LGD1069, prevents the development of estrogen receptor-negative mammary tumors in transgenic mice. Cancer Res. 2002, 62: 6376-80.

112. Lubet RA, Christov K, Nunez NP, Hursting SD, Steele VE, Juliana MM, Eto I, Grubbs CJ. Efficacy of Targretin on methylnitrosourea-induced mammary cancers: prevention and therapy dose-response curves and effects on proliferation and apoptosis. Carcinogenesis. 2005, 26: 441-8.

113. Wu K, Kim HT, Rodriquez JL, Hilsenbeck SG, Mohsin SK, Xu XC, Lamph

WW, Kuhn JG, Green JE, Brown PH. Suppression of mammary tumorigenesis in transgenic mice by the RXR-selective retinoid, LGD1069. Cancer Epidemiol Biomarkers Prev. 2002, 11: 467-74.

114. Camerini T, Mariani L, De Palo G, Marubini E, Di Mauro MG, Decensi A, Costa A, Veronesi U. Safety of the synthetic retinoid fenretinide: long-term results from a controlled clinical trial for the prevention of contralateral breast cancer. J Clin Oncol. 2001, 19: 1664-70.

115. Liby K, Rendi M, Suh N, Royce DB, Risingsong R, Williams CR, Lamph W, Labrie F, Krajewski S, Xu X, Kim H, Brown P, Sporn MB. The combination of the rexinoid, LG100268, and a selective estrogen receptor modulator, either arzoxifene or acolbifene, synergizes in the prevention and treatment of mammary tumors in an estrogen receptor-negative model of breast cancer. Clin Cancer Res. 2006, 12: 5902-9.

116. Suh N, Lamph WW, Glasebrook AL, Grese TA, Palkowitz AD, Williams CR, Risingsong R, Farris MR, Heyman RA, Sporn MB. Prevention and treatment of experimental breast cancer with the combination of a new selective estrogen receptor modulator, arzoxifene, and a new rexinoid, LG 100268. Clin Cancer Res. 2002, 8: 270-5.

117. Rendi MH, Suh N, Lamph WW, Krajewski S, Reed JC, Heyman RA, Berchuck A, Liby K, Risingsong R, Royce DB, Williams CR, Sporn MB. The selective estrogen receptor modulator arzoxifene and the rexinoid LG100268 cooperate to promote transforming growth factor beta-dependent apoptosis in breast cancer. Cancer Res. 2004, 64: 3566-71.

118. Pommier Y. Topoisomerase I inhibitors: camptothecins and beyond. Nat Rev Cancer. 2006, 6: 789-802.

119. Stewart L, Redinbo MR, Qiu X, Hol WGJ, Champoux JJ. A model for the mechanism of human topoisomerase I. Science. 1998, 279: 1534-1541.

120. Wang JC. Cellular roles of DNA topoisomerases: a molecular perspective. Nat Rev Mol Cell Biol. 2002, 3: 430-40.

121. Pommier Y. DNA topoisomerase I inhibitors: chemistry, biology, and interfacial inhibition. Chem Rev. 2009, 109: 2894-2902.

122. Teicher B. Next generation topoisomerase I inhibitors: Rationale and biomarker strategies. Biochem Pharmacol. 2008, 75: 1262-1271.

123. Wall ME, Wani MC, Cook CE, Palmer KH, McPhail AT, Sim GA, Plant

antitumor agents. I. The isolation and structure of camptothecin, a novel alkaloidal leukemia and tumor inhibitor from Camptotheca acuminata. J Am Chem Soc. 1966, 88: 3888-3890.

124. Thomas CJ, Rahier NJ, Hecht SM. Camptothecin: current perspectives. Bioorg Med Chem. 2004, 12: 1585-1604.

125. Schaeppi U, Fleischman RW, Cooney DA. Toxicity of camptothecin (NSC-100880). Cancer Chemother Rep 3. 1974, 5: 25-36.

126. Luzzio MJ, Besterman JM, Emerson DL, Evans MG, Lackey K, Leitner PL, McIntyre G, Morton B, Myers PL, Peel M, et al. Synthesis and antitumor activity of novel water soluble derivatives of camptothecin as specific inhibitors of topoisomerase I. J Med Chem. 1995, 38: 395-401.

127. Mi Z, Burke TG. Differential interactions of camptothecin lactone and carboxylate forms with human blood components. Biochemistry. 1994, 33:10325-36.

128. Paull KD, Hamel E, Malspeis L. Prediction of biochemical mechanism of action from the in vitro antitumor screen of the National Cancer Institute. In Cancer Chemotherapeutic Agents, Foye WO, Ed. American Chemical Society: Washington, DC, 1995; pp 9-45.

129. Paull KD, Shoemaker RH, Hodes L, Monks A, Scudiero DA, Rubinstein L, Plowman J, Boyd MR. Display and analysis of patterns of differential activity of drugs against human tumor cell lines: development of mean graph and COMPARE algorithm. J Natl Cancer Inst. 1989, 81: 1088-92.

130. Antony S, Agama KK, Miao ZH, Takagi K, Wright MH, Robles AI, Varticovski L, Nagarajan M, Morrell A, Cushman M, Pommier Y. Novel indenoisoquinolines NSC 725776 and NSC 724998 produce persistent topoisomerase I cleavage complexes and overcome multidrug resistance. Cancer Res. 2007, 67: 10397-405.

131. Antony S, Agama KK, Miao ZH, Hollingshead M , Holbeck SL , Wright MH , et al. Bisindenoisoquinoline bis-1,3-{(5,6-dihydro-5,11-diketo-11H-indeno[1,2-c]isoquinoline)-6-propylamino}propane bis(trifluoroacetate) (NSC 727357), a DNA intercalator and topoisomerase inhibitor with antitumor activity. Mol Pharmacol. 2006, 70: 1109–20.

132. Kim SH, Oh SM, Song JH, Cho D, Le QM, Lee SH, Cho WJ, Kim TS. Indeno[1,2-c]isoquinolines as enhancing agents on all-trans retinoic acidmediated differentiation of human myeloid leukemia cells. Bioorg Med

Chem. 2008, 16: 1125–32.

133. Park EJ, Kondratyuk TP, Morrell A, Kiselev E, Conda-Sheridan M, Cushman M, Ahn S, Choi Y, White JJ, van Breemen RB, Pezzuto JM. Induction of retinoid X receptor activity and consequent upregulation of p21WAF1/CIP1 by indenoisoquinolines in MCF7 cells. Cancer Prev Res. 2011, 4: 592-607.

134. Ahuja HS, Szanto A, Nagy L, Davies PJ. The retinoid X receptor and its ligands: versatile regulators of metabolic function, cell differentiation and cell death. J Biol Regul Homeost Agents. 2003, 17: 29-45.

135. Wan H, Dawson MI, Hong WK, Lotan R. Overexpressed activated retinoid X receptors can mediate growth inhibitory effects of retinoids in human carcinoma cells. J Biol Chem 1998, 273: 26915–22.

136. Monden T, Kishi M, Hosoya T, Satoh T, Wondisford FE, Hollenberg AN, et al. p120 acts as a specific coactivator for 9-cis-retinoic acid receptor (RXR) on peroxisome proliferator-activated receptor-g/RXR heterodimers. Mol Endocrinol. 1999, 13:1695–703.

137. Thorne J, Campbell MJ. The vitamin D receptor in cancer. Proc Nutr Soc. 2008, 67: 115-27.

138. Jerry W. High throughput lead discovery of ligands for the vitamin D receptor. PhD's thesis, Univeristy of Illinois at Chicago, Chicago, 2012.

139. Muccio DD, Brouillette WJ, Alam M, Vaezi MF, Sani BP, Venepally P, Reddy L, Li E, Norris AW, Simpson-Herren L, Hill DL. Conformationally defined 6-s-trans-retinoic acid analogs. 3. Structure-activity relationships for nuclear receptor binding, transcriptional activity, and cancer chemopreventive activity. J Med Chem. 1996, 39: 3625-35.

140. Cushman M, Cheng L. Stereoselective Oxidation by Thionyl Chloride Leading to the Indeno[1,2-c]isoquinoline System. J. Org. Chem. 1978, 43: 3781-3.

141. Guillouzo A, Morel F, Fardel O, Meunier B. Use of human hepatocyte cultures for drug metabolism studies. Toxicology. 1993, 82:209-19.

142. Winter HR, Unadkat JD. Identification of cytochrome P450 and arylamine N-acetyltransferase isoforms involved in sulfadiazine metabolism. Drug Metab Dispos. 2005, 33: 969-76.

143. Jahn U, Dinca E. Toward the elucidation of the metabolism of 15-E(2)-isoprostane: the total synthesis of the methyl ester of a potential

central metabolite. J Org Chem. 2010, 75: 4480-91.

144. Wu YS, Coumar MS, Chang JY, Sun HY, Kuo FM, Kuo CC, Chen YJ, Chang CY, Hsiao CL, Liou JP, Chen CP, Yao HT, Chiang YK, Tan UK, Chen CT, Chu CY, Wu SY, Yeh TK, Lin CY, Hsieh HP. Synthesis and evaluation of 3-aroylindoles as anticancer agents: metabolite approach. J Med Chem. 2009, 52: 4941-5.

145. Xu D, Penning TM, Blair IA, Harvey RG. Synthesis of phenol and quinone metabolites of benzo[a]pyrene, a carcinogenic component of tobacco smoke implicated in lung cancer. J Org Chem. 2009, 74: 597-604.

146. Tiwari A, Riordan JM, Waud WR, Struck RF. Synthesis and antitumor activity of several new analogues of penclomedine and its metabolites. J Med Chem. 2002, 45: 1079-85.

147. Chen L, Conda-Sheridan M, Reddy PV, Morrell A, Park EJ, Kondratyuk TP, Pezzuto JM, van Breemen RB, Cushman M. Identification, synthesis, and biological evaluation of the metabolites of 3-amino-6-(3'-aminopropyl)-5H-indeno[1,2-c]isoquinoline-5,11-(6H)dione (AM6-36), a promising rexinoid lead compound for the development of cancer chemotherapeutic and chemopreventive agents. J Med Chem. 2012, 55: 5965-81.

148. Li Y, Shin YG, Yu C, et al. Increasing the throughput and productivity of Caco-2 cell permeability assays using liquid chromatography-mass spectrometry: application to resveratrol absorption and metabolism. Comb Chem High Throughput Screen 2003, 6: 757-67.

149. Shin YG, Bolton JL, van Breemen RB. Screening drugs for metabolic stability using pulsed ultrafiltration mass spectrometry. Comb Chem High Throughput Screen. 2002, 5: 59-64.

150. Zhang ZY and Kaminsky LS. Determination of metabolic rates and enzyme kinetics. In: Drug Metabolism in Drug Design and Development: Basic Concepts and Practice, eds. Zhang D, Zhu M and Humphreys WG, pp. 419-425. John Wiley & Sons, Inc., Hoboken, NJ, USA, 2007.

151. Nikolic D, Fan PW, Bolton JL, van Breemen RB. Screening for xenobiotic electrophilic metabolites using pulsed ultrafiltration-mass spectrometry. Comb Chem High Throughput Screen. 1999, 2: 165-175.

152. Yu C, Shin YG, Chow A, Li Y, Kosmeder JW, Lee YS, Hirschelman WH, Pezzuto JM, Mehta RG, van Breemen RB. Human, rat, and mouse metabolism of resveratrol. Pharm Res. 2002, 19: 1907-14.

153. Chovan LE, Black-Schaefer C, Dandliker PJ, Lau YY. Automatic mass spectrometry method development for drug discovery: application in metabolic stability assays. Rapid Commun Mass Spectrom. 2004, 18: 3105-12.

154. Riley RJ, McGinnity DF, Austin RP. A unified model for predicting human hepatic, metabolic clearance from in vitro intrinsic clearance data in hepatocytes and microsomes. Drug Metab Dispos. 2005, 33: 1304-11.

155. Pommier Y, Barcelo JA, Rao VA, Sordet O, Jobson AG, Thibaut L, Miao Z H, Seiler JA, Zhang H, Marchand C, Agama K, Nitiss JL and Redon C. Repair of topoisomerase I-mediated DNA damage. In Prog. Nucleic Acid Res. Mol. Biol., Moldave, K., Ed. 2006, 81: 179.

156. Bailly C. Topoisomerase I poisons and suppressors as anticancer Drugs. Curr Med Chem. 2000, 7: 39-58.

157. Hsiang YH, Hertzberg R, Hecht S, Liu LF. Camptothecin induces protein-linked DNA breaks via mammalian DNA topoisomerase I. J Biol Chem. 1985, 260: 14873-8.

158. Staker BL, Hjerrild K, Feese MD, Behnke CA, Burgin AB, Stewart L. The mechanism of topoisomerase I poisoning by a camptothecin analogue. Proc Natl Acad Sci. USA. 2002, 99: 15387-15392.

159. Sordet O, Khan QA, Kohn KW, Pommier Y. Apoptosis induced by Topoisomerase inhibitors. Curr Med Chem Anticancer Agents 2003, 3, 271-290.

160. Kohlhagen G, Paull KD, Cushman M, Nagafuji P, Pommier Y. Protein-linked DNA strand breaks induced by NSC 314622, a novel noncamptothecin topoisomerase I poison. Mol Pharmacol. 1998, 54: 50-8.

161. Pommier Y, Cushman M. The indenoisoquinoline noncamptothecin topoisomerase I inhibitors: update and perspectives. Mol Cancer Ther. 2009, 8: 008-14.

162. Chrencik JE, Staker BL, Burgin AB, Pourquier P, Pommier Y, Stewart L, Redinbo MR. Mechanisms of camptothecin resistance by human topoisomerase I mutations. J Mol Biol. 2004, 339: 773-84.

163. Relling MV, Nemec J, Schuetz EG, Schuetz JD, Gonzalez FJ, Korzekwa KR. *O*-demethylation of epipodophyllotoxins is catalyzed by human cytochrome P450 3A4. Mol Pharmacol. 1994, 45: 352-8.

164. Küpfer A, Schmid B, Pfaff G. Pharmacogenetics of dextromethorphan O-demethylation in man. Xenobiotica. 1986, 16: 421-33.

165. Paar WD, Frankus P, Dengler HJ. The metabolism of tramadol by human liver microsomes. Clin Investig. 1992, 70: 708-10.

166. Qiu F, Zhu Z, Kang N, Piao S, Qin G, Yao X. Isolation and identification of urinary metabolites of berberine in rats and humans. Drug Metab Dispos. 2008, 36: 2159-65.

167. Sooryakumar D, Dexheimer TS, Teicher BA, Pommier Y. Molecular and cellular pharmacology of the novel noncamptothecin topoisomerase I inhibitor Genz-644282. Mol Cancer Ther. 2011, 10: 1490-9.

168. Benedetti MS, Malnoë A, Broillet AL. Absorption, metabolism and excretion of safrole in the rat and man. Toxicology. 1977, 7: 69-83.

169. Klungsøyr J, Scheline RR. Metabolism of piperonal and piperonyl alcohol in the rat with special reference to the scission of the methylenedioxy group. Acta Pharm Suec. 1984, 21: 67-72.

170. Lim HK, Foltz RL. In vivo and in vitro metabolism of 3,4-(methylenedioxy)methamphetamine in the rat: identification of metabolites using an ion trap detector. Chem Res Toxicol. 1988, 1: 370-8.

171. Springer D, Fritschi G, Maurer HH. Metabolism and toxicological detection of the new designer drug 3',4'-methylenedioxy-alpha-pyrrolidinopropiophenone studied in urine using gas chromatography-mass spectrometry. J Chromatogr B Analyt Technol Biomed Life Sci. 2003, 793: 377-88.

172. Skehan P, Storeng R, Scudiero D, Monks A, McMahon J, Vistica D, Warren JT, Bokesch H, Kenney S, Boyd MR. New colorimetric cytotoxicity assay for anticancer-drug screening. J Natl Cancer Inst. 1990, 82: 1107-12.

173. Boyd MR, Paull KD. Some practical considerations and applications of the national cancer institute In vitro anticancer drug discovery screen. Drug Development Res. 1995, 34: 91-109.

174. Cramer PE, Cirrito JR, Wesson DW, Lee CY, Karlo JC, Zinn AE, Casali BT, Restivo JL, Goebel WD, James MJ, Brunden KR, Wilson DA, Landreth GE. ApoE-directed therapeutics rapidly clear β-amyloid and reverse deficits in AD mouse models. Science. 2012, 335: 1503-6.

Appendix

Antiproliferative potencies and topoisomerase I inhibitory activities of

hydroxyindenoisoquinolines.

Compound	Cytotoxicity (GI$_{50}$ in μM)[a]	
	MGM[b]	Top 1 Cleavage[c]
LMP400	4.64±1.25	+++++
LMP776	0.079±0.023	+++++
M1 of LMP400	0.602	++++
M2 of LMP400	0.056	+++(+)
M1 of LMP776	0.224	++
M2 of LMP776	0.043	++++

[a]The cytotoxicity GI50 values are the concentrations corresponding to 50% growth inhibition. [b]Mean graph midpoint for growth inhibition of all human cancer cell lines successfully tested, ranging from 10^{-8} to 10^{-4} M. [c]Compound-induced DNA cleavage due to Top1 inhibition is graded by the following rubric relative to 1 μM camptothecin: 0, no inhibitory activity; +, between 20 and 50% activity; ++, between 50 and 75% activity; +++, between 75% and 95% activity; ++++, equipotent, +++++ more potent. [d]For MGM GI50 values in which a standard error appears, the GI50 values for individual cell lines are the average of two determinations; values without standard error are from one determination.

NAME   Lian Chen

EDUCATION   Ph.D., Pharmacognosy, University of Illinois, Chicago, Illinois, 2012

                        B.S., Clinical Medicine, Wuhan University, Wuhan, China, 2006

RESEARCH   Research Assistant, University of Illinois at Chicago (UIC), Chicago,
EXPERIENCE   IL (01/2010 – 12/2012)

INTERNSHIP   Johnson & Johnson, Raritan, NJ, 2010
EXPERIENCE   Biogen Idec, San Diego, CA, 2009

TEACHING   Teaching Assistant, University of Illinois at Chicago (UIC), Chicago,
EXPERIENCE   IL (01/2008 – 01/2010)

PROFESSIONAL   American Society of Mass Spectrometry
MEMBERSHIPS   American Association of Pharmaceutical Scientists

PUBLICATIONS   **Chen L**, Conda-Sheridan M, Reddy PV, Morrell A, Park EJ, Kondratyuk TP, Pezzuto JM, van Breemen RB, Cushman M. Identification, synthesis, and biological evaluation of the metabolites of 3-Amino-6-(3-aminopropyl)-5H-indeno[1,2-c]isoquinoline-5,11-6H)dione (AM6-36), a promising rexinoid lead compound for the development of cancer chemotherapeutic and chemopreventive agents. *J Med Chem*. 2012, 55: 5965-81.

                        Cinelli MA, Reddy PV, Lv PC, Liang JH, **Chen L**, Agama K, Pommier Y, van Breemen R, Cushman M. Identification, synthesis, and biological evaluation of metabolites of the experimental cancer treatment drugs indotecan (LMP400) and indimitecan (LMP776) and investigation of isomerically hydroxylated indenoisoquinoline analogues as topoisomerase I poisons. *J Med Chem*. 2012, 55: 10844-62.

                        Kabirov KK, Kapetanovic IM, Benbrook DM, Dinger N, Mankovskaya I, Zakharov A, Detrisac C, Pereira M, Martín-Jiménez T, Onua E, Banerjee A, van Breemen RB, Nikolić D, **Chen L**, Lyubimov AV. Oral toxicity and pharmacokinetic studies of SHetA2, a new chemopreventive agent, in rats and dogs. *Drug Chem Toxicol*. 2013, 36:284-95.

Chang M, Li Y, Angeles R, Khan S, **Chen L**, Kaplan J, Yang L. Development of methods to monitor ionization modification from dosing vehicles and phospholipids in study samples. *Bioanalysis*. 2011, 3:1719-39.

Marler L, Conda-Sheridan M, Cinelli MA, Morrell AE, Cushman M, **Chen L**, Huang K, van Breemen R, Pezzuto JM. Cancer chemopreventive potential of aromathecins and phenazines, novel natural product derivatives. *Anticancer Res*. 2010, 30:4873-82.

Conda-Sheridan M, Beck DE, Reddy PV, Nguyen TX, Hu B, **Chen L**, White JJ, Park EJ, Kondratyuk TP, Pezzuto JM, van Breemen RB, Cushman M. Design, synthesis, and biological evaluation of indenoisoquinolines rexinoids with chemopreventive potential. *J Med Chem*. (submitted)

PRESENTATIONS Conda-Sheridan M, Reddy PV, **Chen L**, Park EJ, Kondratyuk TP, Pezzuto JM, van Breemen RB, Cushman M. Indenoisoquinolines: a new class of rexinoids with promising chemopreventive potential. *242nd American Chemical Society National Meeting*, Denver, Colorado, August 28- September 1, 2011.

Chen L, Li J, Cushman M, Pezzuto J, van Breemen RB. In vitro hepatic metabolism of 3-Amino-6-(3-aminopropyl)-5,6-dihydro-5,11-dioxo-11H-indeno[1,2-c] isoquinoline dihydrochloride, a promising cancer cChemoprevention agent. *58th American Society for Mass Spectrometry Conference on Mass Spectrometry*, Salt Lake City, Utah, May 23-27, 2010.

Chang M, Angeles R, **Chen L**, Khen S, Kaplan J, Yang L. Oral Presentation. Effect of PEG 400 on discovery bioanalysis. *61st Pittsburgh Conference on Analytical Chemistry and Applied Spectroscopy*, Orlando, FL, Feb 28–March 5, 2010.

Chen L, Liu D, Pezzuto JM, van Breemen RB. Screening fatty acids for ligands of human retinoid X receptor-α using ultrafiltration mass spectrometry. *60th Pittsburgh Conference on Analytical Chemistry and Applied Spectroscopy*, Chicago, IL, March 8–13, 2009.